UNIVERSITY OF OKLAHOMA

GRADUATE COLLEGE

INTERACTION OF CLIMATE AND SPACE IN VARIATION OF THE FUNCTIONAL NICHE OF FRESHWATER MUSSELS (FAMILY: UNIONIDAE)

A DISSERTATION

SUBMITTED TO THE GRADUATE FACULTY

in partial fulfillment of the requirements for the

Degree of

DOCTOR OF PHILOSOPHY

By

TRACI GLYN POPEJOY DUBOSE
Norman, Oklahoma
2020

INTERACTION OF CLIMATE AND SPACE IN VARIATION OF THE FUNCTIONAL NICHE OF FRESHWATER MUSSELS (FAMILY: UNIONIDAE)

A DISSERTATION APPROVED FOR THE
DEPARTMENT OF BIOLOGY

BY THE COMMITTEE CONSISTING OF

Dr. Caryn C. Vaughn, Chair

Dr. Thomas M. Neeson

Dr. Carla L. Atkinson

Dr. Michael A. Patten

Dr. Cameron D. Siler

FOR MY DAD
who always encouraged my curiosity

ACKNOWLEDGEMENTS

I am extremely appreciative of the opportunity to complete my degree in the Department of Biology at the University of Oklahoma. The wonderful faculty, staff, and students of this department encourages scientific rigor and broad thinking while supporting the curiosities of its researchers. First and foremost, I would like to thank my advisor and hero, Dr. Caryn C. Vaughn, for teaching me to be a better scientist, a better writer, and a better teacher. I greatly appreciate her patience, her encouragement, and her confidence in my skill. She is the best mentor a person could hope for.

This dissertation would not have been possible without the guidance of my committee: Dr. Carla Atkinson, Dr. Tom Neeson, Dr. Michael Patten, and Dr. Cam Siler. Each member provided insightful comments and advice that greatly improved my research. Their wide-ranging expertise enhanced my dissertation and inspired me to be a better scientist. I count myself lucky to benefit from their time and care in their guidance of my degree and my career. Ranell Madding, Trina Steil, and Kyle Baker provided cheery hellos, great conversations, and logistical support that made this research possible.

I owe sincere and earnest thanks to all my lab mates. Thank you to Dr. Brent Tweedy and Dr. Noé Ferreira Rodríguez for providing career advice and guidance through the perils of graduate school. I loved all the fun times in the field and neat ecological conversations with Katy Murphy, Patrick Olsen, Ed Higgins, Jonathan Lopez, and Janell Hartwell. Previous Vaughn lab members (Dr. Dan Allen, Dr. Brandon Sansom, and Dr. Heather Galbraith) have given me invaluable advice and good memories from conferences as well. I also appreciate the good conversations, happy memories, and friendly peer-reviews from Michelle Busch.

Finally, I would not have completed this degree without the support of my family, especially my husband Sean DuBose. Sean provided impromptu field assistance, a kind ear when I detailed about my excitement at freshwater mussels, and strength through the trials and tribulations of graduate school. I thank my dog, Drake, for never caring about my research or degree and always giving me a smile and tail-wag. While Sean supported me by my side, my family supported me from afar. I would like to thank Vickie Popejoy and Staci Shelton for their career advice and cheerful pictures of my nieces. I appreciate the unwavering support I have received from Glynadee Popejoy, Sue Popejoy, and Donna Popejoy. I am thankful for Vaughn and Janet DuBose's support and curiosity about my degree and study system. Their support, encouragement, and love made my success possible; I hope to reciprocate this support and that this research makes them proud.

TABLE OF CONTENTS

Acknowledgements v

Table of Contents vii

List of Tables ix

List of Figures x

Abstract xi

Chapter 1 Latitudinal variation in freshwater mussel potential maximum length in eastern North America 1

Abstract 2

Introduction 3

Methods 7

Results 13

Discussion 14

Acknowledgements 19

References 20

Tables 29

Figures Captions 36

Chapter 2 Freshwater mussels engineer macroinvertebrate habitat through different mechanisms at different spatial scales 48

Abstract 51

Introduction 52

Methods 56

Results 62

Discussion 65

Acknowledgements 71

References 72

Tables 81

Figure Captions 84

Appendix 91

Chapter 3 Drought-induced, punctuated loss of freshwater mussels alters ecosystem function across temporal scales 99

Abstract 100

Introduction 101

Two case studies of drought-driven mussel losses in the southern United States 107

An experiment quantifying the effects of a mussel die-off on ecosystem function 109

Scaling up: Short and long-term nutrient releases following a mass mortality event 116

Implications & conclusions 118

Acknowledgments 120

References 120

Figure Captions 129

Appendix 137

LIST OF TABLES

CHAPTER 1

Table 1-1. Mussel shells from 5 biogeographic provinces, 14 rivers and 28 sites were thin-sectioned to generate length at age data for two different mussel clades. APLI indicates *A. plicata*, LCAR indicates *L. cardium,* and LORN indicates *L. ornata*. 29

Table 1-2. Sample information and von Bertalanffy growth parameters from each site. N represents the number of unique shells (from individual mussels) included in the analysis. Total annuli are the number of annuli identified and thus total observations of lengths at age for that site and species. The intercept and slope describe the line between shell length and shell width used to estimate shell length from back-calculated length at age observations. Adjusted R^2 for all length-width regressions were greater than 0.898. COFECHA removes age related growth using a cubic spline; the spline that resulted in the highest interseries correlation is reported. -- indicates only one shell was sectioned for that species from that site. Median values from the posterior distribution of the von Bertalanffy growth equation are reported. Parameters of the von Bertalanffy growth equation are: L_∞ (the potential maximum length), K (the growth characteristic), and T0 (size at age 0). 30

Table 1-3. Climatic variables used in the model comparison. Variable type 'characteristics' are from the NHDPlus. Discharge and velocity are also from the NHDPlus; all other flow characteristics are derived from USGS daily flow data. 'Temperature' variables are derived through prediction with NOAA air temperatures. Units are within parenthesis in the definition. 34

CHAPTER 2

Table 2-1. Macroinvertebrate abundance, richness, and diversity at the reach, enclosure, and shell spatial scale. ALIG represents *A. ligamentina* while APLI represents *A. plicata*. Enclosure treatments describe the dominant species, followed by whether the shells were live or sham shells. For example, ALIG Live is *A. ligamentina* dominated, live shells. Bold font indicates statistically significant at $p < 0.05$ using an ANOVA and Tukey's post hoc test..... 81

Table 2-2. Results from the ANOVA-like permutation test and forward and backward model selection of the CCA. Degrees of freedom for the global tests are found within parenthesis. Bold font indicates statistically significant at $p < 0.05$. 82

Table 2-3. Fall median (inter-quartile range) discharge for the Kiamichi, Glover, and Little River (USGS 2016). We recorded discharge at each reach (2016) the enclosure site (2017). September and October are considered fall for this table. 83

LIST OF FIGURES

CHAPTER 1

Figure 1-1. Diagram of mussel shell anatomy and species 39

Figure 1-2. Map of sites (black dots), associated rivers, and the watersheds from which shells were collected. 40

Figure 1-3. Variation in *Lampsilis* spp. (A) and *A. plicata* (B) potential maximum length 41

Figure 1-4. *Amblema plicata* and *Lampsilis* spp. L∞ exhibited positive relationships with latitude 42

Figure 1-5. Evidence for potential drivers between mussel maximum size and climatic variables. 43

Figure 1-6. Direction of the association between exploratory climatic variables and potential maximum length. 44

CHAPTER 2

Figure 2-1 Conceptual figure of mussel engineering effects at different spatial scales 86

Figure 2-2. Location of field sites and enclosure experiment 87

Figure 2-3. Macroinvertebrate density at each spatial scale. 88

Figure 2-4. CCA of macroinvertebrate communities and environmental factors 89

Figure 2-5. Macroinvertebrate community variation explained by the environmental variables. 90

CHAPTER 3

Figure 3-1. Conceptual model of ecosystem function shift due to unionids die-offs. 131

Figure 3-2. Map of case study locations in the Southeastern United States 132

Figure 3-3. Water column nutrients and chlorophyll *a* concentration among treatments 133

Figure 3-4. Organic matter decomposition among treatments after the die-off 134

Figure 3-5. Modelled short-term release of nutrients from soft tissue after a die-off 135

Figure 3-6. Modelled long-term releases of nutrients from shell after a die-off 136

ABSTRACT

Animals are an integral part of ecosystems: they consume and process materials, thus connecting the cycling of nutrients and matter through ecosystems. Freshwater mussels (order Unionoida) are a diverse group of bivalve mollusks that are highly imperiled. They reside on the bottom of rivers in discrete patches known as mussel beds and are aquatic ecosystem engineers that can have a strong impact on ecosystem function. Filter feeding mussels remove seston from the water and release nutrients (nitrogen and phosphorus) back to the riverbed and water through their egesta and excreta. These recycled nutrients fertilize and increase the abundance of algae, which are then eaten by stream animals such as insect larvae. Mussels also store nutrients in their soft body parts and shell, which are released when they die and can lead to algae blooms. Finally, mussel shells change near-bed hydrodynamics and provide habitat for other organisms. While all mussels perform these functions, different species exhibit considerable variation in their behavior, life history, and physiology, all of which describes their 'functional niche' or ecological role. This variation makes mussels ideal study organisms for investigating how species characteristics change through space and how this impacts ecosystem function. My dissertation contains three chapters: (1) variation in potential maximum size characteristics in freshwater mussels along a latitudinal gradient, (2) the impact of mussel ecosystem engineering on macroinvertebrates, and (3) how the effects of drought-driven mass mortality of mussels impacts ecosystem function. Collectively, my dissertation chapters examine how species' characteristics allow them to cope with their changing environment.

My first chapter addresses mussel's adherence to a general ecogeographic pattern, neo-Bergmann's rule, that states larger animals are found in areas of lower temperatures (or higher latitudes). To examine this, I radially dissected shells from two mussel taxa that inhabit different

thermal niches (*Amblema plicata* and *Lampsilis* spp.) to access annually deposited rings. From those annuli, I calculated von Bertalanffy growth parameters to describe the asymptotic maximum size of the mussels. As latitude is correlated with temperature, precipitation, and productivity gradients, I compared how different climatic gradients predicted this potential maximum length. I found that mussels grow larger at higher latitudes. Watershed precipitation and annual water temperature were negatively related to potential maximum size in both taxa. There is some evidence that thermal niche alters the size-latitude relationship. As climate change alters precipitation patterns and water temperatures, mussel taxa are likely to reach a smaller maximum size, which has implications for individual fecundity and thus population viability in the future.

For my second chapter, I used an integrative approach combining field experiments and a large field survey to investigate how the mechanisms and magnitude of ecosystem engineering by mussels changes with spatial scale. I used enclosures that contained assemblages of live mussels and "sham mussels". I sampled macroinvertebrates at two levels in the enclosures: in the sediment of the enclosure (~0.25m^2 scale) and the shell of the mussels (~10 cm^2 scale). On a larger spatial scale and as a part of a larger investigation of consumer control of biogeochemical cycles, I sampled the macroinvertebrates at stream reaches with and without mussel beds (~1,000 m^2 scale). I predicted that mussels' alteration of near-bed velocity would be greatest at the ~0.25 m^2 scale, while their control of food availability would be largest at the shell scale. I found that at larger scales (~1,000 m^2), discharge and food availability drove macroinvertebrate community structure. At the shell scale (~10 cm^2), live mussel presence predicted macroinvertebrate community structure the best, likely through bottom-up trophic effects. In rivers experiencing altered flow and nutrient regimes, ecosystem engineering effects of freshwater mussels are likely

to diminish, causing ecosystem function loss.

Globally, droughts are becoming more frequent and intense, due to climate change and increasing human water withdrawal. As sedentary animals, mussels are sensitive to drought and because they are ecosystem engineers, their loss can have profound impacts on stream ecosystems. Several drought-driven mussel die-offs have been documented in the southern Great Plains, but we do not know the ecosystem impacts of these mortality events. For my third chapter, I conducted an experiment that simulated a mussel die-off and measured the resulting changes in ecosystem function. In three scenarios (control tanks, tanks with a live mussel community, and tanks with a mussel community that experienced a die-off), I measured water column nutrients, algae concentration, and organic matter decomposition before and after the mussel mortality event. After the die-off, nutrients increased in mortality tanks with nitrogen (ammonium) increasing by 94%. This rapid nutrient release stimulated algal production and subsequent decomposition in the mortality tanks. Based on this and previous studies, I developed a conceptual model that predicts that mass mortality of mussels likely reduces ecosystem function for many years through the loss of filtration capacity, nutrient recycling and storage, and habitat. This model should aid development of management strategies (such as water release from dams) that sustain river function in the face of drought.

Freshwater mussels make important contributions to ecosystem function, however the magnitude of this effect is likely to shift due to anthropogenic climate change leading to mussel declines and changing mussel habitat. Through their bio-filtration, habitat provisioning, and influence on nutrient cycling, mussels contribute to ecosystem services (ecosystem functions that are beneficial to and used by humans). Thus, as rivers dry and mussel populations dwindle, stream ecosystems will provide less ecosystem services, such as water provision and recreation,

to human populations. By better understanding how mussels effect stream ecosystems and how important traits vary across space, water managers and conservation biologists can better conserve these threatened animals.

CHAPTER 1

LATITUDINAL VARIATION IN FRESHWATER MUSSEL POTENTIAL MAXIMUM LENGTH IN EASTERN NORTH AMERICA

Keywords:

macroecology, Bergmann's rule, temperature-size rule, thermo-conformer, poikilotherm

Formatted for publication in *Global Ecology and Biogeography*

DuBose, TP, Vaughn, CC, Patten, MA. In prep. Latitudinal variation in freshwater mussel potential maximum length in Eastern North America

ABSTRACT

As body size often predicts energetic requirements and fecundity, understanding the drivers behind size variation is important. In testament to this importance, many ecogeographic patterns describe body size variation (i.e. Bergmann's rule). Neo-Bergmann's rule states that larger individuals are found at higher latitudes and this size variation is attributable to temperature gradients. In ectotherms, this macroecological pattern has mixed support within the literature — both the direction and mechanism of size correlation with latitude varies. We asked if two taxa of freshwater mussels with different thermal niche preferences, *Amblema plicata* and *Lampsilis* spp. (*Lampsilis cardium* and *Lampsilis ornata*, a monophyletic clade), follow Bergmann's rule and what mechanisms might drive that latitudinal variation. *Lampsilis* spp. is a thermally sensitive clade intolerant of high temperatures, while *A. plicata* is more tolerant of a wide range of temperatures. We predicted that *Lampsilis* spp. at southern latitudes would have stunted growth in the summer, and that this would produce a steeper relationship with latitude than in *A. plicata*. We collected and thin-sectioned 114 *A. plicata* shells from 24 sites and 96 *Lampsilis* spp. shells from 16 sites across a latitudinal gradient in the eastern U.S from Texas to Minnesota. We used back-calculated size-at-age data to determine von Bertalanffy growth parameters for each taxon across this gradient. We found that at higher latitudes, both mussel taxa reached a larger potential maximum size. Using Bayesian model selection, we found that watershed precipitation explained mussel potential maximum size (L_∞) better than average water temperature, annual minimum flow ratio, and species identity. Increased watershed precipitation and average water temperature were associated with smaller potential maximum size. As climate change alters precipitation patterns, stream productivity and increases water temperature,

understanding size variation and its cause in mussels will be important for managing these vulnerable populations.

INTRODUCTION

Macroecologists employ ecogeographic rules to evaluate geographic patterns and assess potential mechanisms underlying those patterns at large spatial scales (Millien et al., 2006). Because body size among animals is highly variable, relatively easy to measure, and allometrically related to ecologically important traits (e.g. energetic requirements, longevity, and fecundity), it has historically been the parameter of interest for major ecogeographic rules (i.e. Bergmann's rule [Smith & Lyons, 2013]). While there is some debate regarding the usefulness of these rules (Geist, 1987), evaluating potential patterns in and mechanisms driving body size across different systems allows insight into fundamental ecological processes (Meiri, 2011). Nested processes, such as phylogenetic constraints, physiological constraints, and inter- and intraspecific competition, affect individual body size, thus different mechanisms can generate contrasting macroecological patterns at different taxonomic levels (Olalla-Tárraga, 2011). In this study we address neo-Bergmann's rule, here defined as body size increases as temperature decreases within a species (i.e. increasing latitude in the Northern Hemisphere). Since climate change is altering continental patterns of temperature and precipitation, understanding how those climatic factors might affect individual organismal body size is important for conservation (Jaramillo et al., 2017).

Different mechanisms can lead to body size variability in homeotherms and poikilotherms. In homeotherms, who must maintain a constant internal body temperature, thermal regulation and food availability are often implicated as the processes generating an increase in body size with latitude (Huston & Wolverton, 2011; Turvey & Blackburn, 2011). In

contrast, in poikilotherms, whose internal body temperature varies with external environmental temperature, temperature preferences, temperature-dependent oxygen limitations, food availability, and phylogenetic constraints are posited mechanisms causing geographic variation in body size (Stillwell, 2010). In aquatic ecosystems, water temperature, oxygen concentration, and food availability all interact to affect individual growth rates of ectotherms (Garvey & Marschall, 2003; Angilletta et al., 2004).

Water temperature, which dictates the saturation potential of dissolved oxygen, mediates the metabolism and production of most organisms, and thus regulates the stream-derived food supply within freshwater systems (Allan & Castillo, 2007). For example, in lungless salamanders, temperature dependent-oxygen regulation results in larger body sizes at lower water temperatures (Rollinson & Rowe, 2018); since aquatic organisms might encounter reduced oxygen absorption at higher temperatures and larger body sizes, they reduce body sizes at higher temperatures to maintain their aerobic scope. Freshwater fish exhibit different ecogeographic patterns based upon their thermal niche, with cold-water species following Bergmann's rule while warm-water species do not follow Bergmann's rule (Rypel, 2014). While Bergmann's rule and converse-Bergmann's rule are common among marine bivalve families, productivity, temperature and phylogeny did a poor job of consistently explaining these macroecological patterns (Berke et al., 2013). We aimed to investigate latitudinal body size variation within freshwater mussels to begin exploring potential processes that drive body size within that guild.

Freshwater mussels (Bivalvia: Unionoida, hereafter mussels) are sedentary filter-feeders that exhibit a wide range in functional traits and growth characteristics. Although mussels are typically described as long-lived and slow growing, they actually exhibit considerable variation in size and age across species (Haag & Rypel, 2011). While mussels within the Margartiferidae

family have a maximum age of 25 – 200 years, reach a potential maximum length of 109 mm, and grow slowly, Anodontini tribe mussels have a mean maximum age of 11 years, a mean potential maximum length of 85 mm, and grow quickly (Haag & Rypel, 2011). Growth characteristics can vary within species in populations from different river basins as well. For example, *Amblema plicata* in the Sipsey River, Alabama grew much more slowly than *A. plicata* within the Little Tallahatchie River, Mississippi, though both populations reach the same potential maximum length at 109 mm (Haag & Rypel, 2011). Since mussels are generally slow growing, it is infeasible to track growth in natural settings over their lifespan. However, mussels create durable records of past growth patterns in their shell through annual calcium/aragonite depositions (annuli), similar to tree rings (Neves & Moyer, 1988; Haag & Commens-Carson, 2008). By slicing through these shells (a method called thin-sectioning), we have access to these records and can then determine age, annual growth, and a proxy for maximum size.

Mussels are ectothermic poikilotherms with indeterminate growth. Their size and growth rates should depend on temperature and food availability; thus, as these environmental variables change, so should the mussels' growth characteristics. Most ectotherms grow more slowly but reach larger body sizes in colder environments (Angilletta et al., 2004). While this pattern can result from size dependent mortality, growing slowly and reaching a larger size at maturity can increase an individual's fecundity, especially in populations with distinct reproductive/growing seasons (Arendt, 2011). Thus, at higher latitudes and colder temperatures, mussels might grow more slowly and reach a larger body size in order to maximize their fecundity.

In addition, growth rates and body size should vary across species with different physiological tolerances to summer temperatures. Spooner and Vaughn (2008) evaluated resource acquisition and assimilation in eight mussel species and described two thermal guilds:

thermally tolerant species, where the highest resource acquisition and assimilation occurred at 35°C, and thermally sensitive species, where mussels decreased their resource acquisition and assimilation at 35°C and showed evidence of catabolism. As growth is an anabolic process, when thermally sensitive species encounter high temperatures, they cannot grow during that time period. Many freshwater mussels are likely living close to their thermal maximum during the summer (Spooner & Vaughn, 2008; Khan et al., 2019). As such, thermally sensitive species should reach a smaller potential maximum size at lower latitudes due to thermal stress during growing seasons. By investigating how size varies across a latitudinal gradient the driving climatic variables, we can better predict how climate change and associated changes in water temperature might affect mussel size.

To investigate the impact of climate on mussel size, we compared mussel size in two taxa with different thermal tolerances across a latitudinal gradient in the eastern United States. We used Bayesian model comparison to explore what climatic variables, specifically stream characteristics, water temperature, flow regime, and land use (as a proxy for productivity) might drive macroecological patterns in mussel size. We predicted that mussel size would be positively related to latitude, and thus follow Bergmann's Rule, because of increased temperatures resulting in lower growth rates at lower latitudes. We further predicted that the relationship between size and latitude would be stronger (higher slope between size and latitude) in the thermally sensitive species (*Lampsilis* spp.) than in the more tolerant species (*Amblema plicata*), because they stop growing and catabolize their own tissue at higher water temperatures.

METHODS

Shell sources and measurements

We obtained mussel shells of recently dead *Amblema plicata* and *Lampsilis* spp. from five biogeographic regions, 14 rivers, and 28 sites across the eastern U.S. (Table 1-1; Figure 1-1). We approached malacologists within the Mississippian Region to collect fresh-dead shell during their field seasons; the sites represent a haphazard collection of areas where they found shell. Since we are interested in intraspecific size variation and how it relates to thermal niche, we targeted species that had broad geographic distributions that represented different thermal niches. Both *A. plicata* and the *Lampsilis* clade are within the Ambleminae subfamily but represent two distinct phylogenetic tribes: Amblemini and Lampsilini. While tribes represent monophyletic clades within the family Unionidae, *Lampsilis* is likely not a monophyletic genus (Campbell et al., 2005). For this manuscript, *Lampsilis* spp. includes *Lampsilis cardium* and *Lampsilis ornata*, which have similar shell morphologies and represent a monophyletic group. In terms of thermal niche, *Lampsilis cardium* is thermally sensitive with high oxygen consumption and reduced filtering at 35°C while *Amblema plicata* is thermally tolerant, filters most efficiently at 35°C with lower oxygen consumption (Spooner & Vaughn, 2008). As such, we had shells from two taxa that represent different thermal niches from sites haphazardly spread across a latitudinal gradient.

For each shell, we measured the longest axis (length) and the second longest axis (width) with dial calipers to the nearest tenth of a mm. Following Sansom et al. (2016) and standard methods for sectioning bivalve shells (Neves & Moyer, 1988), we prepared radial thin sections of one valve from each individual. As disturbances can create discontinuous and dark bands in the thin section, two researchers evaluated annuli on the resulting thin section independently

(Haag & Commens-Carson, 2008). True annuli, those representing winter annuli, are more diffuse and have a hook at the ventral shell margin (Haag & Commens-Carson, 2008). Once true annuli were identified, we photographed each thin section under a stereomicroscope and used Adobe Photoshop (CS6 Extended 2012) to create composite images (Figure 1-1). We then measured the distance between the annuli at the intersection of the prismatic and nacreous layers using ImageJ with the ObjectJ plugin (Schneider et al., 2012; Vischer & Nastase, 2020). For some individuals, the umbo was extensively eroded; as such, early growth years were not measured for those shells (Figure 1-1). Instead, we measured the linear distance between the umbo and the first identifiable annuli. We also measured the distance along the nacreous layer on the shell and the linear extent of the shell for later calculation of length at different ages.

Preparation of length-age data

Following Rypel et al. (2008) and Sansom et al. (2016), we cross dated and checked our annuli identification using the software COFECHA (Grissino-Mayer, 2001). COFECHA removes age-related growth variation and creates a master chronology of standardized growth index at each year represented within the series. We determined the optimal cubic spline (a function to remove age related and long-term trends from the annuli growth measurements) for each population by applying splines one through 44 and using the one with the highest interseries correlation (Table 1-2; Black et al., 2005). By comparing each shells' standardized index (age related growth removed) to the master chronology, COFECHA aids quality control by identifying deviations from the master chronology (potential dating errors). We checked each error identified by the program, added or removed annuli when appropriate, and reran COFECHA.

Once quality control was complete, we used the annual growth increments to calculate proportional annual growth. At each age, we divided the previous growth by the total growth measured to calculate the proportional annual growth (Vigliola & Meekan, 2009). We then used that proportion to estimate the shell width of the individual at each recorded age. As freshwater mussel size is usually reported as length, we used species- and site-specific regressions to relate the estimated width at each age to its expected length. Based on this methodology, we created a back-calculated length by age table for each species at multiple sites along a latitudinal gradient.

Bayesian growth model

We evaluated *Amblema plicata* and *Lampsilis* spp. growth using a hierarchical Bayesian modeling framework. Because we used back-calculated lengths, our model accounted for individual variation as our length-age data are not independent (Vigliola & Meekan, 2009). We used a von Bertalanffy model of growth to describe the growth characteristics of each site.

$$L_i = L_{\infty ij} * \left(1 - e^{-K_{ij}\left(Age_i - T0_{ij}\right)}\right) + \epsilon_i \quad (1)$$

$$\epsilon_i \sim Gamma(0.1, 0.1) \quad (2)$$

$$\begin{matrix} Lmax_{ij} \\ K_{ij} \\ T0_{ij} \end{matrix} \sim \boldsymbol{N(\mu_j, \tau_j)T(0, 10^6)} \quad (3)$$

where L_i is the length (mm) of mussel i, and Age_i is the estimated age for mussel i. The three von Bertalanffy model parameters are: L_∞ represents the asymptotic length or potential maximum size, K represents the rate of approaching the asymptotic maximum size or the growth characteristic, and $T0$ is a modelling artifact and represents the hypothetical age at which size equals 0. These model parameters were assumed to come from a normal distribution with a site-level mean $\boldsymbol{\mu_j}$ and precision $\boldsymbol{\tau_j}$. ϵ_i is the residual error, assumed to be distributed as $N(0.01,0.01)$. Individual-level von Bertalanffy growth parameters were pulled from the distribution of the site-

level parameters. The site-level $L_{\infty j}$ was derived from a normal distribution with mean from a uniform distribution bounded from 60 to 160 and its precision from *Gamma(0.01, 0.01)*. The site-level K_j value was derived from a normal distribution with mean from a uniform distribution bounded from 0.01 to 1 and its precision from *Gamma(0.01, 0.01)*. The site-level $T0_j$ was derived from a normal distribution with mean *N(0, .1)* and precision from *Gamma(0.0001, 0.0001)*. These priors were based on minimum and maximum parameter values from the literature (Haag & Rypel, 2011). For all Bayesian models, we used the *R* package *rjags* to run the JAGS (Version 4.3.0) analysis, which completes a Markov Chain Monte Carlo analysis using a Gibbs sampler (Plummer, 2003, 2019). We checked convergence of the final posterior distributions with the Brooks-Gelman-Rubin statistics, $\hat{R} < 1.1$, and visually. We ran three concurrent Markov chains for 70,000 iterations with the first 10,000 iterations discarded for burn-in and further thinned by retaining every fourth value; each chain resulted in 17,500 total iterations for each species for analysis.

Regressing L_∞ with latitude to assess if mussels follow Bergmann's rule

Using the median value (μ_j from above) and precision of L_∞ distribution at each site *j*, we used a Bayesian regression to relate latitude to the potential maximum length for each species. Because *A. plicata* and *Lampsilis* spp. have different potential maximum sizes, we calculated percent maximum length using the maximum median potential maximum length for each species as the denominator (L_∞ in Table 1-2). If *A. plicata* and *Lampsilis* spp. follow Bergmann's rule, the slope between latitude and percent maximum length will be positive. Conversely, if the slope is negative, these species will follow converse-Bergmann's rule. Overlap of the slopes 95% credible interval with zero would indicate no relationship between scaled L_∞ and latitude.

$$\mu_j = beta_s * Latitude_j + precision_j + alpha \quad (4)$$

$$beta_s \sim N(mu\_b, tau\_b) \quad (5)$$

$$alpha \sim N(0{,}50)T(-100{,}100) \quad (6)$$

We evaluated the difference between *A. plicata*'s slope ($beta_{apli}$) and *Lampsilis* spp.'s slope ($beta_{lamp}$) by subtracting the slopes. If there is no difference between the slopes (or species' L_∞ relationship with latitude), the 95% credible interval will overlap with zero. The species $beta_s$ was derived from a normal distribution with mean from a normal distribution of mean 0 and standard deviation 10 and its precision from *Gamma(0.01, 0.01)*. We ran three concurrent Markov chains for 500,000 iterations with the first 30,000 iterations discarded for burn-in and further thinned by retaining every third value; each chain resulted in 166,666 total iterations. We also used a bootstrapped linear model to assess the direction and statistical significance of each species relationship with latitude (Figure 1-A1).

Investigation of macroecological drivers of maximum size

As latitude is often a proxy for other environmental factors (i.e. temperature), we investigated the climatic and landscape variables driving maximum length across our sites. We pulled daily mean stream discharge (cubic feet per second; cfs) from the oldest to youngest year recorded on the shells at each site from the closest United States Geological Survey (USGS) gage (Table 1-A2; USGS, 2016). We then used the *EFlows* package in *R* to calculate hydrologic indicator statistics, which describe ecologically important qualities of stream discharge (Table 2; Poff & Allan, 1995; Henriksen et al., 2006; Mills & Blodgett, 2017). We gathered stream characteristics such as stream elevation and cumulative drainage area from the National Hydrology Dataset Plus (*R* package *NHDPlusTools* (Blodgett, 2018; USGS, 2019). We quantified land cover within a 100 m area of a site location using the National Land Cover Database and the *R* packages *FedData* (Homer et al., 2012; Bocinski, 2019). Using modified

multiple regressions with stream characteristics to determine the intercept and slope (eq. 7 and eq. 8 respectively) of a linear model (Segura et al., 2015), we estimated annual mean and annual maximum water temperature using meteorological data queried from National Oceanic and Atmospheric Administration (*R* package *rnoaa*; Chamberlain, 2019).

$$Slope = 0.055\ln(DA) - 0.004BF - 0.047\ln(H) - 0.001P + 0.002F1 + 0.993 \quad (7)$$

$$Intercept = -0.62\ln(DA) - 0.24T - 0.06U1 + 0.04F1 + 9.8 \quad (8)$$

where *DA* is the drainage area of the watershed, *H* is stream elevation, *P* is the annual mean precipitation (cm), *F1* is the amount of forest within 100 m of the site, *T* is the annual mean air temperature (°C), and *U1* is the amount of developed land within 100 m of the site. When comparing the temperature estimates (calculated with eq.7 & eq. 8) to water temperature at USGS gages, they had a 0.79 Pearson's correlation coefficient (four watersheds, 12 years). This data compilation allowed us to investigate if water temperature, stream characteristics, land cover, and stream flow characteristics explain freshwater mussel potential maximum length.

We used Bayesian model selection to evaluate which linear regression between the variables and L_∞ fit the data best (*R* packages *BayesFactor* (Morey & Rouder, 2018). Bayesian model selection compares the relative evidence for competing hypothesis in the data through the ratio of the marginal likelihoods (Bayes Factor). As the *BayesFactor* package uses priors that make the Bayes Factor scale invariant, variable measurement scale was not altered (Rouder & Morey, 2012). Our null hypothesis was that species identity would provide the best explanation for L_∞. For models that have Bayes Factors greater than one, the alternative hypothesis is supported (or the model predicted L_∞ better than species identity). For models with Bayes Factors less than one, L_∞ is better explained by species identity. For the top model in each

predictor category (Table 1-3), we ran four Markov chains for 10,000 iterations to assess the direction of the relationship between the climatic variable and potential maximum length.

RESULTS

We sectioned 114 *A. plicata* shells from 24 sites and 96 *Lampsilis* spp. shells from 16 sites (Figure 1-2). Interseries correlation (the correlation of annual growth increments, a measure of growth synchronicity) varied from 0.155 to 0.890 across sites (Table 1-2). Using proportional back-calculated sizes, we used 2839 length at age observations to estimate the von Bertalanffy growth parameters.

Mussel growth parameters exhibit variability across sites

The growth parameters of both species varied widely between sites (Figure 1-3; Table 1-2). For *A. plicata*, L_∞ posterior means ranged from 78.6 to 173.2 mm. *Amblema plicata*'s *K* growth parameter posterior means ranged from 0.015 to 0.602 years^{-1} and *T0* ranged from -2.46 to 1.26. For *Lampsilis* spp., L_∞ posterior means ranged from 78.1 to 131.6 mm. *Lampsilis* spp.'s *K* growth parameter ranged from 0.213 to 0.762 years^{-1} and *T0* ranged from -2.32 to 2.34. While the 95% credible intervals overlap, the L_∞ for *A. plicata* and *Lampsilis* spp. appear to diverge as latitude increases for rivers that contain both species.

Amblema plicata & Lampsilis spp. follow Bergmann's Rule

Scaled L_∞ increased with latitude (Figure 1-4). The slope between *Lampsilis* spp.'s L_∞ and latitude had a posterior mean of 1.99 percent potential maximum length·latitude^{-1} (95% credible interval: 1.92, 2.05) while the slope between *A. plicata*'s L_∞ and latitude had a posterior mean of 1.65 percent potential maximum length·latitude^{-1} (95% credible interval: 1.52, 1.79; Figure 1-4). The intercept of the regression had a posterior mean of 0.004 (95% credible interval: -0.271, 0.293). The difference between these two species slopes had a posterior median of -0.33

percent potential maximum length·latitude^{-1} (95% credible interval: -0.48, -0.19). As the difference between the two taxa's slopes does not overlap with zero, *Lampsilis* spp.'s slope was larger than *A. plicata*'s slope (Figure 1-4).

Annual precipitation in a watershed best explains mussel size

As latitude is correlated with climate, we evaluated how multiple climatic factors might explain L_∞ using Bayesian model comparison (Table 1-3; Figure 1-5). Of the variables in our model, annual mean precipitation in a watershed explained more variation than latitude and species identity (BF = 75.8). Based on the model, increased watershed precipitation was negatively related to potential maximum length (Figure 1-6B). Annual average water temperatures, annual maximum water temperatures, and elevation likely explained similar variation in L_∞ because of our method for water temperature prediction (BF = 6.6, 5.7, and 5.1 respectively). Larger potential maximum size was negatively related to average water temperature (Figure 1-6C). The percentage of streamside crops was positively related to potential maximum length, though the evidence was only anecdotal (BF = 1.83; Figure 1-6D). Two discharge metrics related to low flow magnitude (minimum flows and baseflow) better explained L_∞ than species identity, though the evidence was anecdotal ($3 > BF > 1$). Generally, more stable flows (ratio between minimum flow and median flow is close to one) had larger potential maximum size (Figure 1-6E).

DISCUSSION

Understanding macroecological patterns in organism traits is important for predicting the effects of climate change. We found that freshwater mussels with different thermal traits followed neo-Bergmann's Rule and increased in potential maximum size with latitude. In addition, in general, thermally tolerant *A. plicata* achieved a larger potential maximum size than

thermally sensitive *Lampsilis* spp. *Lampsilis* spp. had a higher slope between potential maximum length and latitude than *A. plicata*. This macroecological pattern in mussel size was best explained by annual precipitation received in a watershed, which likely affects mussel growth by storm induced flood pulses.

Temperature, flow, and food availability are often considered important drivers of mussel growth and potential maximum size (Haag, 2012). We found that sites with higher annual precipitation falling in a watershed and with higher water temperatures had lower potential maximum length for both species. Precipitation in a watershed alters stream ecosystems in two main ways. Runoff from the watershed into the stream increases flow, and during storms can result in rapid, large changes in discharge. This runoff also brings terrestrially-derived organic material, sediment, and nutrients into streams (Allan & Castillo, 2007). We found that annual minimum flows were positively related to mussel potential maximum size. In a separate study, Rypel et al. (2009) found that mussel annual growth rates were highest in low flow years and were negatively correlated with the number of spates in a year. Thus, we suspect that the disturbance caused by spates in high flow years – due to increased watershed precipitation – reduced the potential maximum size of mussels at our sites. High flow events reduce mussel growth rates, likely through increased energy expenditure to maintain their position within the stream substrate and reduced resource assimilation (VO_2 respiration) because of increased suspended sediments (Payne et al., 1999; Hardison & Layzer, 2001; Hastie et al., 2003). In contrast, several studies have documented that increased stream productivity typically increases mussel growth rates and potential maximum size. Fritts et al. (2017) used sclerochronology and stable isotopes to evaluate changes over time in age, growth, and food sources in the Illinois River over a 1000 year period and found L_∞ for two mussel species (*A. plicata* and *Quadrula*

quadrula) has increased by 50% since 850, likely due to eutrophication increasing food availability. After measuring the growth of propagated juveniles in rivers throughout Kentucky, Haag et al. (2019) found that lower productivity and cooler temperatures led to decreased juvenile mussel growth. Finally, Bauer (1992) found that the growth rate and longevity of *M. margaritifera,* was highest in areas with higher water temperature and more productive waters. Thus, like other studies investigating how climate affects ectotherms' body size variation (Vinarski, 2014), the interaction of food availability, temperature, and stream flow drive mussel growth and size characteristics.

Mussels are ectothermic poikilotherms who generally can be grouped into two thermal niches, sensitive and tolerant. We expected and provide evidence that a thermally sensitive clade (*Lampsilis* spp.) has smaller body sizes at lower latitudes, likely due to thermal stress during summer growing months. Thermally sensitive mussel species can respond to the stress of high water temperature in multiple, overlapping ways. High water temperatures can cause mussels to catabolize their tissue rather than grow new tissue (Spooner and Vaughn 2008), leading to decreased growth. High water temperatures can also lead to decreased filtration, reduced oxygen consumption, and/or cause them to close their valves reducing food acquisition, which would also lead to decreased growth (Spooner & Vaughn, 2008; Haney et al., 2019). Both catabolism and reduced filtration would lead to smaller mussels at lower latitudes. In addition, recent work has shown that mussels can acclimate to different thermal regimes (Galbraith et al., 2012). Malish and Woolnough (2019) quantified mussels' physiological responses to slight increases in temperature (as predicted with climate change) and found that while *L. cardium* is still more thermally sensitive than *A. plicata* in Michigan, mussels from high latitudes had higher filtration rates and lower oxygen consumption than mussels at lower latitudes (Oklahoma). They posit that

mussels at lower latitudes might be acclimated to higher temperatures than mussels at higher latitudes and thus the relationship between latitude, high temperatures, and thermal traits is not straightforward. Understanding how thermal preference in freshwater mussels shifts among populations, species, and space is an important avenue of research for predicting how impending climate change will impact freshwater mussel populations (Spooner & Vaughn, 2008; Ganser et al., 2013; Payton et al., 2016).

It is unsurprising that environmental characteristics superseded species identity in predicting potential maximum length. While growth characteristics are typically phylogenetically conserved, there is considerable variation among species and populations (Haag & Rypel, 2011). While different species' annual growth rates might respond to different environmental cues, populations within the same river often exhibit synchrony, meaning their growth rates are similar even though individual sites might have different environmental characteristics (Rypel et al., 2009; Sansom et al., 2016). In a common exposure experiment, Denic et al. (2015) found that mussel growth characteristics reflected local environmental conditions instead of the originating population. Growth characteristics seem to be highly plastic, as evidenced by the difference in growth and appearance of juvenile *L. cardium* in different Kentucky streams (Haag et al., 2019). The additive effect of differences in resource availability and local acclimation might obscure phylogenetic control of potential maximum size in this invertebrate with indeterminant growth.

Since size is associated with age estimates and (intraspecific) fecundity estimates in mussels, conservation biologists and managers need to understand how the environment shapes size (Christian et al., 2005; Haag & Rypel, 2011). Also, understanding how size distributions reflect population structure and thus viability in a changing environment is important for managing these threatened population in the face of anthropogenic change (Haag, 2012).

Currently, biologists and managers often calibrate environmental flows and habitat requirements for endangered freshwater mussels based upon estimates of mussel growth rates and size distributions (Haag, 2012; Gates et al., 2015). Understanding the variation and drivers in growth characteristics is essential for population reintroduction and augmentation through propagation efforts; if we have a poor understanding of what sustains mussel growth and influences mussel size, we are more likely to mis-identify areas to focus conservation efforts (McMurray & Roe, 2017; Strayer et al., 2019). As some populations within different rivers exhibit different growth characteristics, we need to be judicious when applying growth characteristics from other taxa in other rivers (Haag & Rypel, 2011).

Climate change is often leading to decreases in organism size (Sheridan & Bickford, 2011). For example, over the past 55 years, salamanders in Appalachian habitats have smaller body sizes because of increased metabolism; the largest reductions in size occurred at lower latitudes and in areas with increased temperature (Caruso et al., 2014). In a study assessing temporal shifts in rodent body size, Villar and Naya (2018) found that seven of 17 species experienced reductions in body mass during the twentieth century, though these reductions could not be attributed to shifts in temperature or food availability. As many organisms are getting smaller, documenting macroecological size patterns (such as with Bergmann's rule) can lend important insights into understanding the effects of climate change (Millien et al., 2006).

In aquatic ecosystems, body size is decreasing at the community, population, and individual level, likely due to increasing water temperatures (Daufresne et al., 2009). Invertebrate abundance decreases with stream warming but individual body size increases in some taxa (specifically non-biting midge larvae) while decreasing in others (Piggott et al., 2015). Nelson et al. (2017) found that smaller, cold tolerant taxa were replaced by larger, warm tolerant

taxa in a warming stream, which resulted in a decrease in abundance, but an increase in macroinvertebrate biomass. Higher stream temperatures led to higher emergence of adult mayflies and caddisflies at smaller body sizes in a mesocosm experiment (Sardiña et al., 2016). As individual size decreases, there will likely be compounding effects on food webs and population structure. We found that mussel size increased with latitude. As rivers warm during the next century, maximum mussel size will likely decrease as mussels approach their thermal maximum, and northern and southern populations may become more similar in size. Since larger mussels can filter more water, this decrease in size could lead to changes in ecosystem function and services, such as decreased biofiltration. Reduced body size also might affect an organism's ability to cope with increasingly extreme climatic events, such as droughts and spates (Sheridan & Bickford, 2011; Norkko et al., 2013). The interactions between rising stream temperatures, shifts in precipitation patterns, and increased water withdrawal will likely stress and reduce aquatic organisms' body size with ramifying effects for stream ecosystems.

Based on our results and the literature, we conclude that the environment in which a mussel grows likely has a larger influence on its growth characteristics than its evolutionary history. At large spatial scales, the interaction of flow disturbance and food availability drove potential maximum size in both mussel species. Global change is altering precipitation patterns, increasing stream water temperatures, and altering food availability. We predict these changes will lead to decreases in mussel size, which will likely lead to decreased ecosystem function.

ACKNOWLEDGEMENTS

Funding for supplies and shell shipping costs provided by OU Department of Biology Adams Scholarship, OU Graduate Student Senate Research Award, and OU Loren G. Hill Zoology Excellence Fund. Special thanks goes to A. Holt who contributed to thin-sectioning

shells. We greatly appreciate advice from B. Samson and C.R. Randklev on thin-sectioning technique and R. Turner for access to the thin-sectioning lab. We thank C.L. Atkinson, J. Adams, S. Douglass, E. Grossman, D. Hornbach, K. Key, C.R. Randklev, A. Rosenberger, B. Sietman, J. Stoeckel, J. Tiemann, R.M., Vinsel, D. Woolnough, and the Illinois Natural History Museum for providing shells. We thank the Vaughn lab, for their advice on the manuscript. This paper was completed as part of a dissertation at the University of Oklahoma and is a contribution to the program of the Oklahoma Biological Survey.

REFERENCES

Allan, J.D. & Castillo, M.M. (2007) *Stream Ecology: structure and function of running waters*. Springer Netherlands.

Angilletta, M.J., Jr., Steury, T.D. & Sears, M.W. (2004) Temperature, growth rate, and body size in ectotherms: fitting pieces of a life-history puzzle. *Integr Comp Biol*, *44*, 498-509.

Arendt, J.D. (2011) Size-fecundity relationships, growth trajectories, and the temperature-size rule for ectotherms. *Evolution*, *65*, 43-51.

Bauer, G. (1992) Variation in the Life Span and Size of the Freshwater Pearl Mussel. *Journal of Animal Ecology*, *61*, 425-436.

Berke, S.K., Jablonski, D., Krug, A.Z., Roy, K. & Tomasovych, A. (2013) Beyond Bergmann's rule: size-latitude relationships in marine Bivalvia world-wide. *Global Ecology and Biogeography*, *22*, 173-183.

Black, B.A., Boehlert, G.W. & Yoklavich, M.M. (2005) Using tree-ring crossdating techniques to validate annual growth increments in long-lived fishes. *Canadian Journal of Fisheries and Aquatic Sciences*, *62*, 2277-2284.

Blodgett, D. (2018) *nhdplusTools: Tools for Accessing and Working with the NHDPlus*. United States Geological Survey.R package version 0.3.8

Bocinski, R.K. (2019) *FedData: Functions to Automate Downloading Geospatial Data Available from Several Federated Data Sources*.R package version 2.5.7

Campbell, D.C., Serb, J.M., Buhay, J.E., Roe, K.J., Minton, R.L. & Lydeard, C. (2005) Phylogeny of North American amblemines (Bivalvia, Unionoida): prodigious polyphyly proves pervasive across genera. *Invertebrate Biology*, *124*, 131-164.

Caruso, N.M., Sears, M.W., Adams, D.C. & Lips, K.R. (2014) Widespread rapid reductions in body size of adult salamanders in response to climate change. *Glob Chang Biol*, 20, 1751-9.

Chamberlain, S. (2019) *rnoaa: 'NOAA' Weather Data from R.*R package version 0.9.5

Christian, A.D., Harris, J.L., Posey, W.R., Hockmuth, J.F. & Harp, G.L. (2005) Freshwater Mussel (Bivalvia: Unionidae) Assemblages of the Lower Cache River, Arkansas. *Southeastern Naturalist*, *4,* 487-512.

Daufresne, M., Lengfellner, K. & Sommer, U. (2009) Global warming benefits the small in aquatic ecosystems. *Proc Natl Acad Sci U S A*, *106*, 12788-93.

DeCicco, L. & Blodgett, D. (2017) *hydroMap: Watershed boundaries*. R package version 0.1.4

Denic, M., Taeubert, J.-E., Lange, M., Thielen, F., Scheder, C., Gumpinger, C. & Geist, J. (2015) Influence of stock origin and environmental conditions on the survival and growth of juvenile freshwater pearl mussels (Margaritifera margaritifera) in a cross-exposure experiment. *Limnologica*, *50,* 67-74.

Fritts, A.K., Fritts, M.W., Haag, W.R., DeBoer, J.A. & Casper, A.F. (2017) Freshwater mussel shells (Unionidae) chronicle changes in a North American river over the past 1000years. *Sci Total Environ*, *575,* 199-206.

Gabry, J. & Mahr, T. (2019) *bayesplot: Plotting for Bayesian Models*. R package version 1.7.1

Galbraith, H.S., Blakeslee, C.J. & Lellis, W.A. (2012) Recent thermal history influences thermal tolerance in freshwater mussel species (Bivalvia: Unionoida). *Freshwater Science*, *31,* 83-92.

Ganser, A.M., Newton, T.J. & Haro, R.J. (2013) The effects of elevated water temperature on native juvenile mussels: implications for climate change. *Freshwater Science*, *32,* 1168-1177.

Garvey, J.E. & Marschall, E.A. (2003) Understanding latitudinal trends in fish body size through models of optimal seasonal energy allocation. *Canadian Journal of Fisheries and Aquatic Sciences*, *60*, 938-948.

Gates, K.K., Vaughn, C.C. & Julian, J.P. (2015) Developing environmental flow recommendations for freshwater mussels using the biological traits of species guilds. *Freshwater Biology, 60,* 620-635.

Geist, V. (1987) Bergmann's rule is invalid. *Canadian Journal of Zoology*, 65, 1035-1038.

Grissino-Mayer, H.D. (2001) Evaluating crossdating accuracy: A manual and tutorial for the computer program COFECHA. *Tree-Ring Research, 57,* 205-221.

Haag, W.R. (2010) A hierarchical classification of freshwater mussel diversity in North America. *Journal of Biogeography, 37,* 12-26.

Haag, W.R. (2012) *North American Freshwater Mussels: Natural History, Ecology and Conservation*. Cambridge U Press, Cambridge, UK.

Haag, W.R. & Commens-Carson, A.M. (2008) Testing the assumption of annual shell ring deposition in freshwater mussels. *Canadian Journal of Fisheries and Aquatic Sciences*, *65,* 493-508.

Haag, W.R. & Rypel, A.L. (2011) Growth and longevity in freshwater mussels: evolutionary and conservation implications. *Biol Rev Camb Philos Soc*, *86,* 225-47.

Haag, W.R., Culp, J.J., McGregor, M.A., Bringolf, R. & Stoeckel, J.A. (2019) Growth and survival of juvenile freshwater mussels in streams: Implications for understanding enigmatic mussel declines. *Freshwater Science*, *38,* 753-770.

Haney, A., Abdelrahman, H. & Stoeckel, J.A. (2019) Effects of thermal and hypoxic stress on respiratory patterns of three unionid species: implications for management and conservation. *Hydrobiologia*, *847,* 787-802.

Hardison, B.S. & Layzer, J.B. (2001) Relations between complex hydraulics and the localized distribution of mussels in three regulated rivers. *Regulated Rivers-Research & Management*, *17,* 77-84.

Hastie, L.C., Cosgrove, P.J., Ellis, N. & Gaywood, M.J. (2003) The threat of climate change to freshwater pearl mussel populations. *Ambio*, *32,* 40-6.

Henriksen, J.A., Heasley, J., Kennen, J.G. & Nieswand, S. (2006) Users' manual for the Hydroecological Integrity Assessment Process software (including the New Jersey Assessment Tools). In: (ed. U.S.Geological Survey), p. 72

Homer, C.H., Fry, J.A. & Barnes, C.A. (2012) The National Land Cover Database. , U.S. Geological Survey Fact Sheet 2012-3020, 4 p.

Huston, M. & Wolverton, S. (2011) Regulation of animal size by eNPP, Bergmann's rule, and related phenomena. *Ecological Monographs*, *81,* 349-405.

Jaramillo, E., Dugan, J.E., Hubbard, D.M., Contreras, H., Duarte, C., Acuna, E. & Schoeman, D.S. (2017) Macroscale patterns in body size of intertidal crustaceans provide insights on climate change effects. *PLoS One*, *12,* e0177116.

Khan, J.M., Hart, M., Dudding, J., Robertson, C.R., Lopez, R. & Randklev, C.R. (2019) Evaluating the upper thermal limits of glochidia for selected freshwater mussel species (Bivalvia: Unionidae) in central and east Texas, and the implications for their conservation. *Aquatic Conservation: Marine and Freshwater Ecosystems*, *29,* 1202-1215.

Malish, M.C. & Woolnough, D.A. (2019) Varied physiological responses of Amblema plicata and Lampsilis cardium exposed to rising temperatures. *Freshwater Science*, 38, 842-855.

McMurray, S.E. & Roe, K.J. (2017) Perspectives on the controlled propagation, augmentation and reintroduction of freshwater mussels (Mollusca: Bivalvia: Unionoida). *Freshwater Mollusk Biology and Conservation*, *10,* 1-12.

Meiri, S. (2011) Bergmann's Rule – what's in a name? *Global Ecology and Biogeography*, *20*, 203-207.

Millien, V., Kathleen Lyons, S., Olson, L., Smith, F.A., Wilson, A.B. & Yom-Tov, Y. (2006) Ecotypic variation in the context of global climate change: revisiting the rules. *Ecol Lett*, *9*, 853-69.

Mills, J. & Blodgett, D. (2017) *EflowStats: Hydrologic Indicator and Alteration Stats*. R package version 5.0.1

Morey, R.D. & Rouder, J.N. (2018) *BayesFactor: Computation of Bayes Factors for Common Designs*. R package version 0.9.12-4.2

Nelson, D., Benstead, J.P., Huryn, A.D., Cross, W.F., Hood, J.M., Johnson, P.W., Junker, J.R., Gislason, G.M. & Olafsson, J.S. (2017) Experimental whole-stream warming alters community size structure. *Glob Chang Biol, 23,* 2618-2628.

Neves, R.J. & Moyer, S.N. (1988) Evaluation of Techniques for Age Determination of Freshwater Mussels (Unionidae). *American Malacological Bulletin, 6,* 179-188.

Norkko, A., Villnäs, A., Norkko, J., Valanko, S. & Pilditch, C. (2013) Size matters: implications of the loss of large individuals for ecosystem function. *Scientific Reports, 3,* 2646.

Olalla-Tárraga, M.Á. (2011) "Nullius in Bergmann" or the pluralistic approach to ecogeographical rules: a reply to Watt et al. (2010). *Oikos*, *120,* 1441-1444.

Payne, B.S., Miller, A.C. & Shaffer, L.R. (1999) Physiological Resilience of Freshwater Mussels to Turbulence and Suspended Solids. *Journal of Freshwater Ecology*, *14,* 265-276.

Payton, S.L., Johnson, P.D. & Jenny, M.J. 2016. Comparative physiological, biochemical and molecular thermal stress response profiles for two unionid freshwater mussel species. *Journal of Experimental Biology, 219,* 3562-3574.

Piggott, J.J., Townsend, C.R. & Matthaei, C.D. (2015) Climate warming and agricultural stressors interact to determine stream macroinvertebrate community dynamics. *Glob Chang Biol*, *21,* 1887-906.

Plummer, M. (2003) JAGS: A program for analysis of Bayesian graphical models using Gibbs sampling. *Proceedings of the 3rd international workshop on distributed statistical computing* pp. 1-10.

Plummer, M. (2019) *rjags: Bayesian graphical models using MCMC*.R package version 4-10

Poff, N.L. & Allan, J.D. (1995) Functional-Organization of Stream Fish Assemblages in Relation to Hydrological Variability. *Ecology, 76,* 606-627.

Rollinson, N. & Rowe, L. 2018. Temperature-dependent oxygen limitation and the rise of Bergmann's rule in species with aquatic respiration. *Evolution, 72,* 977-988.

Rouder, J.N. & Morey, R.D. (2012) Default Bayes Factors for Model Selection in Regression. *Multivariate Behavioral Research*, *47,* 877-903.

Rypel, A.L. (2014) The cold-water connection: Bergmann's rule in North American freshwater fishes. *Am Nat*, *183,* 147-56.

Rypel, A.L., Haag, W.R. & Findlay, R.H. (2008) Validation of annual growth rings in freshwater mussel shells using cross dating. *Canadian Journal of Fisheries and Aquatic Sciences*, *65,* 2224-2232.

Rypel, A.L., Haag, W.R. & Findlay, R.H. (2009) Pervasive Hydrologic Effects on Freshwater Mussels and Riparian Trees in Southeastern Floodplain Ecosystems. *Wetlands*, *29,* 497-504.

Sansom, B.J., Atkinson, C.L. & Vaughn, C.C. (2016) Growth and Longevity Estimate for Mussel Population in Three Ouachita Mountain Rivers. *Freshwater Mollusk Biology and Conservation, 19,* 19-26.

Sardiña, P., Beardall, J., Beringer, J., Grace, M. & Thompson, R.M. (2016) Consequences of altered temperature regimes for emerging freshwater invertebrates. *Aquatic Sciences, 79,* 265-276.

Schneider, C.A., Rasband, W.S. & Eliceiri, K.W. (2012) NIH Image to ImageJ: 25 years of image analysis. *Nature Methods, 9,* 671-675.

Segura, C., Caldwell, P., Sun, G., McNulty, S. & Zhang, Y. (2015) A model to predict stream water temperature across the conterminous USA. *Hydrological Processes, 29,* 2178-2195.

Sheridan, J.A. & Bickford, D. (2011) Shrinking body size as an ecological response to climate change. *Nature Climate Change, 1,* 401-406.

Smith, F.A. & Lyons, S.K. (2013) *Animal body size: linking pattern and process across space, time, and taxonomic group*. University of Chicago Press.

Spooner, D.E. & Vaughn, C.C. (2008) A trait-based approach to species' roles in stream ecosystems: climate change, community structure, and material cycling. *Oecologia, 158,* 307-17.

Stillwell, R.C. (2010) Are latitudinal clines in body size adaptive? *Oikos*, *119,* 1387-1390.

Strayer, D.L., Geist, J., Haag, W.R., Jackson, J.K. & Newbold, J.D. (2019) Essay: Making the most of recent advances in freshwater mussel propagation and restoration. *Conservation Science and Practice*, 1

Turvey, S.T. & Blackburn, T.M. (2011) Determinants of species abundance in the Quaternary vertebrate fossil record. *Paleobiology*, *37*, 537-546.

U. S. Geological Survey [USGS] (2016) National Water Information System data available on the World Wide Web (USGS Water Data for the Nation), accessed February 04, 2020, at URL [http://waterdata.usgs.gov/nwis/].

U. S. Geological Survey [USGS] (2019) National Hydrography Dataset Plus. (ver. USGS National Hydrography Dataset Best Resolution (NHD)), accessed February 04 , 2020 at URL [https://www.usgs.gov/core-science-systems/ngp/national-hydrography/access-national-hydrography-products]

Vigliola, L. & Meekan, M.G. (2009) The Back-Calculation of Fish Growth From Otoliths. In: Green B.S., Mapstone B.D., Carlos G., Begg G.A. (eds) Tropical Fish Otoliths:

Information for Assessment, Management and Ecology. Reviews: Methods and Technologies in Fish Biology and Fisheries, vol 11. Springer, Dordrecht

Villar, C.H. & Naya, D.E. (2018) Climate change and temporal trends in body size: the case of rodents. *Oikos, 127*, 1186-1194.

Vinarski, M.V. (2014) On the applicability of Bergmann's rule to ectotherms: The state of the art. *Biology Bulletin Reviews*, *4,* 232-242.

Vischer, N. & Nastase, S. (2020) *ObjectJ: Non-destructive marking and linked results plugin for ImageJ*. University of Amsterdam.version 1.04x

TABLES

Table 1-1. Mussel shells from 5 biogeographic provinces, 14 rivers and 28 sites were thin-sectioned to generate length at age data for two different mussel clades. APLI indicates *A. plicata*, LCAR indicates *L. cardium,* and LORN indicates *L. ornata*.

Biogeographic Province	River	Sites	Species
Interior Highlands	Kiamichi River	K2, KT, K4, KS, K7	APLI, LCAR
	Little River	LY	APLI, LCAR
Mobile Basin	Sipsey River	Barry, Wendell3, MusselMania, Wendell2	APLI, LORN
St Lawrence-Great Lakes	French Creek	Samson	APLI
	Grand River	Lyons	LCAR
Upper Mississippi	Big River	41-O, MO41, 51-C	APLI
	Elk Fork Salt River	James	APLI
	Illinois River	Florence	APLI
	Iroquois River	Iroquois	LCAR
	Kishwaukee River	Kishwaukee	LCAR
	Mississippi River	MS1, Illiniwek, Eagle, Upstream, Sylvan	APLI, LCAR
	Saint Croix River	STF, Hudson	APLI, LCAR
Western Gulf	Colorado River	Stok	APLI
	Guadalupe River	Dewitt	APLI

Table 1-2. Sample information and von Bertalanffy growth parameters from each site. N represents the number of unique shells (from individual mussels) included in the analysis. Total annuli are the number of annuli identified and thus total observations of lengths at age for that site and species. The intercept and slope describe the line between shell length and shell width used to estimate shell length from back-calculated length at age observations. Adjusted R^2 for all length-width regressions were greater than 0.898. COFECHA removes age related growth using a cubic spline; the spline that resulted in the highest interseries correlation is reported. -- indicates only one shell was sectioned for that species from that site. Median values from the posterior distribution of the von Bertalanffy growth equation are reported. Parameters of the von Bertalanffy growth equation are: L_∞ (the potential maximum length), K (the growth characteristic), and T0 (size at age 0).

Site	Long.	Lat.	N	Total Annuli	Intercept	Slope	Cubic Spline	Interseries Correlation	Median L_∞	Median K	Median T0
Amblema plicata											
Dewitt	-97.31	29.33	6	59	0.23	1.33	41	0.371	92.4	0.115	-2.29
Stok	-96.42	29.58	9	112	-2.85	1.45	32	0.573	99.9	0.178	-0.97
Wendell2	-88.04	33.04	1	2	0.00	1.19	--	--	104.4	0.383	-1.69
MusselMania	-87.98	33.08	4	58	-1.60	1.29	9	0.272	94.8	0.095	-2.23
Wendell3	-87.96	33.09	6	76	-0.85	1.34	3	0.401	91.7	0.125	-1.84
LY	-94.73	33.95	4	57	-6.51	1.51	8	0.352	97.4	0.082	1.26
K7	-95.58	34.43	2	39	0.40	1.29	7	0.304	104.4	0.100	-2.42
KS	-95.50	34.51	3	50	-1.33	1.30	7	0.447	78.6	0.150	-2.37

K4	-95.34	34.57	1	15	0.83	1.20	--	--	82.9	0.602	-2.22
KT	-95.35	34.57	4	46	-0.37	1.30	44	0.378	124.4	0.048	-2.08
K2	-95.06	34.65	5	89	-3.14	1.36	33	0.541	84.0	0.128	-2.46
51-C	-90.59	38.42	4	82	-1.18	1.49	44	0.281	114.6	0.101	-2.46
MO41	-90.59	38.44	6	116	-2.87	1.49	41	0.176	151.4	0.049	-2.15
41-O	-90.60	38.45	5	85	-5.75	1.54	30	0.336	141.9	0.073	-2.24
James	-92.07	39.43	2	42	0.89	1.40	4	0.402	119.0	0.145	1.24
Florence	-90.61	39.63	9	165	-1.56	1.38	7	0.415	173.2	0.033	-1.32
Sylvan	-90.51	41.51	6	109	-1.39	1.32	3	0.439	104.0	0.073	0.35
Upstream	-90.46	41.52	1	16	-1.21	1.24	--	--	120.8	0.089	-2.17
Eagle	-90.44	41.55	4	87	-1.02	1.25	31	0.364	136.6	0.039	0.15
Illiniwek	-90.40	41.57	2	35	-0.37	1.32	21	0.155	97.1	0.073	-2.24
Samson	-79.98	41.85	7	129	-1.53	1.43	28	0.376	114.3	0.143	-2.17
MS1	-93.19	44.90	2	43	0.58	1.31	24	0.476	95.4	0.136	-2.11
Hudson	-92.77	44.97	16	359	-7.71	1.43	24	0.239	145.1	0.015	-1.49
STF	-92.66	45.40	5	123	-0.43	1.30	2	0.218	114.7	0.053	-2.32

Lampsilis cardium

LY	-94.73	33.95	2	13	0.13	1.40	10	0.882	108.7	0.296	-1.84
K7	-95.58	34.43	3	20	0.29	1.27	10	0.876	87.9	0.513	-1.96
KS	-95.50	34.51	2	14	0.00	1.39	9	0.890	86.3	0.409	0.09
KT	-95.35	34.57	6	39	0.75	1.29	42	0.330	99.2	0.515	-1.46
Iroquois	-87.74	40.79	8	63	-2.87	1.51	2	0.233	131.6	0.213	-1.72
Sylvan	-90.51	41.51	1	9	0.00	1.48	--	--	104.8	0.645	1.64
Eagle	-90.44	41.55	3	29	7.89	1.08	10	0.741	106.2	0.443	-1.00
Kishwaukee	-88.94	42.25	22	259	5.67	1.33	20	0.518	110.0	0.350	-2.11
Lyons	-84.95	42.99	16	112	-0.49	1.52	6	0.330	123.6	0.256	-1.92
MS1	-93.19	44.90	9	112	1.18	1.46	34	0.554	123.1	0.271	-2.02
Hudson	-92.77	44.97	5	52	0.12	1.35	19	0.465	109.9	0.416	-1.64
STF	-92.66	45.40	8	60	0.00	1.43	9	0.607	106.5	0.443	-1.41

Lampsilis ornata

Wendel2	-88.04	33.04	1	6	0.00	1.27	--	--	78.1	0.653	-2.20
MusselMania	-87.98	33.08	2	19	-0.61	1.40	15	0.859	94.1	0.555	-2.32
Wendel3	-87.96	33.09	7	29	0.61	1.26	37	0.556	85.9	0.762	-1.03
Barry	-87.87	33.14	1	9	0.00	1.26	--	--	92.3	0.453	2.34

Table 1-3. Climatic variables used in the model comparison. Variable type 'characteristics' are from the NHDPlus. Discharge and velocity are also from the NHDPlus; all other flow characteristics are derived from USGS daily flow data. 'Temperature' variables are derived through prediction with NOAA air temperatures. Units are within parenthesis in the definition.

Variable	**Definition**
Stream Characteristics	
Drainage Area	Natural logarithm of the total upstream cumulative drainage area (km^2)
Stream Order	Modified Strahler stream order
Elevation	Minimum stream elevation (m)
Stream Slope	Change in smooth elevation over the length of the stream segment (m/m)
Precipitation	Catchment precipitation, based on PRISM data from 1971 to 2000 (cm)
Land Cover	
Forest	Deciduous, evergreen, and mixed forest within 100 m of the site location (%)
Urban	High, medium, low, and open space development within 100 m of the site location. (%)
Cultivated Crops	Percentage of cultivated crops within 100 m of the site location. (%)
Hay Pasture	Percentage of pastureland within 100 m of the site location. (%)
Temperature	
Average Water Temperature	Predicted from the average annual air temperature from weather stations within the watershed using eq. 7 & eq. 8 (°C)
Maximum Water Temperature	Predicted from the average annual maximum air temperature from weather stations within the watershed using eq. 7 & eq. 8 (°C)
Flow	
Discharge	Flow from gage adjustment (cfs), estimated from the enhanced unit runoff method based on data from 1971-2000
Velocity	Velocity from gate adjustment (feet per second), estimated from the enhanced unit runoff method based on data from 1971-2000

Median Daily Flow	Median of the daily mean flow values for the entire discharge record (cfs)
Daily Flow Variability	Mean annual coefficient of variation of daily flows (percent)
Monthly flow variability	Maximum monthly flow – minimum monthly flow / mean monthly flow (dimensionless)
May – August monthly low flows	Mean monthly minimum flow across all years; each month represents one variable (cfs)
May – August monthly high flows	Mean monthly maximum flow across all years; each month represents one variable (cfs)
Minimum flows	Median annual minimum flows (dimensionless)
Base Flow	The ratio of minimum annual flow to mean annual flow for each year (percentage)
Low flood pulse count	Average number of low flow events. Low flow event defined by flows less than the 25^{th} percentile of the flow record (number of events)
High flood pulse count	Average number of high flow events. High flow event defined by flows less than the 75^{th} percentile of the flow record (number of events)
Low flow pulse duration	Average length of a low flow event (days/year)
High flood pulse duration	Average length of a high flow event (days/year)
Reversals	Number of days where the change in flow from one day to the next changes direction (so from falling water to rising and vice versa)
Summer low flow	Mean of the mean monthly low flow from May to August (cfs)
Summer high flow	Mean of the mean monthly high flow from May to August (cfs)

FIGURES CAPTIONS

Figure 1-1. Diagram of mussel shell anatomy and species (A) and depiction of thin-sectioning products from one shell (B). The umbo represents the oldest part of the shell while the ventral margin is actively growing when the animal is alive. Umbos can erode due to both sediment movement and acidic waters. When thin-sectioning, we created a radial thin-section from the umbo to the ventral margin, aiming for perpendicular cuts across outer annuli while avoiding sculpturing. The diagonal across the shell in (B) represents the typical position of this cut. The composite image of the slide-mounted thin-section is displayed with reference to the umbo (and earliest annuli) and the ventral margin (with most recent growth). Closer examination of the composite reveals the three layers of the shell: the leathery periostracum, the prismatic where annuli are measured (demonstrated), and the nacreous inner layer.

Figure 1-2. Map of sites (black dots), associated rivers, and the watersheds from which shells were collected. Watershed color shows the mussel biogeographic province according to Haag (2010). A seventh-order river is represented in dark grey. Code is from the *R* package *hydroMap* (DeCicco & Blodgett, 2017)

Figure 1-3. Variation in *Lampsilis* spp. (A) and *A. plicata* (B) potential maximum length across latitude and at different sites. There was large variation in L_∞ among sites and species at the same site (C). Points represent the posterior median, larger lines represent the 50% credible interval, and the thin line represents the 90% credible interval. The color bar on the x-axis of (C) represents the different bioregions encompassed by the sites (Figure 2). The graph was made with code from the *R* package *bayesplot* (Gabry & Mahr, 2019)

Figure 1-4. *Amblema plicata* and *Lampsilis* spp. L_∞ exhibited positive relationships with latitude. (A) displays the species-specific posterior distributions of the slope from a regression with no intercept relating L_∞ and latitude. Points represent the posterior median, larger lines represent the 50% credible interval, and the thin line represents the 90% credible interval. (B) represents the posterior distribution of the difference between *A. plicata's* slope and *Lampsilis* spp.'s slope. Based on our data, there is a 75% probability that *A. plicata*'s slope is slightly smaller than *Lampsilis* spp.'s slope. The graph was made with code from the *R* package *bayesplot* (Gabry & Mahr, 2019)

Figure 1-5. Evidence for potential drivers between mussel maximum size and climatic variables.
Figure 1-5. Evidence for potential drivers between mussel maximum size and climatic variables.Evidence for potential drivers between mussel maximum size and climatic variables. The x-axis represents the Bayes Factor -1 to improve interpretation; a negative Bayes Factors mean there is more evidence for the null hypothesis while a positive Bayes Factors indicate there is more evidence for the alternative hypothesis.

Figure 1-6. Direction of the association between exploratory climatic variables and potential maximum length. (A) represents the posterior distribution of the top models' coefficients in each variable category from the model comparison (Figure 1-5). The coefficient from 'Minimal Flows' is divided by 10 to facilitate interpretation of other coefficients. (B-E) represents the data input into each model and a line of best fit (linear regression). Minimum flows represent the median of the lowest flow magnitude divided by the median flow magnitude; values closer to 0

represent more extreme variance between normal and low flow, while values closer to 1 represent more steady flow.

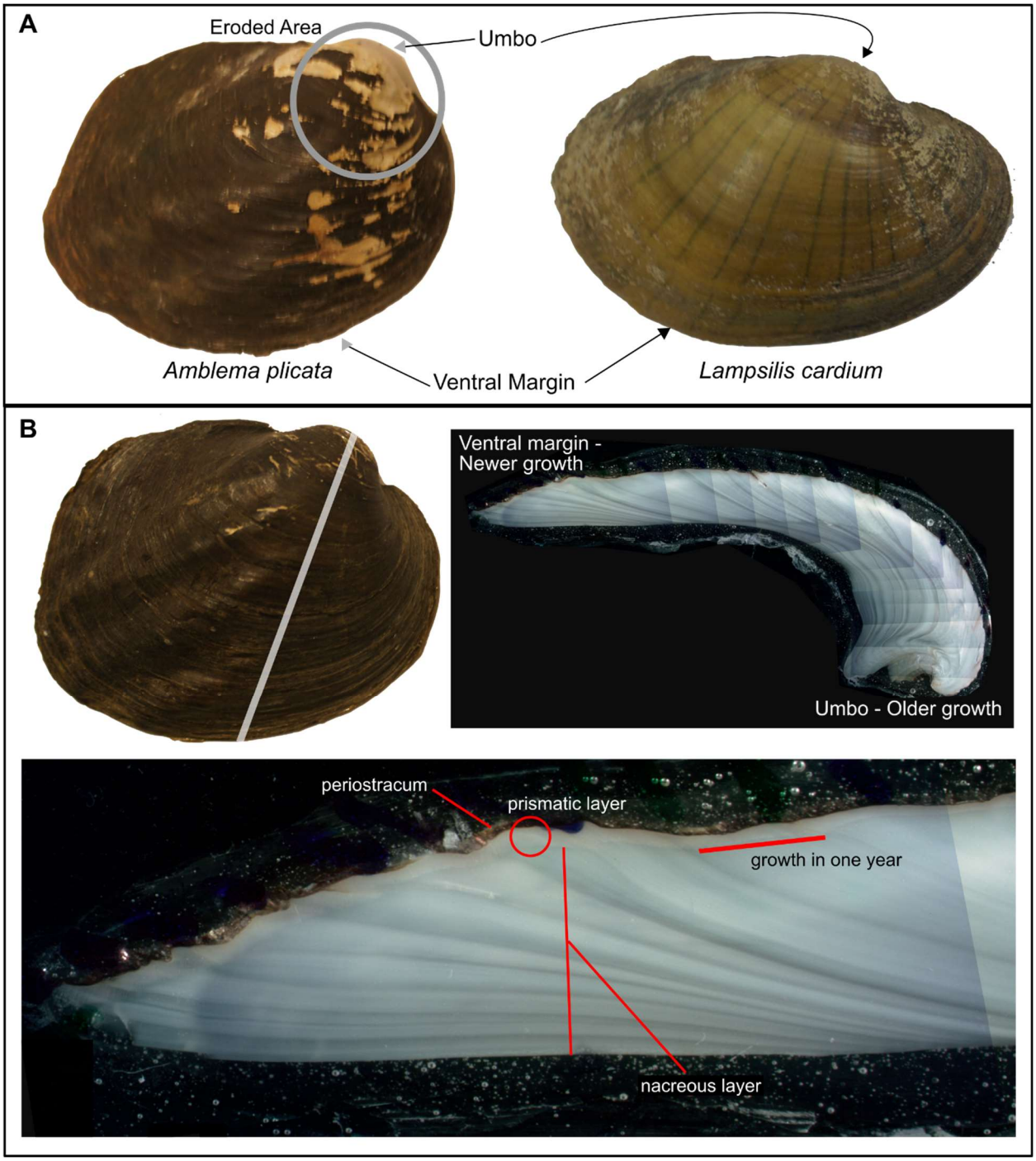

Figure 1-1. Diagram of mussel shell anatomy and species

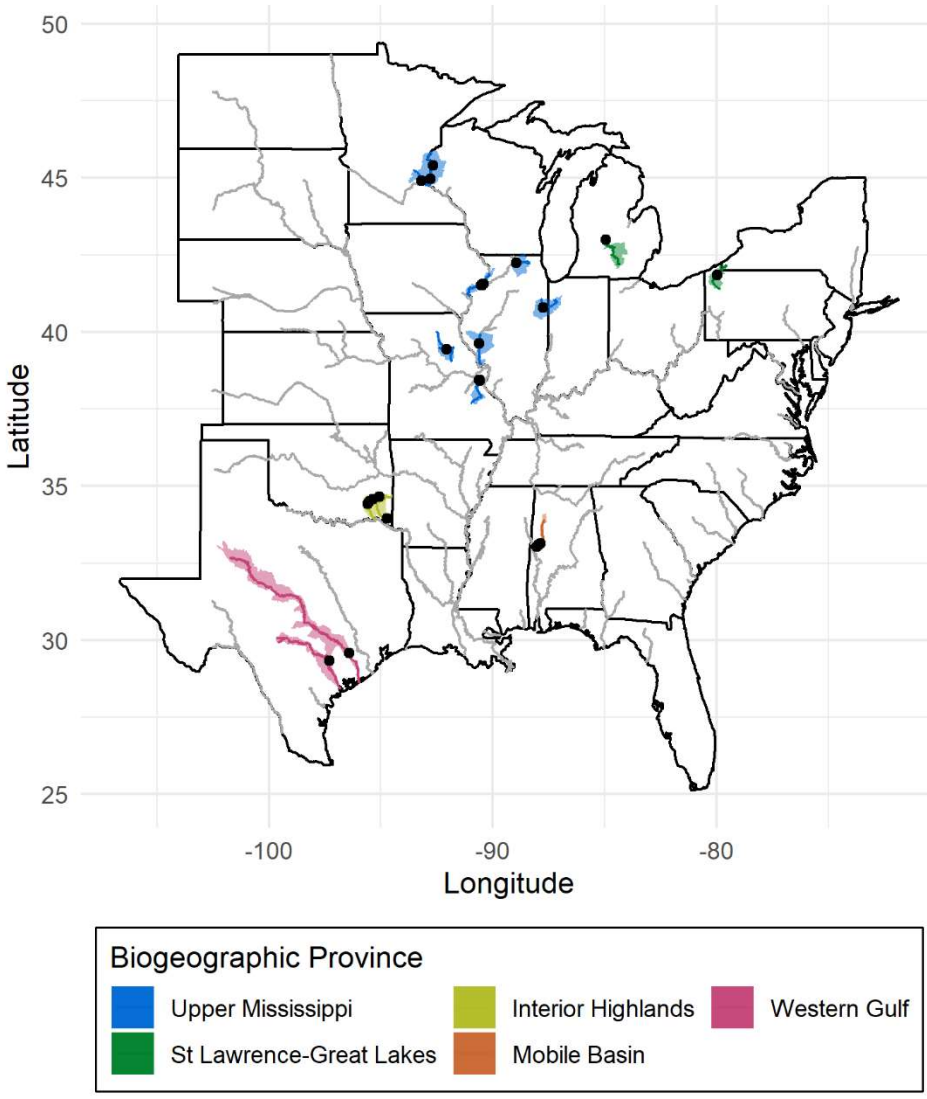

Figure 1-2. Map of sites (black dots), associated rivers, and the watersheds from which shells were collected.

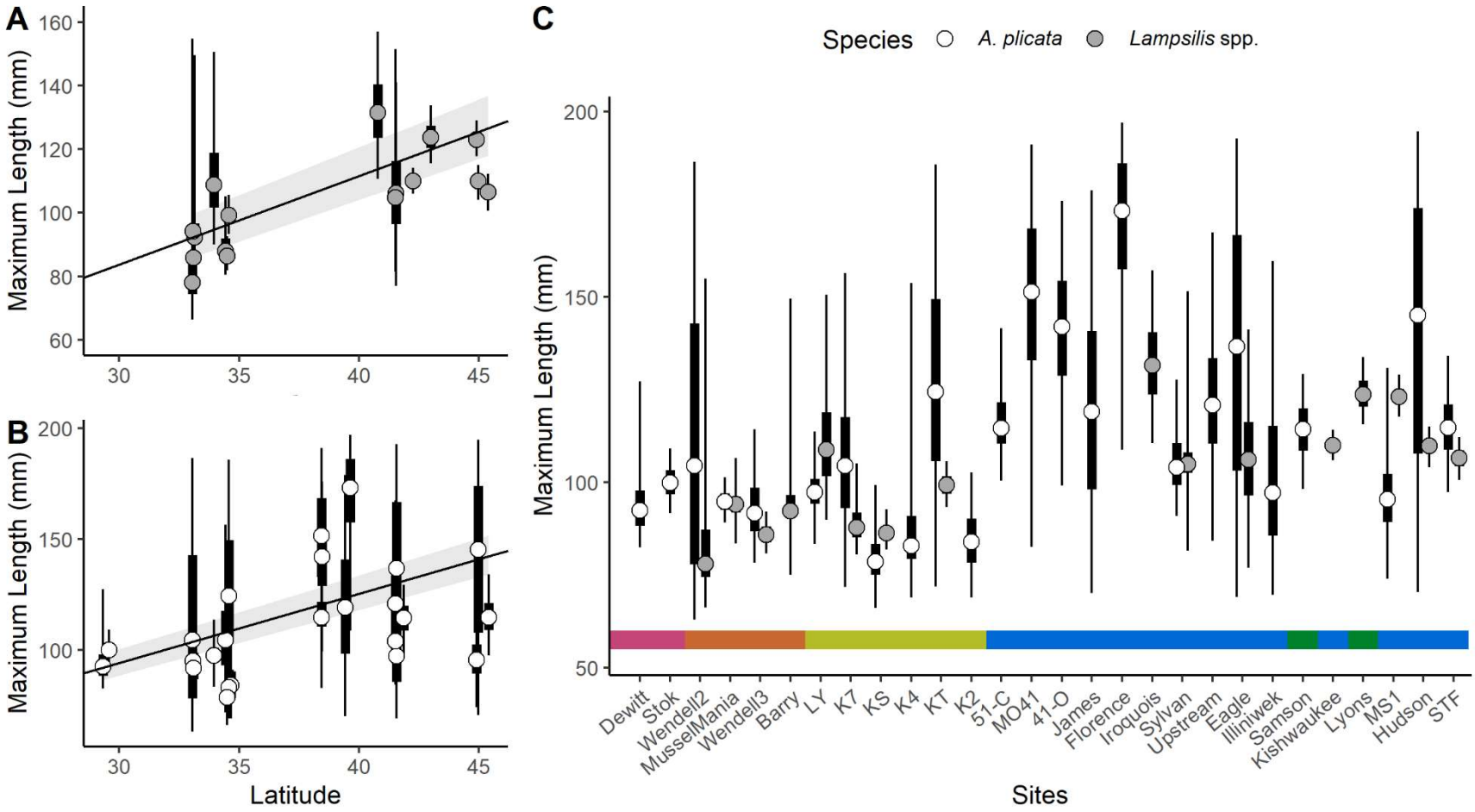

Figure 1-3. Variation in *Lampsilis* spp. (A) and *A. plicata* (B) potential maximum length

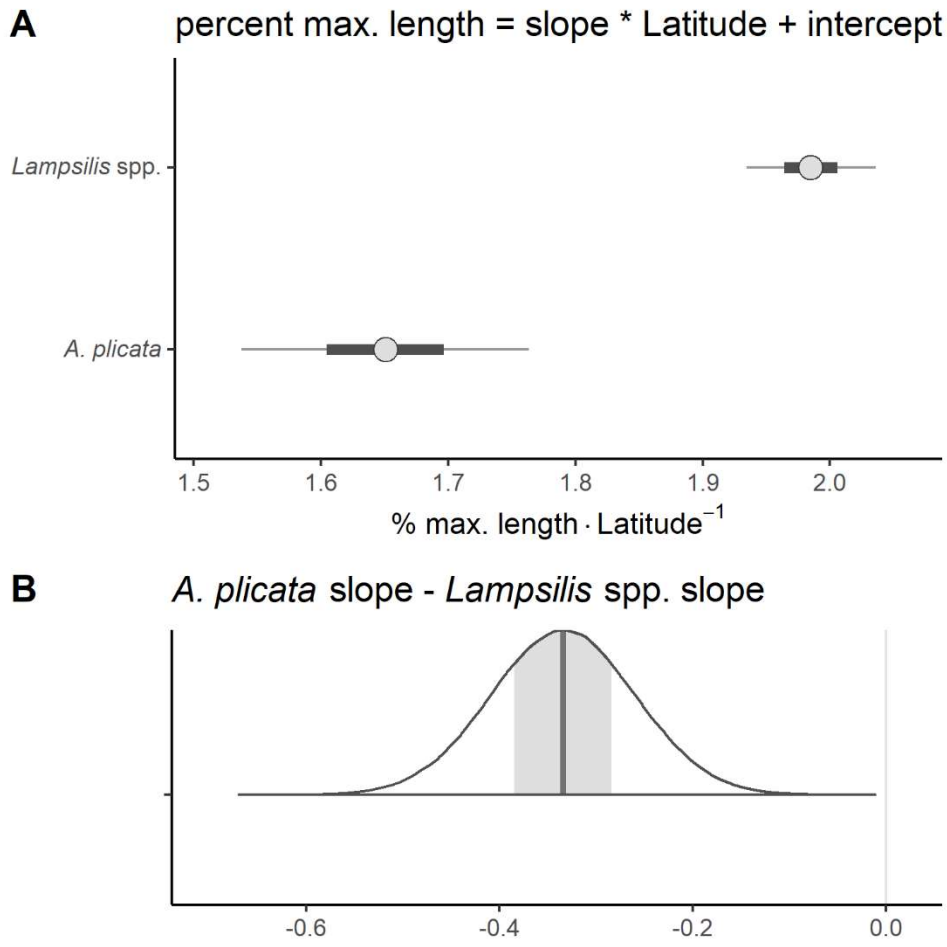

Figure 1-4. *Amblema plicata* and *Lampsilis* spp. L∞ exhibited positive relationships with latitude.

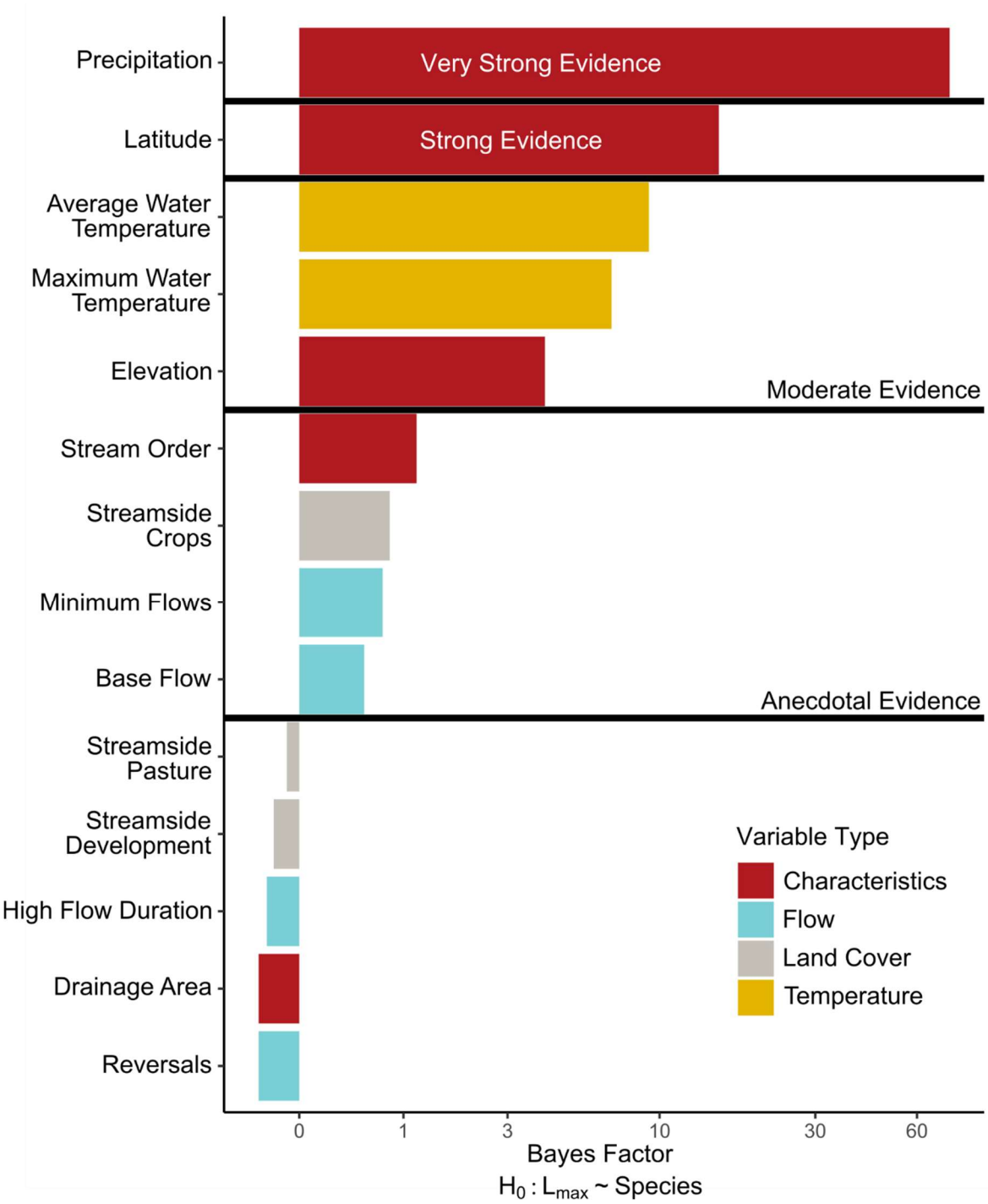

Figure 1-5. Evidence for potential drivers between mussel maximum size and climatic variables.

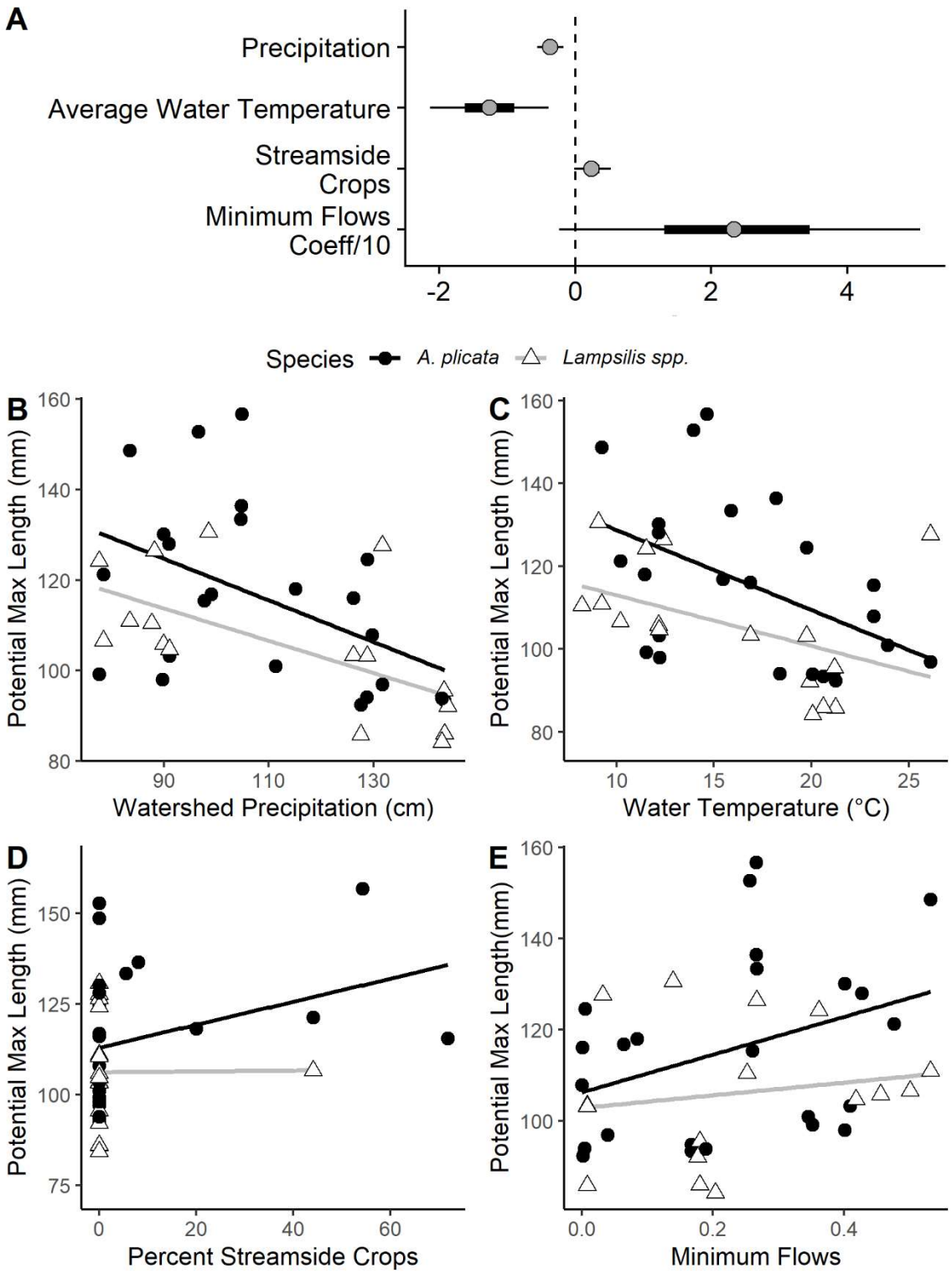

Figure 1-6. Direction of the association between exploratory climatic variables and potential maximum length.

APPENDIX

Table 1-A1. Results from a bootstrapped linear model to assess the direction and statistical significance of each species relationship with latitude. As with the Bayesian regression model, we use percent maximum length to account for different sizes among the taxa; thus this slope has the units Percent maximum length·Latitude^{-1}. After resampling the linear model 1000 times, we report the mean and 95% confidence intervals for each coefficient in the model, the p value, and the R^2 for the linear model. These results do not contradict the results found from the Bayesian regression analysis within the results above. There is overlap between *A. plicata*'s slope and *Lampsilis* spp.'s slope.

Variable	**Mean [95% confidence intervals]**
Intercept	1.385 [-8.32, 34.12]
A. plicata's slope	1.349 [0.765, 2.004]
Lampsilis spp.'s slope	1.688 [1.174, 2.303]
R^2	47.2 % [17.7, 66.0]
p value	$7.28 \cdot 10^{-6}$ [0.000, 0.018]

Table 1-A2. USGS gages and HUC 8 areas used to derive the input values for the exploratory model comparison. Included are the four highest predictors within each variable category (precipitation (cm), annual mean water temperature (°C), cultivated crops (%), and minimum flows). Minimum flows and annual mean water temperature are the average value at that site for the two species. Drainage area represents the natural logarithm of cumulative watershed area (km^2).

Site	Long.	Lat.	HUC 8	USGS Gage	Drainage Area	Precipitation (cm)	Annual Mean Water Temperature (°C)	Cultivated Crops (%)	Minimum Flows
Dewitt	-97.31	29.33	12100202	8175800	9.26	97.7	23.2	71.9	0.26
Stok	-96.42	29.58	12090302	8161000	11.48	111.3	23.9	0.0	0.35
Wendell2	-88.04	33.04	03160107	2446500	7.54	143.0	0.0	0.0	0.00
MusselMania	-87.98	33.08	03160107	2446500	7.47	143.4	21.2	0.0	0.17
Wendell3	-87.96	33.09	03160107	2446500	7.46	143.5	0.0	0.0	0.00
Barry	-87.87	33.14	03160107	2446500	7.37	144.1	19.9	0.0	0.18
LY	-94.73	33.95	11140107	7338500	8.12	131.6	26.1	0.0	0.04
K7	-95.58	34.43	11140105	7335790	7.64	126.1	16.9	0.0	0.00
KS	-95.50	34.51	11140105	7335790	7.60	127.5	21.2	0.0	0.01
K4	-95.34	34.57	11140105	7335790	7.54	128.6	18.4	0.0	0.00
KT	-95.35	34.57	11140105	7335790	7.54	128.7	19.8	0.0	0.01
K2	-95.06	34.65	11140105	7335700	6.72	129.7	23.2	0.0	0.00

51-C	-90.59	38.42	07140104	7018500	7.82	104.7	15.9	5.6	0.27
MO41	-90.59	38.44	07140104	7018500	7.82	104.8	14.6	54.3	0.27
41-O	-90.60	38.45	07140104	7018500	7.82	104.7	18.2	8.1	0.27
James	-92.07	39.43	07110006	5506800	6.36	99.0	15.4	0.0	0.06
Florence	-90.61	39.63	07130011	5586100	11.15	96.6	13.9	0.0	0.26
Iroquois	-87.74	40.79	07120002	5525000	7.56	98.5	9.1	0.0	0.14
Sylvan	-90.51	41.51	07080101	5420500	12.33	91.1	12.2	0.0	0.41
Upstream	-90.46	41.52	07080101	5420500	12.33	90.9	12.1	0.0	0.43
Eagle	-90.44	41.55	07080101	5420500	12.33	89.9	12.2	0.0	0.43
Illiniwek	-90.40	41.57	07080101	5420500	12.33	89.8	12.2	0.0	0.40
Samson	-79.98	41.85	05010004	3021520	6.95	115.1	11.4	20.0	0.08
Kishwaukee	-88.94	42.25	07090006	5438500	7.40	87.7	8.2	0.0	0.25
Lyons	-84.95	42.99	04050004	4116000	8.43	88.2	12.4	0.0	0.27
MS1	-93.19	44.90	07010206	5331000	10.84	77.7	11.5	0.0	0.36
Hudson	-92.77	44.97	07030005	5341550	9.83	83.5	9.2	0.0	0.53
STF	-92.66	45.40	07030005	5340500	9.66	78.5	10.2	44.1	0.49

Figure 1-1A. Correlations between exploratory variables in the model comparison. A Pearson's product-moment correlation test was conducted to assess the direction and magnitude of the correlation between the two variables. In (A), the natural logarithm of drainage area (km^2) is positively correlated with stream order with $t_{26} = 7.40$, $p < 0.001$, $r = 0.82$. In (B), the natural logarithm of drainage area (km^2) is negatively correlated with catchment precipitation (cm) with $t_{26} = -3.70$, $p = 0.001$, $r = -0.58$. In (C), decimal degree latitude is negatively correlated with catchment precipitation (cm) with $t_{26} = -6.53$, $p < 0.001$, $r = -0.79$. The two outlier points in (C) are from west-central Texas.

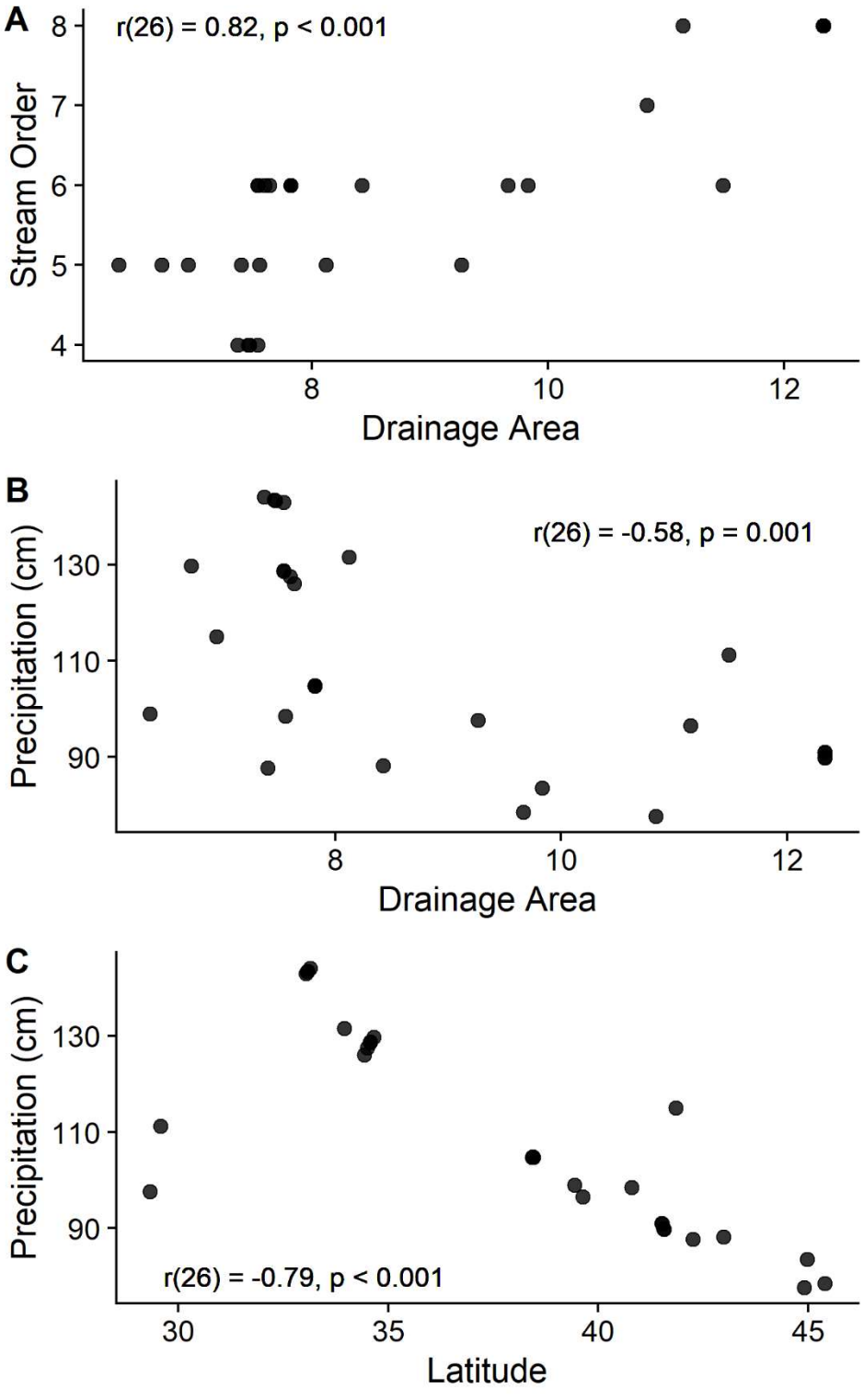
A
r(26) = 0.82, p < 0.001
Stream Order
8
7
6
5
4
8
10
12
Drainage Area
B
r(26) = -0.58, p = 0.001
Precipitation (cm)
130
110
90
8
10
12
Drainage Area
C
Precipitation (cm)
130
110
90
r(26) = -0.79, p < 0.001
30
35
40
45
Latitude

CHAPTER 2 FRESHWATER MUSSELS ENGINEER MACROINVERTEBRATE HABITAT THROUGH DIFFERENT MECHANISMS AT DIFFERENT SPATIAL SCALES

Keywords:

ecosystem engineer, facilitation, spatial scale, context dependence

Formatted for publication in *Oecologia*

DuBose, TP, Vaughn, CC, Hopper, GW, Gido, KB, and Parr, TB. In prep. Freshwater mussels engineer macroinvertebrate habitat through different mechanisms at different spatial scales

ABSTRACT

Ecosystem engineers alter habitat and resource availability within ecosystems, which benefits other organisms, but these effects often depend on abiotic context and spatial scale. We used stream-dwelling freshwater mussels to explore how the mechanisms by which organisms engineer ecosystems might shift with spatial scale and environmental context. We combined a comparative field study and field enclosure experiment to measure mussel and macroinvertebrate community structure, discharge, substrate heterogeneity, and chlorophyll *a* concentration across three spatial scales: mussel shells (~10 cm^2), enclosures (~0.25 m^2) and stream reaches (~1,000 m^2). We used canonical correspondence analysis and variation partitioning to evaluate how mussel abundance, food availability (measured as chlorophyll *a* concentration), substrate heterogeneity, and flow (discharge) influenced macroinvertebrate community structure. At the larger, stream reach scale, macroinvertebrate community structure was primarily controlled by flow and secondarily by food availability. At the mussel-shell scale, macroinvertebrate communities were controlled by the presence of live mussels (rather than mussel shells alone), likely due to mussel-derived food availability. At the reach and enclosure scale, caddisfly larvae and pupae were more common in areas with higher mussel biomass. While chlorophyll *a* was a statistically significant variable at the reach scale, live mussel shells better predicted macroinvertebrate community structure at the shell scale. Mussel movement, biodeposits, or leathery shell surface are likely contributing to macroinvertebrate abundance above the variation explained simply by chlorophyll *a* concentration. Understanding at what spatial scale and by which potential mechanism ecosystem engineers' effect co-occurring animals is important to protect ecosystem function in the face of global change.

INTRODUCTION

Ecosystem engineers alter habitat and resource availability in ecosystems through their behavior, physiology, feeding and growth (Jones et al. 1997). Differences between engineered and non-engineered patches modulates the effect ecosystem engineers have on communities (Jones et al. 1997; Wright et al. 2002). Engineer density, temporal scale, spatial scale and heterogeneity, and abiotic context all influence the difference between engineered and not-engineered patches; thus, ecosystem engineering is context dependent (Coggan et al. 2018; Crain and Bertness 2006). For example, the heterogeneity of shading leads to larval midges in lakes increasing or decreasing net ecosystem production (completed by algae within their tubes and on which they feed) based on light abundance (Phillips et al. 2019). An organism's size, aggregation preference, movement behavior, and dispersal ability dictate their ecosystem engineering effect at different spatial scales (Wright et al. 2002). Thus, the interaction of spatial scale and abiotic factors determines the magnitude of how an organism engineers its surrounding habitat.

Across marine and freshwater ecosystems, bivalves act as ecosystem engineers through their burrowing and filter-feeding activities, the creation of habitat through their hard shell, and their relatively sedentary lifestyles where they live within dense uni- or multispecies aggregations of other bivalves (Vaughn and Hoellein 2018). Aggregations of marine bivalves create a 'facilitation landscape', where beneficial habitats for other organisms are heterogeneously located due to both positive and negative interactions with mussels. Marine bivalves alter the spatial distribution of basal resources through habitat creation from their shells (Donadi et al. 2013; Engel et al. 2017). Marine mussel recruitment and cockle densities are dependent upon the interplay between predation pressure, habitat modification, and intra-guild competition for food resources (Donadi et al. 2013; van der Heide et al. 2014). Just as marine

bivalves' impact on their habitat and thus co-occurring macroinvertebrates shifts with space, we expect freshwater bivalves' impact on macroinvertebrates also to shift (Figure 2-1A).

Freshwater mussels (Bivalvia: Unionoida; hereafter mussels) are sedentary, filter-feeding bivalves that act as ecosystem engineers (Gutiérrez et al. 2003; Vaughn and Hoellein 2018). Mussels are often congregated in dense, diverse, and heterogeneous patches that are hydrologically stable within a river (Sansom et al. 2018; Strayer 1999). Mussels create habitat, alter sediment characteristics, and change near-bed hydrology through their hard shells and activity (Allen and Vaughn 2011; Goodding et al. 2019; Sansom et al. 2017). Mussels also function as nutrient capacitors that transfer nutrients from the water column to the benthos (Strayer 2014). They store nutrients in their soft tissue and shells, remineralize and excrete inorganic nutrients, and biodeposit organic nutrients (feces and pseudo-feces) (Atkinson et al. 2017). Because mussels comprise a high proportion of biomass in streams, their storage and transfer of nutrients influences how nutrients move downstream, depending on ambient nutrient limitation (Atkinson and Vaughn 2015; Spooner et al. 2013). Through habitat provisioning and nutrient regeneration, mussels often increase the biomass and alter the composition of benthic algal communities (Atkinson et al. 2013; Spooner and Vaughn 2012; Vaughn et al. 2008; Vaughn et al. 2007), which benefits macroinvertebrates that use this resource. Mussels' creation of habitat directly facilitates some macroinvertebrates while their regulation of food resources indirectly affects others (Atkinson et al. 2018a).

Mussels have been shown to have a variety of effects on benthic macroinvertebrates, from increasing their abundance and richness, to no effects at all. In combination, these studies suggest that effects mussels have on macroinvertebrates are determined by the strength of the gradient between mussel-engineered patches and non-engineered patches, which varies with

spatial scale. Mussel-derived habitat, such as living mussels' shells, typically harbor increased basal food resources and thus more grazing macroinvertebrates (Spooner et al. 2012), although the increase in grazers could represent a shift in functional groups instead of differences in abundance between mussel-derived habitat and stream sediments (Spooner and Vaughn 2006; Vaughn et al. 2008). When considering within-reach patches (sub-meter samples, hereafter enclosures), some studies found macroinvertebrate abundance was higher near live mussels (Spooner and Vaughn 2006; Vaughn and Spooner 2006), while others found no difference between control and mussel enclosures (Howard and Cuffey 2006). At the larger, reach scale, studies have also produced contradicting conclusions. While some studies found mussel presence and biomass increases macroinvertebrate abundance and diversity at the stream reach scale and in lakes (Aldridge et al. 2007; Chowdhury et al. 2016; Vaughn and Spooner 2006), others found no relationship between mussels and total macroinvertebrate abundance (Richter et al. 2016; Simeone et al. 2018). In some studies, mussel richness and mussel species identity does not alter macroinvertebrate taxon richness (Aldridge et al. 2007; Spooner and Vaughn 2006); in others, mussels increase nonbiting midge larva (Chironomidae) abundance (Spooner et al. 2012). As ecosystem engineers are notoriously context and spatial scale dependent, we posit that contradictions in the literature are evidence of mussels' engineering mechanism and magnitude shifting across space and environmental contexts.

Here we introduce a conceptual figure to describe how two engineering effects by freshwater mussels shift at different spatial scales (Figure 2-1A). We suggest that the mechanism that causes the largest difference between engineered and non-engineered patches will drive macroinvertebrate community structure. Mussels mitigate two potential stressors for macroinvertebrates: flow (which can cause downstream displacement) and food limitation. At

small spatial scales (~10 cm^2), such as on the mussel shell, bed roughness increased by mussel shells is counteracted by mussel burrowing and movement (Allen and Vaughn 2011; Sansom et al. 2017). At moderate scales (such as ~0.25 m^2 enclosures), mussels' hard shells and filtration alter near bed hydrodynamics by increasing bed roughness and thus decreasing near bed velocity (Allen and Vaughn 2010; Sansom et al. 2017). This reduction in near bed velocity helps mussels stay in the sediment rather than being dislodged during floods. In these patches, sediment is larger and more homogenous than patches without mussels (Koerner, 2018). At the stream reach scale, mussel distribution and abundance are constrained by both high and low flows. At high flows, mussels require shear stresses and substrate heterogeneity that prevent dislodgement (Allen and Vaughn 2010; Randklev et al. 2019). At low flows, they need to be in wetted, flowing habitat because of their inability to move very far to escape declining water levels (Atkinson et al. 2014a; Gough et al. 2012). Because of these ecological requirements, at large spatial scales (such as a ~1,000 m^2 river reach) mussel abundance should be correlated with stream flow. As mussels don't alter large-scale flow patterns, the difference between mussel beds and non-engineered patches is dependent upon the hydrological context (such as floods, normal flow, and drought). As such, we predict that the mussel-derived flow modulation will be highest at moderate spatial scales. Mussels affect basal resources at each of these spatial scales through their consumption of seston, habitat provisioning for biofilms (aggregations of heterotrophic and photosynthetic microbes), and alleviation of nutrient limitation (Vaughn et al. 2008; Atkinson et al. 2014b). Mussel shells provide habitat for biofilms and thus can greatly increase food availability compared to near-by rocks (Spooner et al. 2013). At the enclosure scale, mussels' influence on nutrient limitation can increase food resources near freshwater mussels while mussel shells continue to provide habitat for biofilms. At the reach scale, basal resources become

more diffuse and are constrained by factors unrelated to mussels (namely shading and flow). As such, we predict that the influence of mussels on food resources will be highest at small spatial scales and will decrease with increasing spatial scale. Based on these insights, we predict that the mechanism by which mussels facilitate macroinvertebrate shifts in identity and magnitude based upon spatial scale (Figure 2-1).

To evaluate these predictions, we asked how mussels impact macroinvertebrate communities at three spatial scales: on mussel shells, at the enclosure scale, and at the stream reach scale. We measured mussel abundance, macroinvertebrate communities, and environmental measurements in a field survey and a field enclosure experiment. We then quantified how mussel biomass was related to macroinvertebrate density, taxonomic richness, and Simpsons diversity index. We used canonical correspondence analyses to evaluate which environmental variables were correlated with macroinvertebrate taxa and how those environmental variables correlated with mussel biomass. We predicted that (1) at the mussel shell scale, food availability would best explain macroinvertebrate communities, (2) at the enclosure scale, mussel biomass would be correlated with macroinvertebrate communities due to their influence on both hydrodynamics and food availability (measured as chlorophyll *a* concentration), and (3) at the reach scale, macroinvertebrate communities would be best explained by stream discharge, with discharge also controlling mussel density (Figure 2-1B).

METHODS

Study System

We conducted our study in three rivers in southeastern Oklahoma known for their high mussel and macroinvertebrate biodiversity: the Kiamichi, Little and Glover rivers (Matthews et al. 2005) Figure 2-2). Mussel assemblages in these rivers are typically dominated by two species,

Actinonaias ligamentina and *Amblema plicata*, that make up ~70% of mussel biomass but differ morphologically, behaviorally, and physiologically (Hopper et al. 2018; Vaughn 2010). *Amblema plicata* has a ridged shell and tends to be sedentary, while *A. ligamentina* is an active burrower with a smooth shell. The two species differ in their thermal preferences, which influences their filtering and nutrient excretion rates and stoichiometry (Atkinson et al. 2018b; Spooner and Vaughn 2008). Combined, these trait differences lead to differences in the types and abundance of algae and macroinvertebrates that colonize shells and live in the sediment surrounding mussels (Spooner and Vaughn 2006; Spooner et al. 2012).

Reach Scale Field Study

We sampled macroinvertebrates and mussels at 14 sites in 7 paired river reaches in October 2016 (Figure 2-2) as part of a larger study (Hopper et al. 2018). Each paired reach contained a 100 m reach with a large mussel bed and a 100 m reach without mussels or with low densities of mussels. Paired sites averaged 346 m apart. At each site, we quantitatively sampled macroinvertebrates with 5 Surber samples (0.09 m^2) and preserved samples in 5% formalin. We enumerated and identified macroinvertebrates to the family level following Merritt and Cummins (1996) and Voshell (2002). We sampled mussels by excavating 15 – 20 (depending on the size of the mussel bed) 0.25 m^2 quadrats to a depth of 15 cm (Vaughn et al. 1997). We identified mussels to species, measured the longest shell axis of all individuals, and returned mussels alive to the stream bed. We used species-specific length-mass regressions to estimate mussel soft tissue dry mass (Atkinson et al. in press). We estimated areal mussel biomass ($g \cdot m^{-2}$) based on the estimate of dry, soft tissue mass in each quadrat (Hopper et al. 2018).

We measured depth and discharge at a transect across each site (Hach FH 950 Handheld Flow Meter, Loveland, Colorado). We determined sediment size with Wolman pebble counts at

each site (Wolman 1954). We used the R package *GSDtools* (Eaton 2019) to derive D_{10} and D_{60} values (the size of 10% and 60%, respectively) of measured pebbles, and used these to describe substrate heterogeneity (Williams 1980).

Eighteen days prior to sampling, we filled 3 strawberry baskets (100 cm^{-2} area, 6 cm deep) per site with river sediment and buried them flush with the riverbed to allow them to be colonized by biofilms (Bertrand and Gido 2007). We collected the baskets when we sampled macroinvertebrates. We homogenized the sediment in the baskets in a bucket with a known volume of stream water, creating a slurry, filtered a subsample (glass fiber 0.7 μm), placed filters in aluminum foil and froze them. Chlorophyll *a* was extracted in acetone and measured spectrophotometrically with the acid addition method (protocol 10200 H.2; ASTM, 2012).

Small Scale Field Experiment

We conducted a field experiment to examine how mussels influence macroinvertebrates at a small and intermediate spatial scale. A companion component of the experiment examined the effect of mussels on fish activity and is described in Hopper et al. (2019). To avoid the confounding effects of our treatments with legacy mussel effects, we selected a stream reach in the Kiamichi River that was upstream of known, large mussel beds (Figure 2-2). We constructed 50, 0.25 m^2 (50 cm by 50 cm by 20 cm deep) enclosures from 3.3 cm schedule 40 PVS pipe and 2.5 cm diameter poultry netting. Enclosures were buried flush within the riverbed in a checkerboard pattern to minimize cage-effects on downstream enclosures and filled with homogenized sediment collected from the stream reach. This design prevented mussels from escaping the enclosures but allowed for colonization of macroinvertebrates. We placed 6 sediment baskets (described above under Field Study) in each enclosure to collect resident macroinvertebrates. To quantify algal abundance, we attached glass fritted discs (diameter = 2.8

cm) to clay tiles (width = 7.6 cm) with silicone sealant. We then collected one glass fritted disc from each enclosure and stored them in opaque containers on ice for later processing.

We created assemblages of live mussels and "sham mussels" (empty mussel shells filled with sand and sealed with silicone) where we varied which species was dominant, *A. ligamentina* and *A. plicata*, as follows: live *A. ligamentina* dominated (7 live *A. ligamentina*, 3 live *A. plicata*), live *A. plicata* dominated (7 live *A. plicata*, 3 live *A. ligamentina*), sham *A. ligamentina* dominated (7 sham *A. ligamentina*, 3 *A. plicata*), and sham *A. plicata* dominated (7 sham *A. plicata,* 3 *A. ligamentina*). We also had a sediment control containing no mussels. Each treatment was replicated 10 times. Enclosures were stocked on July 12, 2017 and the experiment ran for 12 weeks until October 8, 2017.

We measured discharge and temperature for the experimental reach as described above under Field Study. We measured flow velocity and water depth in the middle of each enclosure and multiplied this by enclosure width to estimate the discharge over each enclosure. We conducted Wolman pebble counts to determine substrate heterogeneity in each enclosure as described above. Chlorophyll *a* was extracted from discs with acetone and measured as described above.

To sample macroinvertebrates within the enclosures, we homogenized sediment in the baskets with river water (as described above under Field Study), sieved the resulting slurry through a 0.175 mm mesh sieve, and preserved the macroinvertebrates in 70% ethanol. We measured the shell length of all mussels for later determination of soft-tissue dry mass using species-specific length-mass regressions. Live mussels were removed and returned to the area of the river from which they were collected.

We quantified algal abundance and macroinvertebrates occurring on mussel shells for a subsample of enclosures. From four enclosures for each treatment, we removed mussels and placed all the mussels of each species from an enclosure in a separate bucket. We then gently scrubbed mussel shells in river water in the bucket to create a slurry. We filtered a subsample of slurry and analyzed it for chlorophyll *a* as described above. We then sieved the remainder of the slurry and preserved macroinvertebrates in 70% ethanol. We measured shell length, width and height on subsampled mussels, and use these data to estimate shell area. We then summed shell surface area for each species in each enclosure separately and used that value to calculate chlorophyll *a* concentration and macroinvertebrate density.

Data analyses

Macroinvertebrate density and diversity

We examined how areal mussel biomass (reach and enclosure scale) or treatment (enclosure and shell scale) affected macroinvertebrate density, taxonomic richness, and Simpsons diversity. To meet statistical assumptions, we $\log_{10}$ transformed macroinvertebrate density and natural log transformed richness, except for data at the shell scale, where transformations were unnecessary (Zuur et al. 2009). We calculated Simpsons diversity, which describes both richness and evenness, with the function *diversity* (R Package vegan; (Oksanen et al. 2014).

For the reach scale, we used mixed linear models to test for differences among our dependent variables based on mussel biomass ($g \cdot m^{-2}$) and a random intercept accounting for geographic location (using HUC12 codes). We conducted a type III ANOVA with Satterthwaithe's method, using *anova*, for the *lmer* mixed models as implemented in the *R* package *lmerTest* and *lme4*, respectively (Bates et al. 2015; Kuznetsova et al. 2017). For the enclosure and shell scales, we evaluated treatment effects with ANOVA (*aov* from *stats* package

in R). If a significant independent variable was identified, we conducted Tukey *post hoc* multiple comparisons in the R package *emmeans* (Lenth, 2018).

Macroinvertebrate community structure

We used canonical correspondence analysis (CCA) with functions *cca* and *vif.cca* (R package vegan; (Greenacre 2017; Oksanen et al. 2014) to evaluate how mussel biomass and important environmental factors (discharge, chlorophyll *a* concentration, and substrate heterogeneity) influenced macroinvertebrate community structure. We standardized environmental variables to reduce the influence of measurement scale. To reduce the influence of rare species, we removed taxa found in only one sample from the reach analysis (< 8%) and in two samples of the enclosure analysis (< 4%); most Surber samples had similar species compositions at the reach level (Figure 2-A1). For the reach data, we included HUC12 as a conditional covariate to factor out spatial effects due to site location within and among the watersheds (Dauwalter 2013). To avoid pseudo-replication of environmental data, we used average macroinvertebrate density in each reach to build the community matrix; a boot-strapped CCA analysis did not change the conclusions of the averaged CCA analysis (Table 2-A1; Figure 2-A2; Figure 2-A3). For the enclosure data, we considered *A. plicata* and *A. ligamentina* separately and whether treatments were live mussel or sham shells. At the shell scale, the environmental variables include chlorophyll *a* concentration, mussel species, and live vs. sham as substrate and discharge were controlled for experimentally. Unlike the reach data analysis, we did not include a conditional spatial variable in this CCA as a Mantel test was not statistically significant ($r = 0.089$, $p = 0.07$) and its inclusion did not increase the total explained proportion of the inertia (similar to variation; Figure A4).

After conducting the CCAs at each spatial scale, we then performed permutation tests with *anova.cca* to determine if the global model explained more inertia than a random normal model. If the global model was significant, we then conducted both forward and backward model selection to determine which variables were significant in explaining inertia within the macroinvertebrate community using the function *ordistep* (R package vegan). We conducted variation partitioning to determine the unique and shared variation explained by either mussel or environmental variables with *varpart* (R package vegan). We present and interpret the global model to investigate how each environmental variable affects the macroinvertebrate community; we use the results of model selection to determine which variables are most important when explaining the community structure and testing our hypothesis.

RESULTS

Macroinvertebrate densities are highest on living mussels at the shell scale.

We predicted that algal food availability, measured as chlorophyll *a* concentration, would be higher on the shells of living mussels, and would drive macroinvertebrate community structure at this scale. Macroinvertebrate densities were higher on shells of live mussels compared to sham shells ($F_{1,28} = 4.51$, $p < 0.04$), but were not different between shells of different species ($F_{1,28} = 2.25$, $p = 0.06$; Table 2-1), and there was not a significant interaction between these factors ($F_{1,28} = 2.57$, $p = 0.10$; Figure 2-3A). Based on the *post hoc* test, live *A. plicata* shells had 1.88 times more macroinvertebrates than sham shells while live *A. ligamentina* shells had 1.12 more times macroinvertebrates than sham shells. Richness was not different among live vs. sham shells ($F_{1,28} = 1.25$, $p = 0.27$), species ($F_{1,28} = 0.003$, $p = 0.95$), or the interaction of the factors ($F_{1,28} = 0.03$, $p = 0.86$). Simpsons diversity index was not different among live vs. sham shells ($F_{1,28} = 0.51$, $p = 0.58$), species ($F_{1,28} = 0.03$, $p = 0.87$), or the interaction of the factors ($F_{1,28} = 0.78$, $p = 0.33$). At

the shell scale, the global model was statistically significant and explained 14.3% of the variation within the community matrix ($F_{3,28} = 1.55$, $p < 0.01$; Table 2-2; Figure 2-5A). Model selection indicated that shell type was the only significant variable within the global model ($p < 0.01$). Differences between the sham and live mussel treatments dominate the first CCA, which explains 48.6% of the total explained variation (Figure 2-4A). Adult beetles (Elmidae) and seed shrimp (Ostracoda) were associated with live *A. plicata* mussels. Chlorophyll *a* was positively related to the first axis and was associated with algal-grazing mayflies (Leptophlebiidae) and caddisflies (Helicopsychidae). Differences between *A. ligamentina* and *A. plicata* shells drove the second CCA and explains 33.5% of the total explained variation. Larval midges (Chironomidae) and caddisflies (Lepidostomatidae) were more often found on *A. ligamentina* shells while craneflies (Tipulidae) and hydra (Hydrazoa) were more often found on *A. plicata* shells. Based on variation partitioning, mussel variables explained 8.9% of the explained variation, chlorophyll *a* concentration explained 4.3%, and together they explained 0.9% of the explained variation (Figure 2-5A).

Mussels had little impact on macroinvertebrates at the enclosure scale.

Contrary to our predictions, mussels had little impact on macroinvertebrate communities at the enclosure scale. Macroinvertebrate abundance did not vary with treatment ($F_{4,45} = 0.83$, $p = 0.52$) and was not related to mussel biomass (Table 2-1; Figure 2-3B). Treatment did not affect richness ($F_{4,45} = 0.78$, $p = 0.54$) or Simpson's diversity ($F_{4,45} = 1.73$, $p = 0.16$). The enclosure scale global model explained only 14.4% of the variation within the macroinvertebrate community and was not statistically significant ($F_{6,43} = 1.23$, $p = 0.12$; Table 2; Figure 5C). This non-significance indicates that our environmental variables were not correlated with community structure and/or variation within the macroinvertebrate community was very low. While not

significant, this analysis revealed that algal-grazing mayflies (Leptophlebiidae) and common stonefly (Perlidae) were positively related to mussel biomass while pale burrower mayflies (Polymitarcyidae) was negatively related to mussels (Figure 2-4B). We also find that snail-case caddisflies (Helicopsychidae) and microcadisflies (Hydroptilidae) were found more often in enclosures with live mussels. While this CCA is not statistically significant, we find that some taxa are more associated with live mussel patches.

Discharge, mussel biomass, and algal abundance explain macroinvertebrate community structure at the stream reach scale.

We predicted that discharge would be the driving force shaping macroinvertebrate community structure at the reach scale, but that mussel biomass would also be important. Mussel biomass by itself did not govern macroinvertebrate abundance ($F_{1,7} = 0.20$, $p = 0.67$; Figure 2-3C), richness ($F_{1,7} = 0.12$, $p = 0.74$; Table 1), or Simpsons diversity ($F_{1,7} = 0.02$, $p = 0.88$). However, mussel biomass, discharge, and algal abundance in combination explained a large proportion of the variation in macroinvertebrate community structure. The reach scale global CCA model was statistically significant ($F_{4,8} = 2.45$, $p < 0.01$; Table 2-2). Discharge explained the most variation ($p = 0.01$), with chlorophyll *a* concentration also explaining a significant portion ($p < 0.04$). Geographic location explained 9.8% of the variation (Figure 2-5C). After accounting for location, the environmental variables explained 50.8% of the variation within the macroinvertebrate community. Discharge drove the first CCA, followed by chlorophyll *a* and mussel biomass, to account for 63.2% of the total explained variation (Figure 2-5C). Mortarjoint casemakers (Odontoceridae), and caddisfly pupae (Trichoptera) had high loadings on the first CCA, while spiny crawler mayflies (Ephemerellidae) and circular-seamed flies (Diptera: Cyclorrhapha) had low loadings. The second CCA represented a gradient between chlorophyll *a*

and discharge and accounted for a total of 18.9% of the total explained variation. Snail-case caddisflies (Helicopsychidae) and copepods were found more often at sites with higher benthic chlorophyll, while adult flies (Diptera) and side-swimmers (Amphipoda) were found more often in areas with higher discharge. Based on variation partitioning, the environmental variables (discharge, chlorophyll a concentration, and substrate heterogeneity) explained 33.9% of the explained variation, mussels alone explained 3.7%, and together mussels and the environmental variables explained 13.3% of the explained variation (Figure 2-5C).

DISCUSSION

We evaluated how mussel biomass and environmental factors (related to potential mussel engineering mechanisms) predict macroinvertebrate community structure at three spatial scales. We found that at the shell scale macroinvertebrates were most abundant on live *A. plicata* shells and live mussels had different macroinvertebrate communities living on their shells than sham shells. Our predictions that mussels would have the largest impact on macroinvertebrate community structure at the enclosure scale were not supported by our data; the environmental variables explained little variation within the macroinvertebrate community. At larger spatial scales, discharge, a proxy for flow, explained the most variation. Comparing the significant predictors in the CCAs at different spatial scales, we find correlative evidence that the mechanism shaping macroinvertebrate communities within mussel beds shifts with spatial scale. While chlorophyll *a* was a statistically significant variable at the reach scale, it did not significantly explain macroinvertebrate variation at the shell scale. Live mussel shell presence explained more, but similar, variation in the macroinvertebrate community than chlorophyll *a* concentration. Mussel biodeposits (as a food resource) or rough periostracum (shell surface that acts as macroinvertebrate habitat) might explain macroinvertebrate community structure more

than chlorophyll *a* concentration alone. We conclude that mussels' effect on macroinvertebrates is spatial-scale dependent and the magnitude of their engineering effects are context dependent.

Different engineering mechanisms drive macroinvertebrate community structure at different spatial scales. Discharge, a proxy for flow, explained the most variation in macroinvertebrate community composition at the reach scale. This is unsurprising as flow has been referred to as the 'master variable' of stream ecosystems as it influences (and thus is correlated with) channel geomorphology, energy sources, and water quality (Poff et al. 1997). For sedentary animals like mussels, high flows potentially push individuals downstream, reducing mussel density and intra-guild facilitation (Peck et al. 2014; Sansom et al. 2018); while at low flows, mussels lack a quick, long-distance dispersal to withstand low flow events (Gough et al. 2012). Discharge, chlorophyll *a*, and mussel density explained similar variation within the community on the first axis; on the second axis, chlorophyll *a* and discharge diverge though both are statistically significant. As flow regulates both food resources and mussel occurrence in rivers, flow was the driving factor of macroinvertebrate communities at larger spatial scales. At smaller spatial scales, we found that living mussels vs. dead shells explained macroinvertebrate community structure better than chlorophyll *a* concentration. Chlorophyll *a* explained similar variation as the presence of live mussels. Live mussels are likely engineering macroinvertebrate habitats through multiple mechanisms; while supplementing the green-food web through algae on their shells, macroinvertebrates could be feeding on mussel pseudofeces or prefer living on the rough, proteinaceous outer layer of mussel shells. While chlorophyll *a* significantly explained some variation at the reach spatial scale, it was surpassed by a different mechanism at the small shell spatial scale. Thus, our hypothesis that mussels' engineering mechanism shifts at different spatial scales is supported.

Just as spatial scale shifts the prevalence of different engineering mechanisms, abiotic context shifts the magnitude of an engineer's effect at different spatial scales. Abiotic context modulates the difference between engineered and non-engineered patches, often in predictable ways. The effects of mussels on macroinvertebrates are known to vary with environmental context, particularly with flow (Vaughn et al. 2007). In summer, when flow is low and water temperatures warmer, mussel excretion typically contributes disproportionately to nutrient pools, stimulates primary production, and thus increases food resources available to macroinvertebrates (Atkinson and Vaughn 2015). In contrast, high flow events often both reduce macroinvertebrate abundance and dilute effects of mussel excretion, thus they can mask the effects of mussels on macroinvertebrates (Spooner and Vaughn 2006). We had atypically high flows during our field experiment. Typically, the maximum 50% (median) daily mean value for the closest United States Geological Survey gage (07335700) over the course of our experiment is 0.06 $m^3 \cdot s^{-1}$ and the maximum 75% daily mean value is 0.42 $m^3 \cdot s^{-1}$; during our experiment discharge peaked at 15.7 $m^3 \cdot s^{-1}$ (USGS, 2016; Figure A5). We think these higher flows likely inhibited macroinvertebrate colonization in our experimentally-created mussel patches, thus reducing the difference between engineered and non-engineered patches (Table 2-3). The effects of mussels on basal food resources are also context dependent (Spooner and Vaughn 2012); mussel effects on nutrients and their effects on macroinvertebrates are diminished in rivers with higher nutrient concentrations due to agricultural runoff (Spooner et al. 2013). For example, because mussel and control plots had similar basal resources, those patches had similar macroinvertebrate abundances and thus no mussel engineering effect (Richter et al. 2016). As climate change is altering flow regimes and carbon cycling (Carpenter et al. 1992; Trenberth 2011), further investigation into the interaction between mussels, abiotic stressors, and macroinvertebrates is

needed. By investigating the interaction between mussel engineering and the abiotic factors that affect macroinvertebrates, we can better predict how stream communities will change with future losses of mussels and global change.

We found similar relationships between environmental variables, mussels, and macroinvertebrate abundances but different taxonomic associations with mussels than previous research in the region. Vaughn and Spooner (2006) examined the relationship between mussel assemblage structure and macroinvertebrate assemblage structure at the 0.25 m^2 and stream reach scales at 30 sites across 8 rivers in the Ouachita Highlands of Oklahoma and Arkansas. They found that mussel assemblage structure explained the most variation at the 0.25 m^2 scale while spatial variables (location, network position, and watershed area) explained the most variation at the reach scale. We confirm that discharge, which is a function of precipitation, groundwater input, and watershed area, drives macroinvertebrate community structure at the reach scale. Our study shares many conclusions with Vaughn and Spooner (2006), who completed a year-long field experiment in the Kiamichi River where they examined the effects of live and sham shells of *A. ligamentina* and *A. plicata* in monoculture on macroinvertebrates over time at the 0.25 m^2 scale. While we did not find differences in macroinvertebrate abundance or major taxonomic abundances between our treatments, we did find that caddisfly larvae (Trichoptera) were associated with mussel treatments. While we found higher invertebrate abundance on live *A. plicata* shells, Spooner and Vaughn (2006) found invertebrate abundances were equivalent between sham and live mussel shells. Our data confirm that different macroinvertebrate communities occupy live vs. sham shells (Vaughn et al. 2008), we found that herbivorous adult beetles and caddisfly larva were on live shells more often while a trophically diverse caddisflies (collector-gatherers, herbivorous, and predatory genera) associated with sham

shells. Thus, some macroinvertebrates might be inhabiting live mussel shells because of the higher abundance of food on the shells. The incongruency between live mussels harboring increased herbivorous macroinvertebrates but chlorophyll *a* concentration not predicting macroinvertebrate abundance might be explained by herbivore reduction of algal pools through consumption, which we did not measure. Caddisflies, particularly algae-grazing weighted casemaker caddisflies and snail-case caddisflies, might use the leathery periostracum found on live shells to anchor and withstand high flows (Lawfield et al. 2014; Robinson et al. 2017), and are also likely grazing on algae on the shells. Our study confirms that that snail-case caddisflies were associated with live mussels at the shell and enclosure scales, and previous work has shown that algal food availability can control the distribution of this insect (Vaughn 1986). Our research adds to the growing evidence that mussels have complex interactions with macroinvertebrate communities and further investigation into taxa specific facilitation is warranted.

Mussels, both marine and freshwater, create a facilitation landscape for macroinvertebrates, though the strength of this facilitation is dependent upon the spatial scale and abiotic context considered. Within marine mussel beds, mussel filter feeding reduces food available for cockles but at the edges of said beds, cockle settlement increases due to the mussels' reduction of wave energy (Donadi et al. 2013). Similar intra-guild facilitation is evident in aquatic vegetation as *Callitriche platycarpa* plant growth moderates flow velocity and thus facilitates other aquatic macrophytes (Cornacchia et al. 2018). Both freshwater mussels and oysters affect co-occurring invertebrates through mechanisms that shift across space (Arribas et al. 2014; McAfee and Bishop 2019; McAfee et al. 2016). Termites facilitate vegetation and grazers, depending upon water availability, at a local spatial scale while altering soil properties at the landscape scale (Davies et al. 2016; Jouquet et al. 2011). These scale and context dependent

effects create patches with distinct, potentially facilitative, interactions and lead to spatially heterogeneous patches of animals within ecosystems — a facilitation landscape (Cornacchia et al. 2018).

Understanding how effects of ecosystem engineers change with context is important for conserving ecosystems and predicting how ecosystem function will shift with global change (Coggan et al. 2018). Conservation biologists argue that ecosystem engineers conservation directly and indirectly benefit other co-occurring species and thus should be prioritized (Angelini et al. 2011; Crain and Bertness 2006). As an example, conservation of beavers, who engineer riparian ecosystems, enhances Saproxylic beetle conservation through habitat provisioning (Mourant et al. 2018). With urbanization and climate change, the abiotic stage upon which ecosystem engineers act is expected to shift, potentially altering the effectiveness of species conservation through ecosystem engineer restoration. Native freshwater mussels are imperiled ecosystem engineers (FMCS 2016); internationally, 40.6% are considered near threatened, vulnerable, and endangered and 16% are considered data deficient (Ferreira-Rodríguez et al. 2019). Current conservation measures often advocate for supplementing mussel populations through population reintroduction and augmentation (McMurray and Roe 2017). Loss of mussel beds, which are ecological hotspots, has large ramifications for ecosystem function and ecosystem services (Vaughn et al. 2015). With decreasing stream permanency due to global change, we expect mussel beds to decline; while the habitat-generating effects of mussels should remain for years, their effects on basal food resources will be more rapidly reduced (DuBose et al. 2019). As the abiotic context shifts with global change, conservation biologists and water managers should be cognizant of the interacting factors of mussel engineering and sampling

spatial scale for quantifying mussel engineering effects and population measurements (Ries et al. 2019).

Ecosystem engineers can have different effects based upon the spatial scale considered. For freshwater mussels, the mechanism by which mussels engineer stream ecosystems shifts with spatial scale (Figure 1). We investigated how mussels' influence on near-bed hydrodynamics and basal resources affects macroinvertebrate communities at three spatial scales: shell (~10 cm^2), enclosure (~0.25 m^2) and reach (~1,000 m^2). Live mussel shells had different communities residing on them than sham shells, with higher macroinvertebrate abundance on live *A. plicata* shells. We also found evidence that flow and chlorophyll *a* concentration was correlated with macroinvertebrate community structure at the reach scale. Through our conceptual figure, we explain how our results joins the literature in defining mussel engineering as context dependent ecosystem engineers. As global change is altering the abiotic context of ecosystems, ecosystem engineers' impact will change in the future. With flow and nutrient regime alteration, freshwater mussels' effect as ecosystem engineers is likely to shift and might cause the ultimate loss of ecosystem function.

ACKNOWLEDGEMENTS

Funding to conduct field surveys and the enclosure experiment was provided by NSF DEB-1457542; Funding for the enclosure experiment was provided by OU Department of Biology Adams Scholarship, and OU Graduate Student Senate Research Award. We thank Ronnie Rose and many other landowners for allowing us river access. We appreciate M. Couchman, W.S. DuBose, A. Earl, and A. Hageman, and K. Murphy for their efforts installing the enclosure experiment, N. Ferreira Rodríguez, J. Hartwell, E. Higgins, A. Holt, J. Lopez, and B. Tweedy for their assistance collecting enclosure samples, K. Murphy, and D. Kopp for field

sample collection assistance and J. Hartwell for laboratory assistance. We thank the Vaughn lab, C. Curry, and M. Patten for their advice on the manuscript. This paper was completed as part of a dissertation at the University of Oklahoma and is a contribution to the program of the Oklahoma Biological Survey.

REFERENCES

Aldridge DC, Fayle TM, Jackson N (2007) Freshwater mussel abundance predicts biodiversity in UK lowland rivers. Aquatic Conservation: Marine and Freshwater Ecosystems 17:554-564

Allen DC, Vaughn CC (2010) Complex hydraulic and substrate variables limit freshwater mussel species richness and abundance. Journal of the North American Benthological Society 29:383-394.

Allen DC, Vaughn CC (2011) Density-dependent biodiversity effects on physical habitat modification by freshwater bivalves. Ecology 92:1013-1019

Angelini C, Altieri AH, Silliman BR, Bertness MD (2011) Interactions among Foundation Species and Their Consequences for Community Organization, Biodiversity, and Conservation. BioScience 61:782-789.

Arribas LP, Donnarumma L, Palomo MG, Scrosati RA (2014) Intertidal mussels as ecosystem engineers: their associated invertebrate biodiversity under contrasting wave exposures. Marine Biodiversity 44:203-211.

Atkinson CL, Capps KA, Rugenski AT, Vanni MJ (2017) Consumer-driven nutrient dynamics in freshwater ecosystems: from individuals to ecosystems. Biol Rev Camb Philos Soc 92:2003-2023.

Atkinson CL, Christian AD, Spooner DE, Vaughn CC (2014a) Long-lived organisms provide an integrative footprint of agricultural land use. Ecological Applications 24:375-384.

Atkinson CL, Kelly JF, Vaughn CC (2014b) Tracing Consumer-Derived Nitrogen in Riverine Food Webs. Ecosystems 17:485-496.

Atkinson CL, Allen DC, Davis L, Nickerson ZL (2018a) Incorporating ecogeomorphic feedbacks to better understand resiliency in streams: a review and directions forward. Geomorphology 305:123-140

Atkinson CL, Sansom BJ, Vaughn CC, Forshay KJ (2018b) Consumer Aggregations Drive Nutrient Dynamics and Ecosystem Metabolism in Nutrient-Limited Systems. Ecosystems 21:521-535.

Atkinson CL, Vaughn CC (2015) Biogeochemical hotspots: temporal and spatial scaling of the impact of freshwater mussels on ecosystem function. Freshwater Biology 60:563-574.

Atkinson CL, Vaughn CC, Forshay KJ, Cooper JT (2013) Aggregated filter-feeding consumers alter nutrient limitation: consequences for ecosystem and community dynamics. Ecology 94:1359-1369

Bates DM, Maechler M, Bolker B, Walker S (2015) Fitting Linear Mixed-Effects Models Using lme4. Journal of Statistical Software 67:1-48.

Bertrand KN, Gido KB (2007) Effects of the herbivorous minnow, southern redbelly dace (Phoxinus erythrogaster), on stream productivity and ecosystem structure. Oecologia 151:69-81.

Carpenter S, Fischer SG, Grimm NB, Kitchell JF (1992) Global Change and Freshwater Ecosystems. Annual Review of Ecology and Systematics 23:119-139.

Chowdhury GW, Zieritz A, Aldridge DC (2016) Ecosystem engineering by mussels supports biodiversity and water clarity in a heavily polluted lake in Dhaka, Bangladesh. Freshwater Science 35:188-199.

Coggan NV, Hayward MW, Gibb H (2018) A global database and "state of the field" review of research into ecosystem engineering by land animals. J Anim Ecol 87:974-994.

Cornacchia L, van de Koppel J, van der Wal D, Wharton G, Puijalon S, Bouma TJ (2018) Landscapes of facilitation: how self-organized patchiness of aquatic macrophytes promotes diversity in streams. Ecology 99:832-847

Crain CM, Bertness MD (2006) Ecosystem Engineering across Environmental Gradients: Implications for Conservation and Management. BioScience 56:211.

Dauwalter DC (2013) Fish assemblage associations and thresholds with existing and projected oil and gas development. Fisheries Management and Ecology 20:289-301.

Davies AB, Levick SR, Robertson MP, van Rensburg BJ, Asner GP, Parr CL (2016) Termite mounds differ in their importance for herbivores across savanna types, seasons and spatial scales. Oikos 125:726-734

Donadi S et al. (2013) Cross-habitat interactions among bivalve species control community structure on intertidal flats. Ecology 94:489-498

DuBose TP, Atkinson CL, Vaughn CC, Golladay SW (2019) Drought-Induced, Punctuated Loss of Freshwater Mussels Alters Ecosystem Function Across Temporal Scales. Frontiers in Ecology and Evolution 7. doi: 10.3389/fevo.2019.00274

Eaton, B (2019). GSDtools: Tools for analyzing pebble counts used to measure river bed surface texture. R package version 0.0.1.0000.

Engel FG et al. (2017) Mussel beds are biological power stations on intertidal flats. Estuarine, Coastal and Shelf Science 191:21-27.

Ferreira-Rodríguez N et al. (2019) Research priorities for freshwater mussel conservation assessment. Biological Conservation 231:77-87.

Goodding DD, Williams MG, Ford DF, Williams LR, Ford NB (2019) Associations between substrate and hydraulic variables and the distributions of a sculptured and an unsculptured unionid mussel. Freshwater Science 38:543-553

Gough HM, Landis AMG, Stoeckel JA (2012) Behaviour and physiology are linked in the responses of freshwater mussels to drought. Freshwater Biology 57:2356-2366.

Greenacre MJ (2017) Correspondence analysis in practice / Michael Greenacre, Third edition.. edn. Boca Raton, FL : CRC Press, Taylor & Francis Group

Gutiérrez JL, Jones CG, Strayer DL, Iribarne OO (2003) Mollusks as ecosystem engineers: the role of shell production in aquatic habitats. Oikos 101:79-90.

Hopper GW, DuBose TP, Gido KB, Vaughn CC (2019) Freshwater mussels alter fish distributions through habitat modifications at fine spatial scales. Freshwater Science 38:702-712

Hopper GW et al. (2018) Biomass distribution of fishes and mussels mediates spatial and temporal heterogeneity in nutrient cycling in streams. Oecologia 188:1133-1144.

Howard JK, Cuffey KM (2006) The functional role of native freshwater mussels in the fluvial benthic environment. Freshwater Biology 51:460-474.

Jones CG, Lawton JH, Shachak M (1997) Positive and negative effects of organisms as physical ecosystem engineers. Ecology 78:1946-1957

Jouquet P, Traoré S, Choosai C, Hartmann C, Bignell D (2011) Influence of termites on ecosystem functioning. Ecosystem services provided by termites. European Journal of Soil Biology 47:215-222

Koerner, M. (2018) Biogenic modification of sediments by unionid mussels and their implications for sediment transport in the Sipsey River of Alabama. Masters thesis, The University of Alabama.

Kuznetsova A, Brockhoff PB, Christensen RHB (2017) lmerTest Package: Tests in Linear Mixed Effects Models. Journal of Statistical Software 82:1-26.

Lawfield AMW, Gingras MK, Pemberton SG, Erickson JM (2014) Freshwater Unionid Bivalve Shells as Substrata for Trichoptera Attachment. Palaios 29:525-532.

Matthews WJ, Vaughn CC, Gido K, Marsh-Matthews E (2005) Southern Plains Rivers. In: Benke AC, Cushing CE (eds) Rivers of North America, pp 283-311

McAfee D, Bishop MJ (2019) The mechanisms by which oysters facilitate invertebrates vary across environmental gradients. Oecologia 189:1095-1106.

McAfee D, Cole VJ, Bishop MJ (2016) Latitudinal gradients in ecosystem engineering by oysters vary across habitats. Ecology 97:929-939

McMurray SE, Roe KJ (2017) Perspectives on the controlled propagation, augmentation and reintroduction of freshwater mussels (Mollusca: Bivalvia: Unionoida). Freshwater Mollusk Biology and Conservation 10:1-12

Merritt RW, Cummins KW (1996) An introduction to the aquatic insects of North America. Kendall Hunt

Mourant A, Lecomte N, Moreau G (2018) Indirect effects of an ecosystem engineer: how the Canadian beaver can drive the reproduction of saproxylic beetles. Journal of Zoology 304:90-97.

Oksanen J et al. (2014) Vegan: Community Ecology Package, R package version 2.5-6.

Peck AJ, Harris JL, Farris JL, Christian AD (2014) Survival and Horizontal Movement of the Freshwater Mussel Potamilus capax (Green, 1832) Following Relocation within a Mississippi Delta Stream System. American Midland Naturalist 172:76-90.

Phillips JS, McCormick AR, Einarsson Á, Grover SN, Ives AR (2019) Spatiotemporal variation in the sign and magnitude of ecosystem engineer effects on lake ecosystem production. Ecosphere 10:e02760

Poff NL et al. (1997) The natural flow regime. Bioscience 47:769-784.

Randklev CR, Hart MA, Khan JM, Tsakiris ET, Robertson CR (2019) Hydraulic requirements of freshwater mussels (Unionidae) and a conceptual framework for how they respond to high flows. Ecosphere 10

Richter A, Stoeckl K, Denic M, Geist J (2016) Association between the occurrence of the Thick-shelled River Mussel (Unio crassus) and macroinvertebrate, microbial, and diatom communities. Freshwater Science 35:922-933.

Ries PR, Jager ND, Newton TJ, Zigler SJ (2019) Local-scale spatial patterns of freshwater mussels in the Upper Mississippi River. Freshwater Science 38:742-752.

Robinson JL, Wetzel MJ, Tiemann JS (2017) Some Phoretic Associations of Macroinvertebrates on Transplanted Federally Endangered Freshwater Mussels. Northeastern naturalist 24:N29-N34

Sansom BJ, Atkinson JF, Bennett SJ (2017) Modulation of near-bed hydrodynamics by freshwater mussels in an experimental channel. Hydrobiologia 810:449-463.

Sansom BJ, Bennett SJ, Atkinson JF, Vaughn CC (2018) Long-term persistence of freshwater mussel beds in labile river channels. Freshwater Biology 63:1469-1481.

Simeone D, Santos C, Gisane F, Tagliaro CH, Beasley CR (2018) Greater macroinvertebrate diversity and freshwater mussel density in meander margins of an Amazon river. Freshwater Biology 63:1118-1129.

Freshwater Mollusk Conservation Society [FMCS] (2016) A national strategy for the conservation of native freshwater mollusks. Freshwater Mollusk Biology and Conservation 19:1-21

Spooner DE, Frost PC, Hillebrand H, Arts MT, Puckrin O, Xenopoulos MA (2013) Nutrient loading associated with agriculture land use dampens the importance of consumer-mediated niche construction. Ecol Lett 16:1115-1125.

Spooner DE, Vaughn CC (2006) Context-dependent effects of freshwater mussels on stream benthic communities. Freshwater Biology 51:1016-1024.

Spooner DE, Vaughn CC (2008) A trait-based approach to species' roles in stream ecosystems: climate change, community structure, and material cycling. Oecologia 158:307-317.

Spooner DE, Vaughn CC (2012) Species' traits and environmental gradients interact to govern primary production in freshwater mussel communities. Oikos 121:403-416.

Spooner DE, Vaughn CC, Galbraith HS (2012) Species traits and environmental conditions govern the relationship between biodiversity effects across trophic levels. Oecologia 168:533-548.

Strayer DL (1999) Use of flow refuges by unionid mussels in rivers. Journal of the North American Benthological Society 18:468-476.

Strayer DL (2014) Understanding how nutrient cycles and freshwater mussels (Unionoida) affect one another. Hydrobiologia 735:277-292.

Trenberth KE (2011) Changes in precipitation with climate change. Climate Research 47:123-138

U. S. Geological Survey [USGS] (2016) National Water Information System, data available on the World Wide Web (USGS Water Data for the Nation)

van der Heide T et al. (2014) Predation and habitat modification synergistically interact to control bivalve recruitment on intertidal mudflats. Biological Conservation 172:163-169.

Vaughn CC (1986) The role of periphyton abundance and quality in the microdistribution of a stream grazer, Helicopsyche borealis (Trichoptera: Helicopsychidae). Freshwater Biology 16:485-493

Vaughn CC (2010) Biodiversity Losses and Ecosystem Function in Freshwaters: Emerging Conclusions and Research Directions. BioScience 60:25-35.

Vaughn CC, Atkinson CL, Julian JP (2015) Drought-induced changes in flow regimes lead to long-term losses in mussel-provided ecosystem services. Ecology and Evolution 5:1291-1305.

Vaughn CC, Hoellein TJ (2018) Bivalve Impacts in Freshwater and Marine Ecosystems. Annual Review of Ecology, Evolution, and Systematics 49:183-208.

Vaughn CC, Nichols SJ, Spooner DE (2008) Community and foodweb ecology of freshwater mussels. Journal of the North American Benthological Society 27:409-423.

Vaughn CC, Spooner DE (2006) Unionid mussels influence macroinvertebrate assemblage structure in streams. Journal of the North American Benthological Society 25:691-700.

Vaughn CC, Spooner DE, Galbraith HS (2007) Context-dependent species identity effects within a functional group of filter-feeding bivalves. Ecology 88:1654-1662.

Vaughn CC, Taylor CM, Eberhard KJ (1997) A comparison of the effectiveness of timed searches vs. quadrat sampling in mussel surveys, pp 157-162

Voshell JR (2002) A guide to common freshwater invertebrates of North America

Wild C et al. (2011) Climate change impedes scleractinian corals as primary reef ecosystem engineers. Marine and Freshwater Research 62:205-215

Williams DD (1980) Some relationships between stream benthos and substrate heterogeneity. Limnology & Oceanography 25:166-172

Wolman MG (1954) A method of sampling coarse river-bed material. EOS, Transactions American Geophysical Union 35:951-956

Wright JP, Jones CG, Flecker AS (2002) An ecosystem engineer, the beaver, increases species richness at the landscape scale. Oecologia 132:96-101

Zuur AF, Ieno EN, Walker NJ, Savaliev AA, Smith GM (2009) Mixed Effects Models and Extensions in Ecology with R. Springer

TABLES

Table 2-1. Macroinvertebrate abundance, richness, and diversity at the reach, enclosure, and shell spatial scale. ALIG represents *A. ligamentina* while APLI represents *A. plicata*. Enclosure treatments describe the dominant species, followed by whether the shells were live or sham shells. For example, ALIG Live is *A. ligamentina* dominated, live shells. Bold font indicates statistically significant at $p < 0.05$ using an ANOVA and Tukey's post hoc test.

Scale	*Shell Species - Type*	*Approximate shell area (m^2)*	*Log_{10}(individuals · m^{-2})*	*Richness*	*Simpson's index*
Shell	ALIG Live	0.167	2.45 (2.24)	8.9 (4.1)	0.69 (0.13)
	ALIG Sham	0.167	2.40 (2.19)	7.9 (1.9)	0.68 (0.08)
	APLI Live	0.122	**2.68 (2.37)**	9.0 (2.8)	0.66 (0.12)
	APLI Sham	0.122	2.39 (2.03)	7.6 (2.9)	0.72 (0.07)

	Treatment	*Mussel biomass ($g \cdot m^{-2}$)*	*Log_{10}(individuals · m^{-2})*	*Richness*	*Simpson's index*
Enclosure	ALIG Live	280.0	3.33 (2.80)	16.0 (2.7)	0.63 (0.10)
	ALIG Sham	248.1	3.37 (2.65)	14.3 (2.4)	0.53 (0.14)
	APLI Live	189.9	3.36 (2.83)	14.5 (3.6)	0.60 (0.10)
	APLI Sham	162.9	3.38 (3.02)	15.3 (2.8)	0.58 (0.15)
	Control	0.0	3.26 (2.61)	14.1 (2.4)	0.66 (0.13)
Reach	Mussel	93.1	3.31 (3.29)	28.0 (5.3)	0.84 (0.05)
	Control	5.4	3.29 (3.23)	26.6 (5.9)	0.82 (0.06)

Table 2-2. Results from the ANOVA-like permutation test and forward and backward model selection of the CCA. Degrees of freedom for the global tests are found within parenthesis. Bold font indicates statistically significant at $p < 0.05$.

Dataset	**Variable**	**F**	***p* value**	**Adj. *p* value**
Shell	*Global (3,28)*	*1.55*	***0.02***	
	Live vs. Sham	2.05	**0.01**	**0.02**
	Chlorophyll *a*	1.39	0.11	
	Shell species	1.10	0.27	
Enclosure	*Global (6,43)*	*1.21*	*0.12*	
	A. ligamentina biomass			
	A. plicata biomass			
	Alive			
	Discharge			
	Chlorophyll *a*			
	Substrate heterogeneity			
Reach	*Global (4,8)*	*2.58*	***0.01***	
	Discharge	4.18	**0.01**	**0.04**
	Chlorophyll *a*	2.15	**0.04**	**0.12**
	Substrate heterogeneity	2.24	0.06	
	Mussel biomass	0.58	0.72	

Table 2-3. Fall median (inter-quartile range) discharge for the Kiamichi, Glover, and Little River (USGS 2016). We recorded discharge at each reach (2016) the enclosure site (2017). September and October are considered fall for this table.

	Our Study		*USGS data*	
	Reaches 2016	*Enc. 2017*	*Fall daily mean*	*Date Range*
Kiamichi @ Clayton	0.118 (0.035)		0.365 (2.35)	1981-2018
Kiamichi @ Big Cedar	0.103 (0.027)	0.266	0.034 (0.28)	1965-2018
Glover	0.112 (0.009)		0.368 (2.48)	1961-2018
Little	2.130 (0.317)		2.464 (10.7)	1960-2018

FIGURE CAPTIONS

Figure 2-1 Conceptual figure of mussel engineering effects at different spatial scales. A) predicts the degree of mussel engineering (difference between engineered and non-engineered areas) on flow and resource alteration as spatial scale increases. B) depicts the three scales analyzed within this manuscript and the hypothesized mechanism by which mussels drive macroinvertebrate community structure.

Figure 2-2. Locations within Southeastern Oklahoma where the mussel (upside triangle) and control (downside triangle) reaches and the field enclosure experiment (Enc., plus sign) were conducted. USGS gage location indicted with a black square. Code from the R package *hydroMap* (DeCicoo and Blodgett, 2017).

Figure 2-3. Macroinvertebrate density at the reach (A), enclosure (B), and at the shell (C) spatial scale. Both axes are transformed: all axis are $\log_{10}$ transformed except the reach mussel biomass axis, which is $\log_e(1+x)$ transformed.

Figure 2-4. Partial Canonical Correspondence Analysis and Canonical Correspondence Analysis of macroinvertebrate communities and environmental factors at the shell (A), enclosure (B), and reach (C) scale. Factor constraints are indicated as centroids with underlined, navy text while linear combinations of quantitative measures are indicated with vectors and bold, red text. Points represent species; black, labeled points are discussed within the text. Percent of the total variation explained by that CCA axis is displayed.

Figure 2-5. Percentage of macroinvertebrate community variation explained by the environmental variables. The pie-charts depict the conditioned, explained, and unexplained variation within the macroinvertebrate dataset based on the CCA. Using variation partitioning, we then explored how mussel variables (biomass and treatment), the environment (discharge, chlorophyll *a* concentration, and substrate), and the interaction of the two explained the macroinvertebrate communities. Overlap between groups represents shared variation.

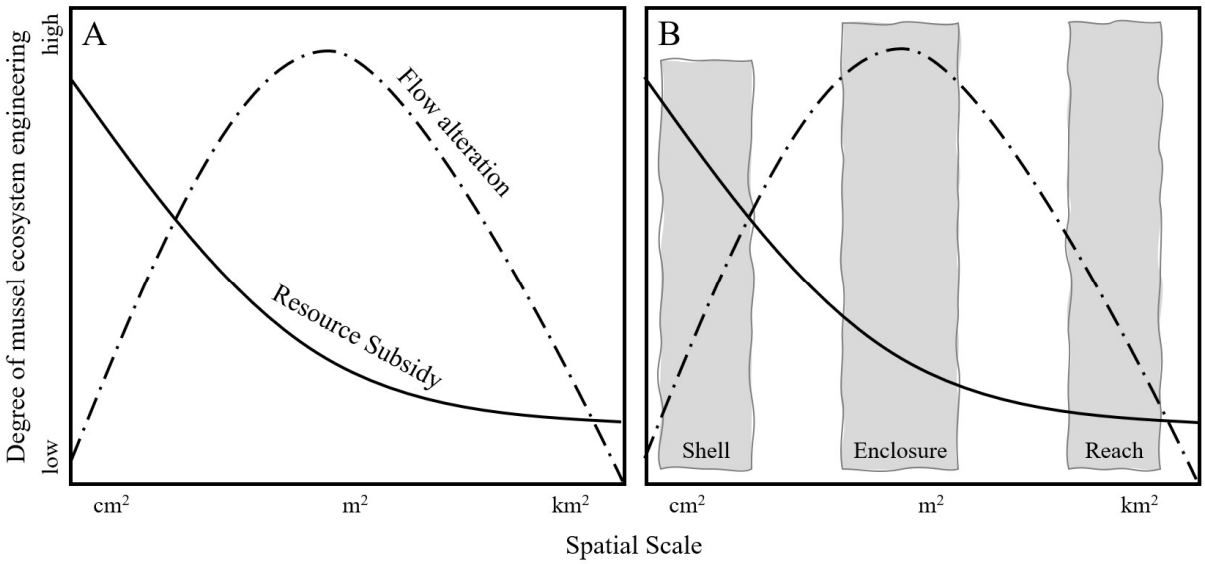

Figure 2-1 Conceptual figure of mussel engineering effects at different spatial scales

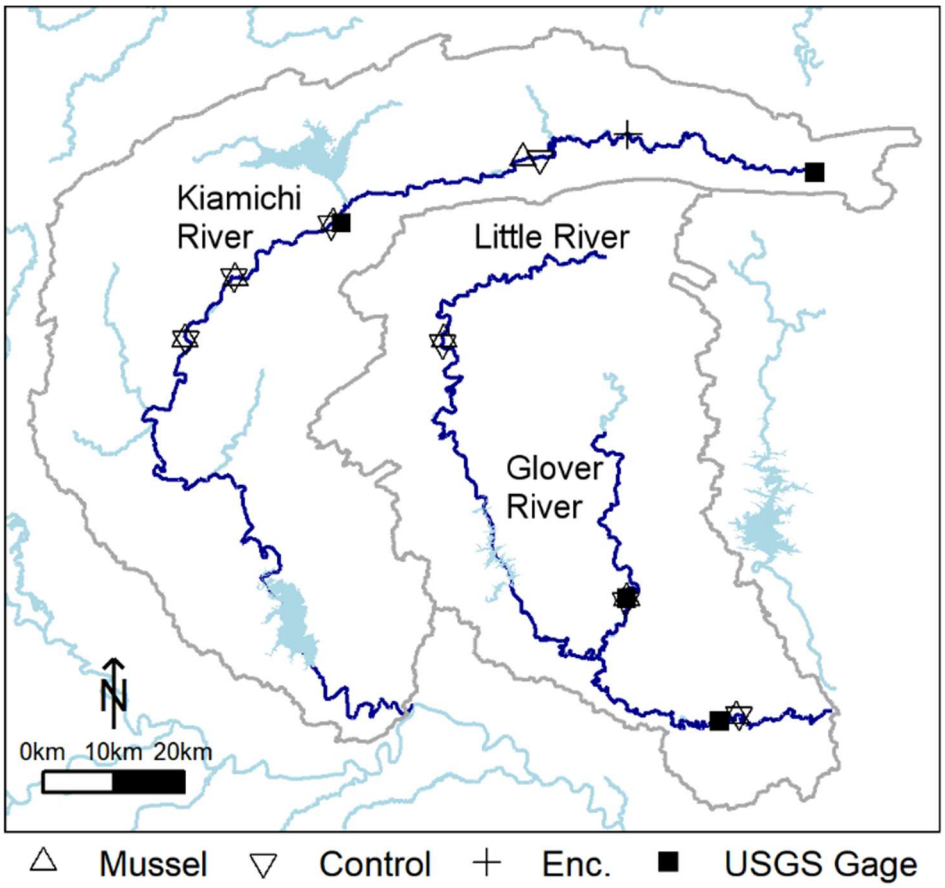

Figure 2-2. Location of field sites and enclosure experiment

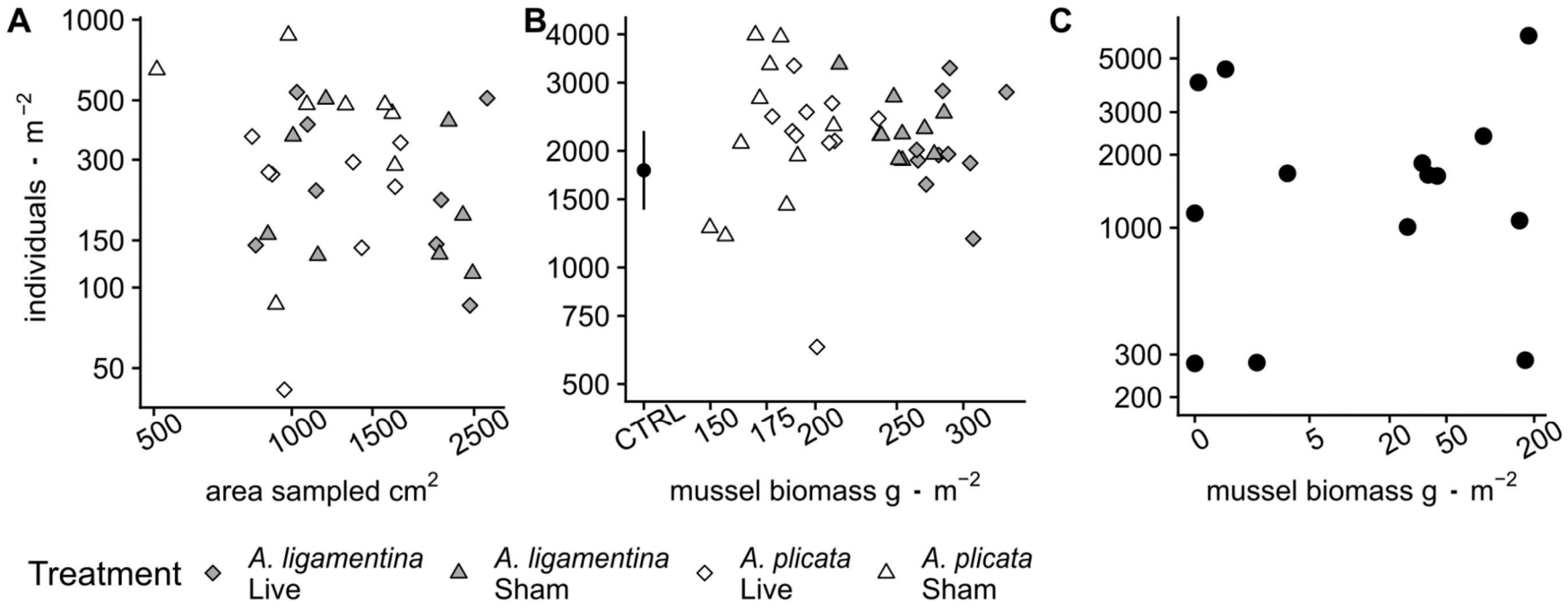

Figure 2-3. Macroinvertebrate density at each spatial scale.

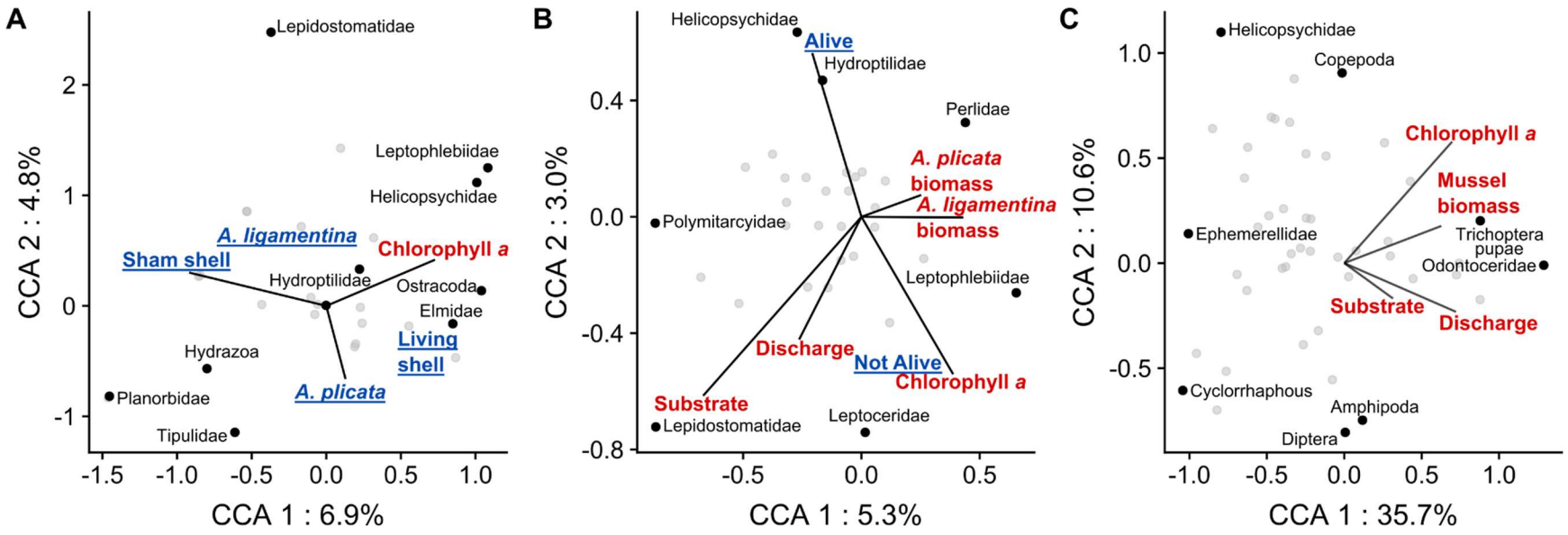

Figure 2-4. CCA of macroinvertebrate communities and environmental factors

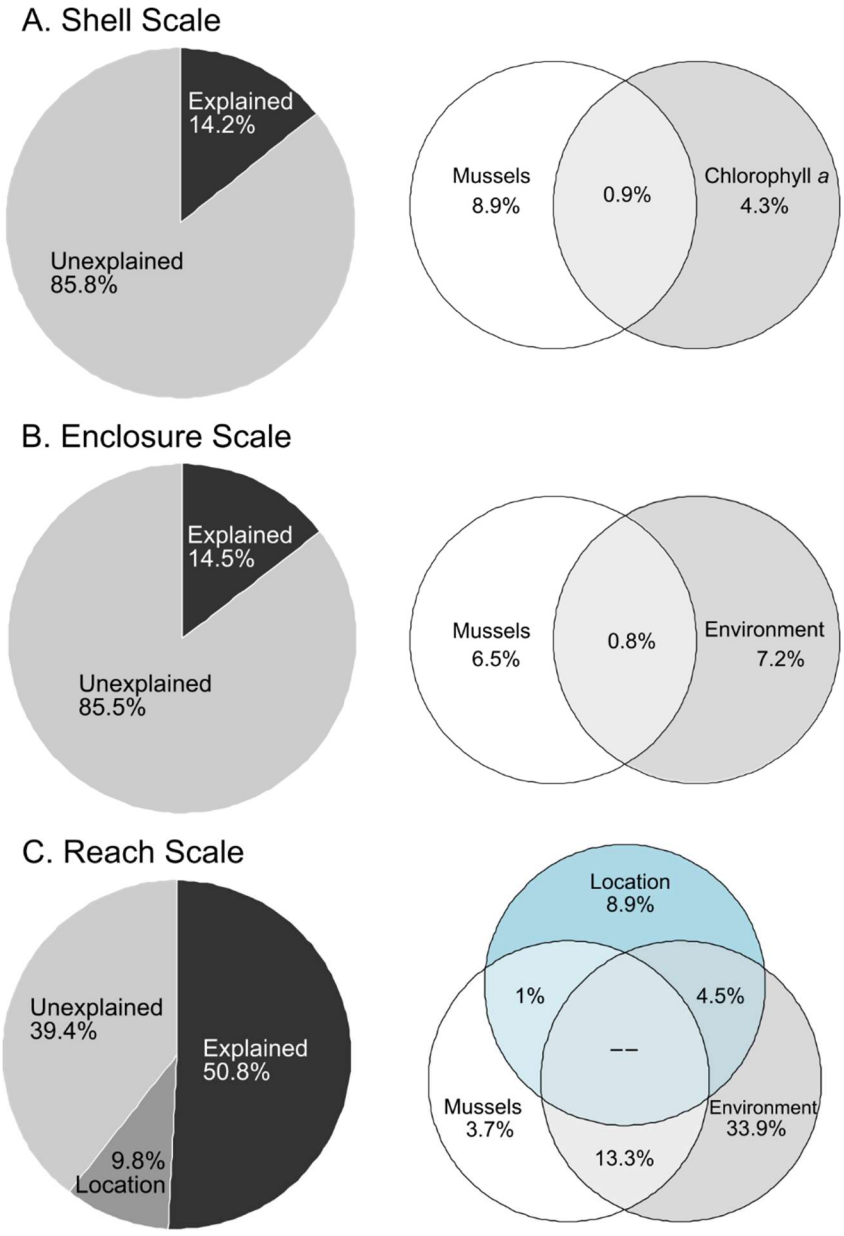

Figure 2-5. Macroinvertebrate community variation explained by the environmental variables

APPENDIX

To fully analyze our data and be clear about the decisions and information that informed our methodology, we present this appendix to describe two major decisions when conducting the constrained ordinations: to average the Surber samples taken at each reach and not include a spatial variable within the enclosure analysis.

Reach Analysis Decision

We first conducted a principle components analysis (PCA) to explore variation within our macroinvertebrate dataset. A PCA is a form of unconstrained ordination that creates orthogonal combinations of species variables to minimizes variation within the dataset; the first principle component describes the most variation within the dataset while the second then attempts to reduce the remaining variation left over from the first principle component. Samples that have similar compositions will be close together on the plot. Based on this PCA, we found that most Surber samples have similar species compositions. Generally, there was minimal variation between Surber samples collected from the same reach (Figure 2-A1). The LY, K2, GL and KS sites are exceptions of this, though the variation is greatest in the second principle component, which only accounted for 15% variation.

The data input into a canonical correspondence analysis, especially rare species, affect the results of the analysis. To explore how averaging the Surber samples potentially altered the results of our CCA, we decided to conduct a bootstrap analysis. We selected one Surber sample per reach (68 Surber samples from 14 reaches) for our community dataset and then completed the CCA; after resampling 1000 times, we report the mean and 95% confidence intervals for the first and second canonical coordinate axis for each environmental variable. These results do not contradict the results found when averaging the Surber samples at each reach (Table 2-A1).

Generally, the loadings are lower in the bootstrap analysis, presumable because of more variation within the macroinvertebrate community. Different loadings are also potentially the result of taking the average of divergent results (though with the same interpretability when considering how the environment affects macroinvertebrate communities; Figure 2-A2). We chose not to present the results of the bootstrap analysis partially because of the difficulty discussing specific taxa's affiliation with environmental constraints, which is the main purpose of constrained ordination (Figure 2-A3).

Enclosure Analysis Decision

We included a conditioned spatial variable within the Reach dataset to account for spatial autocorrelation (Figure 2-A4). We conducted a Mantel test to determine if our macroinvertebrate samples from the sediment within the enclosures was spatially autocorrelated. There was no spatial autocorrelation between the macroinvertebrate abundance based upon a Mantel test ($r = 0.089$, $p = 0.066$). Since the p value was approaching the 0.5 threshold, we decided to run a CCA with a conditioned spatial variable as well to see if it affected the enclosure CCA analysis. Spatial coordinates explained 3.8% of the variation within the macroinvertebrate community. Environmental variables continued to explain 14.4% of the variation within the macroinvertebrate community. We felt that adding more variables to an ordination that already potentially suffered from excessive explanatory variables was not necessary and didn't add or change the explanation of our data.

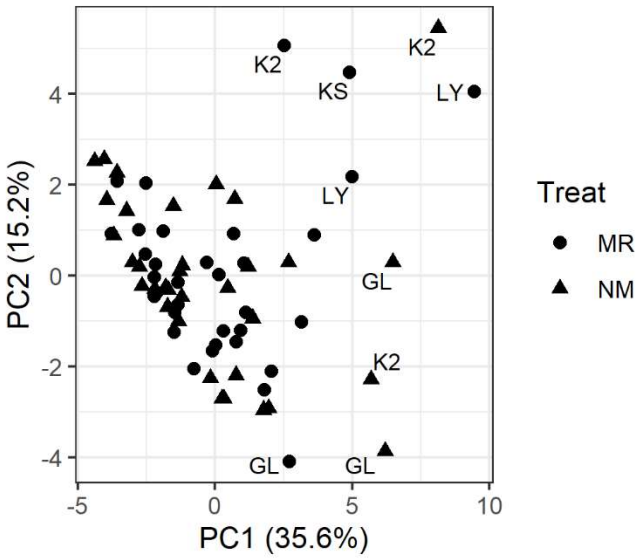

Figure 2-A1. Principle components analysis of the macroinvertebrate abundances within each Surber sample at the reaches from Southeastern Oklahoma.

Table 2-A1. Loadings on the first and second CCA axis for each dataset/analysis completed. Percentages after each axis represent the percentage of the explained variation. Standard deviations are reported within the parenthesis within the Reach Dataset (Bootstrap Analysis). The significance column reports the results of the model selection (see Table 3) and the percentage of bootstrapped models that reported the variable as statistically significant and the most informative variable.

Reach Dataset (Surber samples averaged)			Sig.
Constrained Proportion: 50.8%	*CCA 1 (63.3%)*	*CCA 2 (18.9%)*	
Discharge	0.722	0.177	*
Benthic chlorophyll *a*	0.697	- 0.232	*
Mussel biomass	0.627	0.578	
Substrate heterogeneity	0.315	-0.169	
Reach Dataset (Bootstrap analysis)			
Constrained Proportion: 42.5 %	*CCA 1 (49%)*	*CCA 2 (26%)*	
Discharge	0.407 (0.44)	- 0.084 (0.49)	34.8%
Benthic chlorophyll *a*	0.343 (0.45)	- 0.053 (0.37)	12.5%
Mussel biomass	0.297 (0.43)	- 0.009 (0.39)	4.1%
Substrate heterogeneity	0.009 (0.43)	0.144 (0.41)	16.7%
Enclosure Dataset			
Constrained Proportion: 14.5%	*CCA 1 (5.2%)*	*CCA 2 (3.0%)*	
A. ligamentina biomass	0.43	- 0.00	
Benthic chlorophyll *a*	0.39	- 0.54	
A. plicata biomass	0.25	0.07	
Live vs. control	- 0.21	0.56	
Discharge	- 0.26	- 0.42	
Substrate heterogeneity	- 0.67	- 0.62	
Shell Dataset			
Constrained Proportion: 14.3%	*CCA 1 (48.3%)*	*CCA 2 (33.9%)*	
Shell Type	0.913	- 0.319	*
Shell Species	- 0.122	0.659	
Shell Chlorophyll *a*	- 0.723	- 0.492	

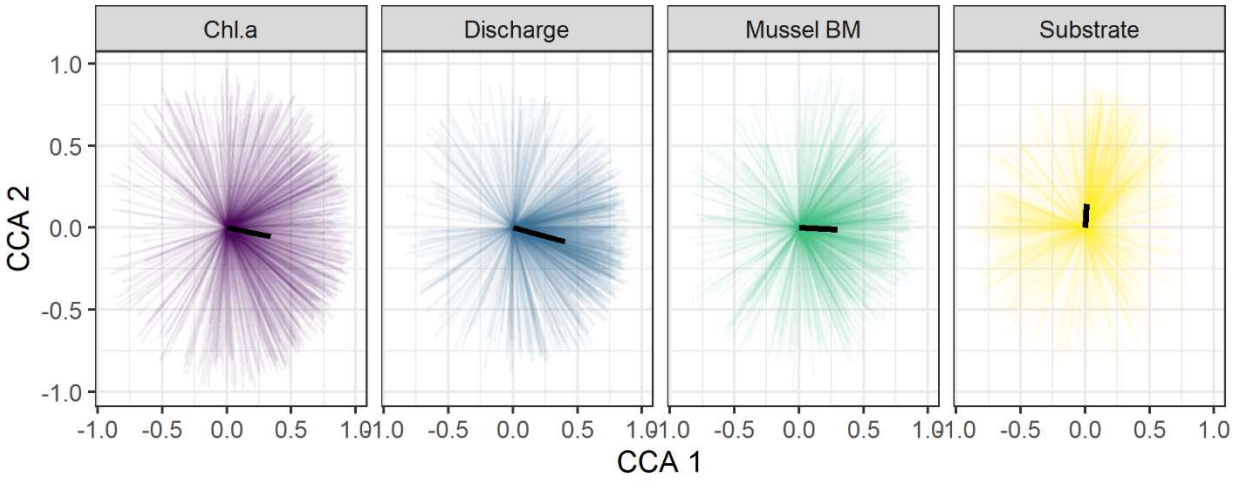

Figure 2-A2. Bootstrapped environmental vectors from the reach dataset. The dark line represents the mean of all vectors.

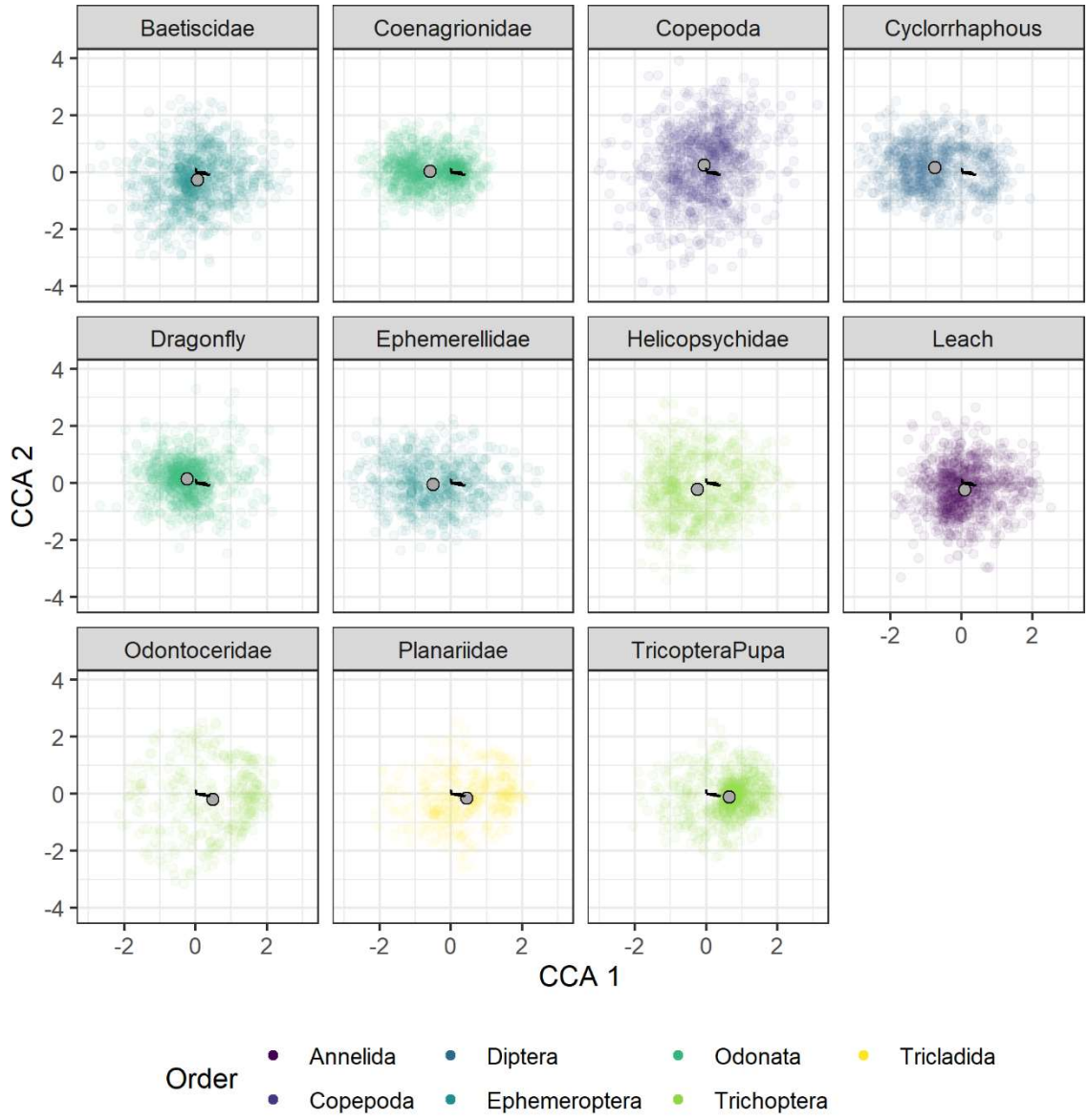

Figure 2-A3. Eleven species with either the highest or lowest loading on the first or second axis of the bootstrapped CCA. Grey points represent the mean while small dark lines represent the mean environmental vectors (as displayed in Figure A 2).

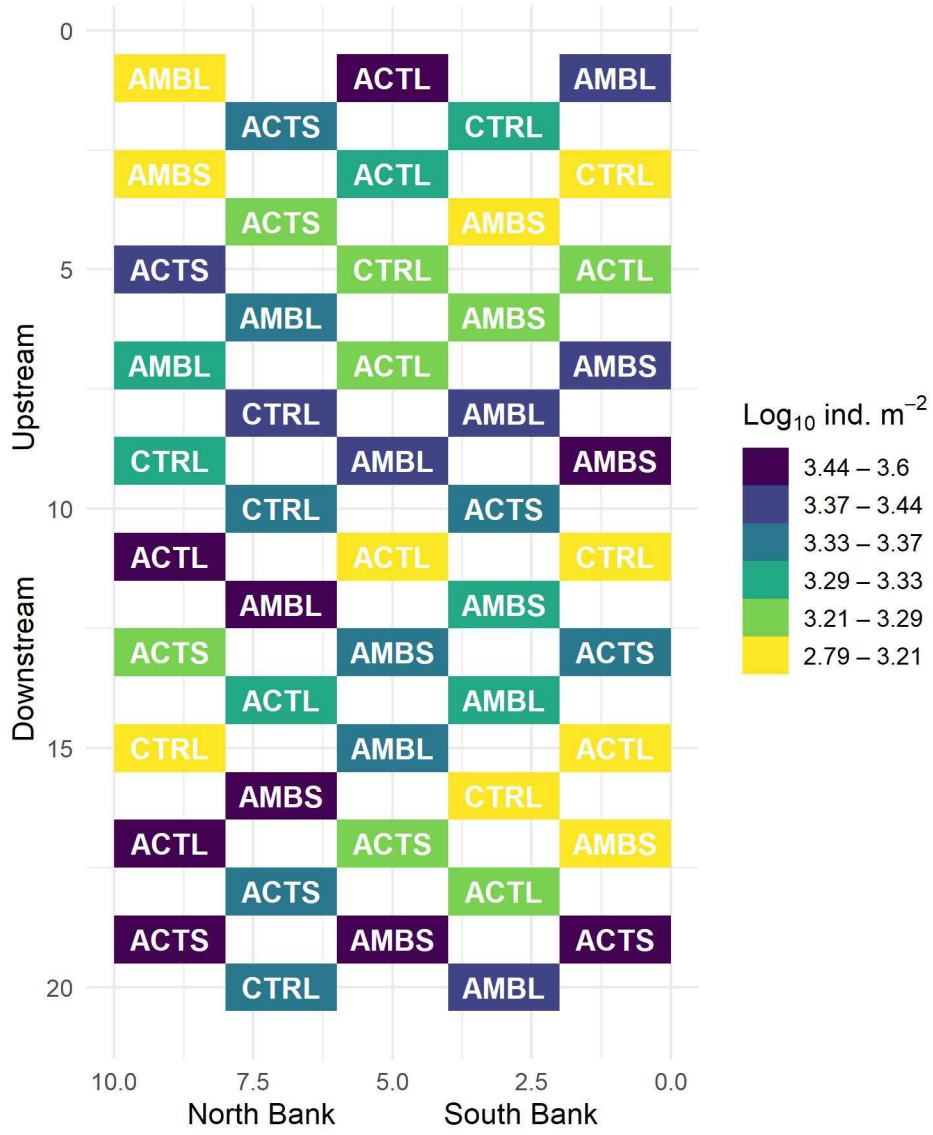

Figure 2-A4. Spatial Distribution of Invertebrate Biomass within the Enclosure Experiments. There was no spatial autocorrelation between the macroinvertebrate abundance based upon a Mantel test ($r = 0.089$, $p = 0.066$). Coordinates given as relative position to the top right enclosure.

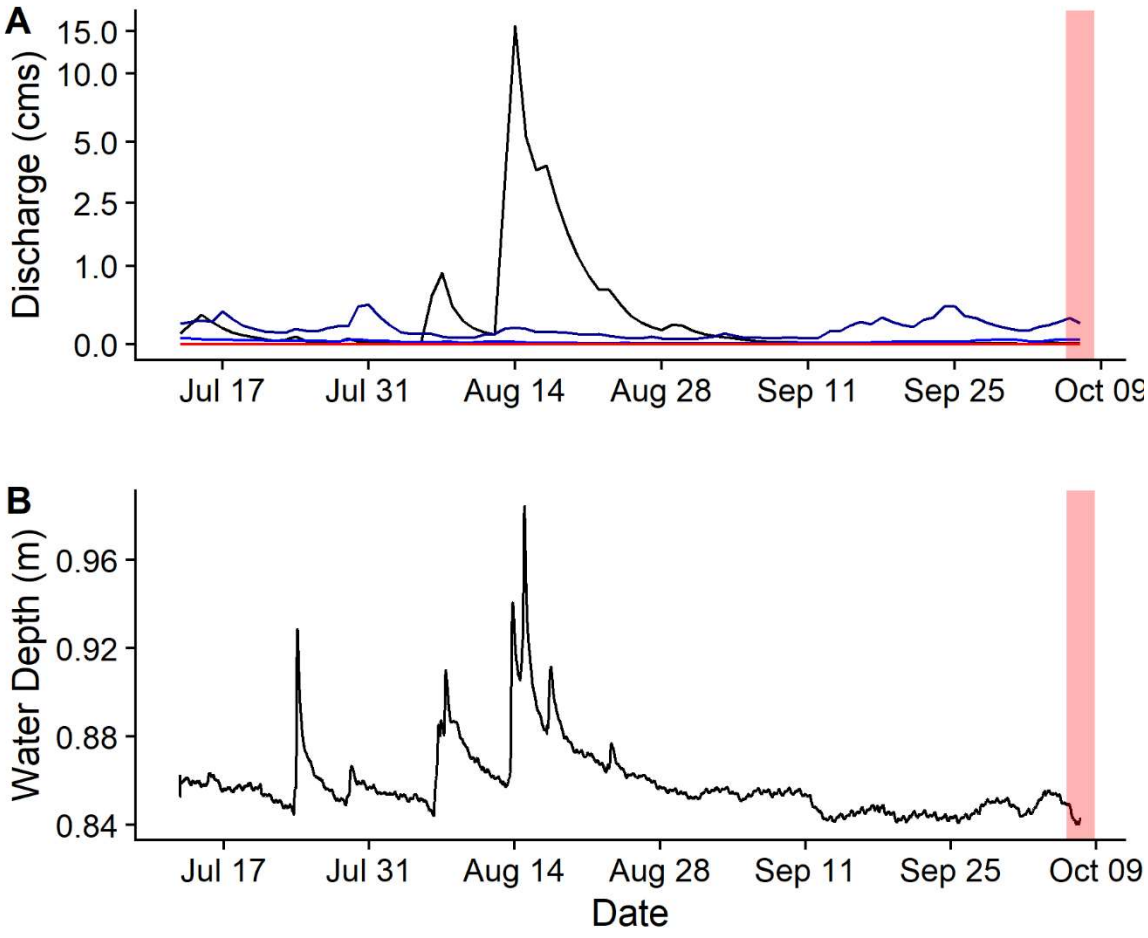

Figure 2-A5. Evidence of high flows occurring during the small scale field experiment. Discharge records (black line, red line) and statistics (dark blue line, blue line) from the USGS Big Cedar station, number 07335700 (A). Discharge from July 12 to October 8, 2017 represented by the black line; the red line represents the discharge during a large hydrologic drought in 2011. The 50% daily mean discharge value is represented by the blue line while the dark blue line represents the 75% daily mean discharge value. The water depth over our field experiment based on the measurements from a HOBO pressure sensor (B). The vertical red box represents when macroinvertebrate data were collected for this manuscript.

CHAPTER 3

DROUGHT-INDUCED, PUNCTUATED LOSS OF FRESHWATER MUSSELS ALTERS ECOSYSTEM FUNCTION ACROSS TEMPORAL SCALES

Keywords:

mass mortality event, resource pulse, die-off, drought, nutrient cycling

Published in *Frontiers in Ecology and Evolution*

DuBose TP, Atkinson CL, Vaughn CC and Golladay SW (2019) Drought-Induced, Punctuated Loss of Freshwater Mussels Alters Ecosystem Function Across Temporal Scales. *Frontier in Ecology and Evolution*. 7:274. doi: 10.3389/fevo.2-19.00274

ABSTRACT

Punctuated, mass mortality events are increasing for many animal taxa and are often related to climatic extremes such as drought. Freshwater mussels are experiencing increased mass mortality events linked to hydrologic drought. Because mussels play important functional roles in rivers it is important to understand the ecosystem effects of these die-offs. Here, we address how mass mortality events of mussels caused by drought may impact stream ecosystem function. We first present a conceptual model, based on the literature, of how mussel mass mortality should affect different ecosystem functions across various ecological time scales, from hours to decades. Next, we highlight two case studies of drought-linked, mussel-mass mortality events from rivers in the southern U.S. We then present the results of an experiment we performed quantifying the ecosystem effects of a punctuated mussel die-off. Finally, we combine our experimental results with field data from a recent mussel die-off to predict how mussel losses will influence ecosystem function. Based on the presented case studies, our mesocosm experiment, and our extrapolated nutrient pulse due to a mussel die-off, we conclude that stream ecosystems are extensively altered following mussel mass mortality events. Mussel loss is governed by drought severity, location within the river network, and species-specific drought tolerances. In the short term, decomposing carrion from mussel die-offs releases a large pulse of nutrients into the water which stimulates food web productivity. In the long term, the overall loss of mussel biomass, and the loss of functional traits as more sensitive species decline, leads to decreases in ecosystem function which may take decades to recover. Drought and human demand for water will make mussel die-offs more likely in the future and it is unlikely that drought sensitive species will recover without changes in water management and restoration of

populations through mussel propagation. Our research provides an example of how the loss of an abundant, long-lived organism has cascading and long-term impacts on ecosystems.

INTRODUCTION

Resource pulses are episodes of increased resource availability in space and time that are relatively rare, of large magnitude, and usually of short duration (Yang et al., 2008). These pulses are widespread and often result from climatic and environmental factors. Resource pulses can result from the mass die-offs of animals, such as 17-year cicadas, spawning salmon, and even wildebeest, and are increasingly recognized as important components of ecosystem function (Yang et al., 2008; Subalusky et al., 2018). Mass mortality events, or die-offs, are increasing in frequency across most taxa (Fey et al., 2015), thus it is important that we understand how these events affect ecosystem function (Baruzzi et al., 2018). In freshwater systems, unionid mussels play important structural and functional roles and are also experiencing increasing mass mortality events globally (Lydeard et al., 2004; Wenger et al., 2018) that are often linked to climatic events such as drought (Vaughn et al., 2015). Thus, they are a useful system for investigating the ecosystem effects of mass mortality events, particularly as related to environmental change (Fey et al., 2015).

Here, we address how mass mortality events of unionid mussels caused by drought may impact stream ecosystem function short-term and long-term. We first present a conceptual model, based on the literature, of how mussel mass mortality should affect different ecosystem functions across various ecological time scales, from hours to decades. Next, we highlight two case studies of drought-linked, mussel-mass mortality events from rivers in the southern U.S. We then present the results of an experiment we performed quantifying the ecosystem effects of a

punctuated mussel die-off. Finally, we combine our experimental results with field data from a recent mussel die-off to predict how mussel losses will influence ecosystem function.

How do mussel mass mortality events impact ecosystem function? A conceptual model

Freshwater mussels (order Unionida, hereafter mussels or unionids) are sedentary mollusks that live burrowed in stream sediments where they filter the water and transfer energy and nutrients from the water column to benthos. Nutrients excreted and biodeposited by mussels stimulate instream microbial, primary, and secondary production and are even exported to riparian areas (Allen et al., 2012; Vaughn, 2018). Mussels provide habitat for other organisms through the biogenic structure of their shells and by changing hydrodynamic conditions at the sediment-water interface (Sansom et al., 2018b). They are long-lived (6-100 years) with high native biodiversity in eastern North America (Williams et al., 1993), often live in high density, multi-species aggregations (hereafter mussel beds) that can persist in rivers for many decades and can make up most of the invertebrate biomass in many perennial rivers (Sansom et al., 2018a). Mass mortality of mussels has been linked to increasing drought, either from emersion (Atkinson et al., 2014) or from low dissolved oxygen and high temperatures associated with decreased water volume (Gagnon et al., 2004), as drying in streams is often accompanied by increased water temperatures and diel oxygen shifts (Mosely et al. 2015). How mussels respond to drought conditions depends on individual species' physiological tolerances, drought severity, and abiotic conditions (Haag and Warren, 2008; Golladay et al., 2004; Gagnon et al., 2004; Gough et al., 2012). When mass mortality of mussels occurs, their loss should influence stream ecosystem functions in a variety of ways across ecological time scales (Figure 3-1). We highlight these predicted effects below.

Mussel mortality feedback loop: Mussel species vary in their physiological tolerance and response to stress (Spooner and Vaughn 2008). Species that are sensitive to low oxygen (hypoxia sensitive) or higher temperatures (thermally sensitive) are less likely to survive during a hydrologic drought, thus thermally tolerant and/or hypoxia tolerant mussels become the dominant species within the assemblage (Gagnon et al., 2004; Atkinson et al., 2014). Mussel soft tissue can decay within seven days, as shown below. Decomposing soft tissue releases a pulse of nitrogen and phosphorus into the water column and interstitial spaces (Figure 3-1A) (Cherry et al., 2005; Atkinson et al., 2014). Depending on stream discharge, this nutrient pulse moves downstream over a few hours/days. Pore water can retain high nutrient concentrations longer, potentially exposing burrowing unionids to lethal nutrient concentrations (Cooper et al., 2005; Gough et al., 2012). After the loss of mussels, shifts in algal production and turbidity are driven by stream discharge. If the stream becomes intermittent (a series of drying pools), turbidity will likely decrease due to increased sedimentation while algal blooms will likely form in stagnant areas (Mosley 2015). During intermittence, the combination of reduced biofiltration and the release of nutrients into the water from mussel soft tissue decay encourages large algal blooms (Gagnon et al., 2004), which leads to high respiration rates at night, further reducing dissolved oxygen concentrations and stressing the remaining mussels, leading to additional mortality (Figure 3-1B). This cycle can also exacerbate feedback among deaths within mussel beds; algal blooms cause mortality in remaining hypoxia-intolerant bivalves, worsening algal blooms and depressing dissolved oxygen, further stressing and eventually killing hypoxia-tolerant mussels. If the stream remains perennial, turbidity will increase through the addition of suspended solids from upstream and algal blooms become less likely. Algal blooms and/or increased turbidity can persist because of a reduction in biofiltration by freshwater mussels (Figure 3-1C).

Reduced biofiltration: Immediately after a mass mortality event, biofiltration is greatly reduced in part to both residual stress on the remaining living mussels and biomass loss from mussel mortality (Vaughn et al., 2015). Biofiltration by the remaining mussels will gradually increase within the following days, but is likely to remain low until mussel biomass is replaced, unlikely for at least a decade (Figure 3-1E). Reduced biofiltration drastically increases the time required for the remaining mussels to filter a given amount of water, reducing material exchange between the water column and benthos (Baustian et al., 2014; Vaughn et al., 2015).

Reduced nutrient capacitance and storage: Short-term nutrient storage in mussel soft tissue is greatly reduced through decomposition (Atkinson et al., 2014). As mussels filter feed, they act as 'nutrient capacitors', accumulating, storing, and releasing energy and nutrients (carbon, nitrogen, and phosphorus) at different rates based on their age and species' traits (Strayer, 2014; Atkinson et al., 2018). Following mass-mortality, remaining mussel assemblages have lower abundance, age diversity, and species diversity, reducing their ability to filter seston and excrete nutrients. This reduced nutrient capacitance may result in longer nutrient spirals and more downstream transport of nutrients, likely due to an increase in nutrient uptake length (Figure 3-1D) (Atkinson et al., 2014). Shells of deceased mussels lose approximately 50% mass by 15 years through mechanical and chemical dissolution, which reduces the nutrient storage and shell habitat within the mussel bed as particle size becomes more homogeneous (Figure 3-1E) (Atkinson et al., 2018).

Changes in habitat provided by shells: Live mussels and their spent shells modify physical the environment in streams, providing unique habitat for other organisms. Tissue decay potentially creates interstitial spaces within the substrate, which can be used by both

macroinvertebrates and fish. Shells vary in shape and size across species and age and can accumulate in the sediment at different rates; thus, shell habitat can harbor variable macroinvertebrate communities depending on the shells species of origin (Bódis et al., 2014). While shells represent hard surfaces for macroinvertebrates, they dissolve over time. Shell dissolution is fastest in flowing waters with low calcium carbonate concentrations and thin, small shells dissolve faster than thicker, larger shells (Strayer and Malcom, 2007; Ilarri et al., 2015; Ilarri et al., 2019). While bivalve soft tissue decomposes quickly, shells persist for many decades (5 to 30 years), providing habitat for other stream biota (Strayer and Malcom, 2007; Ilarri et al., 2015; Atkinson et al., 2018). Over time, the benthos will be more homogenous as old shells dissolve and new relic shells are produced by a less diverse mussel assemblage ultimately altering benthic microhabitat characteristics and macroinvertebrate community structure (Figure 3-1E) (Ilarri et al., 2018).

Shifts in community composition and ecosystem function: During droughts, species sensitive to low oxygen (hypoxia sensitive) or higher temperatures (thermally sensitive) face greater risk of mass mortality leading to differential survival resulting in tolerant species becoming dominant within an assemblage, changing community structure (Gagnon et al., 2004; Atkinson et al., 2014). Surviving mussels may contribute to population recovery if conditions are suitable for reproduction. Most mussels have an ectoparasitic larval phase that requires a host fish (Barnhart et al., 2008). Drought concentrates fish into drying pools as they to attempt to escape harsh conditions or die due to increased biotic and abiotic stressors (Matthews and Marsh-Matthews, 2003; Lennox et al., 2019). While mussel reproduction is unlikely limited by host density (Haag and Stoeckel, 2011), different mussel species exhibit different host specificity and infection phenology (Barnhart et al., 2008). Thus, predicting the recruitment success is

difficult due to unionid's unique life histories. As it takes mussels anywhere from 9 months -10 years to reach sexual maturity, with most mussels reaching maturity around 4 years old (Haag, 2012), thus in die-off affected areas, biomass is unlikely to rebound for at least a decade. Future mussel assemblage structure is dependent on the surviving mussel assemblage, the surviving fish assemblage, and the recurrence frequency of droughts. If drought frequency decreases or remains constant, the mussel community could return to its former, pre-drought structure if no mussel species were extirpated from the river basin. If droughts increase in frequency and severity as projected in many regions (Palmer et al., 2008; USGCRP, 2017), we anticipate the mussel community will become dominated by tolerant mussel species (Figure 3-1E).

Mussel species with different temperature tolerances have different, temperature-dependent biofiltration and nutrient excretion rates. Thus, when the proportion of thermally sensitive vs. tolerant species in a mussel assemblage changes, this can impact ecosystem function (Spooner and Vaughn, 2008; Vaughn et al., 2015; Atkinson et al., 2018). For example, in rivers in southern Oklahoma, *Actinonaias ligamentina* is a thermally sensitive species with higher filtration and nutrient excretion rates at summer temperatures than other mussels in the assemblage. Because of its temperature intolerance, it also has a higher mortality rate during drought than other species. Thus, when this species is lost, the overall biofiltration (Figure 3-1C) and nutrient recycling capacity (Figure 3-1F) of the community is decreased for an extended time period, even if the biomass of other species remains stable (Vaughn et al., 2015). Further, mussel species excrete at different N:P ratios, and losses can also lead to shifts in excretion stoichiometry (Figure 3-1F) (Atkinson et al., 2018). These changes can cascade through the food web impacting algal, macroinvertebrate (Novaias et al., 2017) and even fish dynamics.

TWO CASE STUDIES OF DROUGHT-DRIVEN MUSSEL LOSSES IN THE SOUTHERN UNITED STATES

Drought-induced mussel mass mortality events have been documented for two diverse, well-studied river systems in the southern U.S., the Lower Flint River in Georgia and the Kiamichi-Little River system in Oklahoma (Figure 3-2). These case-studies allow for a deeper understanding of how drought affects mussel assemblages, the subsequent changes in stream ecosystems, and the potential recovery time for mussel assemblages.

Lower Flint River, Georgia

The lower Flint River of southwestern Georgia experienced an extended period of below normal rainfall from 1999 until 2013. This period included three multiyear droughts that were classified as severe/exceptional. The summer of 2000 was particularly disastrous for unionids as streams in the region experienced unprecedented low flows and transitioned from perennial to intermittent. Forty-six historically-species-rich sites in lower Flint tributaries were surveyed in 1999 prior to drought onset, and a subset of these were resampled in 2000 (Gagnon et al., 2004). Stream drying had not been previously observed but became common during subsequent growing seasons (Rugel et al., 2012). Stream flow was essential for maintaining dissolved oxygen concentrations within the tolerances of freshwater mussels; dissolved oxygen between 5 mg L^{-1} and 3 mg L^{-1} resulted in 24% mortality and when dissolved oxygen fell below 3 mg L^{-1} up to 76% of mussels died (Gagnon et al., 2004; Golladay et al., 2004). These degraded physicochemical conditions differentially impacted species within the mussel communities. Riffle specialists in medium-sized streams suffered the highest mortality, while drought-tolerant, small stream species and species in larger tributaries whose habitat was buffered from drought

conditions fared better (Gagnon et al., 2004). In medium-sized streams, community composition shifted towards more generalist species from riffle specialists (Gagnon et al., 2004).

The lower Flint River has been surveyed since this drought. Through 2013, there was little evidence of recovery from mortality associated with the 1999-2001 drought (Smith et al., 2015). During most summers since the initial drought, conditions were stressful, likely preventing the reproduction of surviving unionids. Reproduction of mussel populations, as evident from observation of juvenile mussels, was not apparent until rainfall approached average levels (2013-2015) (Smith et al., 2015). The extended period of below normal rainfall (1999-2013) and subsequent below normal stream flows were likely exacerbated by anthropogenic water withdrawal; the mid reaches of tributaries of the lower Flint cross the Dougherty Plain physiographic district, which is a recharge area for a heavily developed agricultural water source (Golladay et al., 2004). This case study provides evidence that mussel biomass might not recover from mass mortality events for over a decade and that anthropogenic and climate alterations can alter stream benthic communities for extended periods.

Kiamichi and Little Rivers, Oklahoma

The Kiamichi and Little Rivers in southeastern Oklahoma are adjacent, major tributaries to the Red River. This region experienced a period of exceptional drought during 2011-12 where the Kiamichi River experienced 84 days of no flow (defined as discharge < 0.01 m^3 s^{-1}) and 36 weeks of extreme low flow, defined as flows below the 10^{th} percentile of flow frequency (Atkinson et al., 2014). The Little River, and its major tributary the Mountain Fork River, experienced 39 and 40 weeks of extreme low flow, respectively (Atkinson et al., 2014).

These severe drought conditions led to a mass mortality event as mussels became isolated in shallow drying pools or emersed. Mussel losses and their effects on ecosystem function were

documented in two related studies. Atkinson et al. (2014) sampled mussels at three sites in each river prior to the drought (2010) and at the end of the drought (2012) and assessed changes in mussel abundance and mussel-provided nutrient cycling and storage. Sixty percent of unionids died during the drought, but thermally sensitive species had a higher mortality rate, resulting in a community shift towards more thermally tolerant species. In the second study, Vaughn et al. (2015) compared mussel biomass and ecosystem services (biofiltration, nutrient cycling, and nutrient storage) at four sites in the Kiamichi River across several decades (1991, 2004, 2011). 1991 was a wet period and 2004 and 2011 were drought periods with significant mussel losses. They found that mussel biomass decreased over 60% across these sites and that ecosystem function losses mirrored the biomass losses. The sites experienced mussel biomass losses of ~28% and corresponding declines in nitrogen recycling (22%), phosphorus recycling (15%), and ~30% declines in areal storage of nitrogen and phosphorus (Vaughn et al., 2015).

AN EXPERIMENT QUANTIFYING THE EFFECTS OF A MUSSEL DIE-OFF ON ECOSYSTEM FUNCTION

While case studies have documented how native mussel communities change after mass mortality events, no studies have experimentally demonstrated how these losses impact ecosystem function. With our conceptual model and case studies in mind, we designed an experiment to measure ecosystem function changes that occur following a punctuated mussel mass mortality event. We conducted a mesocosm experiment at the University of Oklahoma Biological Station in the summer of 2018 where we induced mussel mortality and measured effects on ecosystem structure (water column nutrient concentrations and algal abundance) and ecosystem function (decomposition rates and ecosystem metabolism) over time. We predicted

that decaying mussel tissue would increase nutrient concentrations, which would stimulate both algal growth and microbial respiration and decomposition.

Mesocosm experiment methods

We used 18, 1.52 m diameter, 946 L circular tanks to simulate drying stream pools. Each mesocosm (tank) was lined with ~15 cm of gravel (1:1 ratio of 10mm and 38mm diameter gravel). We had 9 control mesocosms with no mussels and 9 mesocosms containing 31 mussel individuals, to replicate a natural mussel community in the region. Each mussel treatment mesocosm contained 13 *Actinonaias ligamentina*, 9 *Cyclonaias pustulosa*, 5 *Amblema plicata*, two *Tritogonia verrucosa*, one *Lampsilis cardium*, and one *Plectomerus dombeyanus*. This represented a low, but natural density of mussels (11.9 mussels/m^2) and reflected the freshwater mussel community of the upper Kiamichi River (Atkinson et al., 2012).

We describe sampling events and present our results relative to the day of the mussel mass mortality event: negative values indicate days before and positive values days after the mussels died. We filled mesocosms with water 12 days (day -45; see Table 3-A1 for sampling dates and measurements) before adding mussels to allow the mesocosms to be naturally colonized by algae and macroinvertebrates. On day -33, we added mussels. On day -14, we introduced 10 largemouth bass (*Micropterus salmoides*; mean standard length = 95 mm, SD = 16 mm) to simulate how fish are concentrated in drying pools during early periods of drought. We removed the fish on day -2 to simulate their movement downstream during the drought as drying pools became too stressful for them (Magoulick and Kobza, 2003). Fish may have impacted water column nutrients on day -3 but had little impact on mesocosm nutrient concentrations and algal abundance (see Results below). We induced a punctuated mass mortality event on 2 July 2018 (day 0) by sacrificing the mussels in 5 of the 9 mussel mesocosms, while maintaining the 9

non-mussel controls. To produce the carrion for this stage of this experiment, we cut the adductor muscles of 155 mussels. We returned the mussel carrion to the mesocosms to allow for natural decomposition of soft tissue.

We sampled mesocosms 3 times before and 4 times after the mass mortality event, resulting in the following sampling days: -20, -15, -3, 4, 11, 25, and 39. On each sampling day we measured dissolved oxygen (DO), conductivity, and water temperature at midday (Table 3-A2). To measure water column phosphorus and nitrogen concentrations, we collected 20 mL filtered water samples (Grade F, 0.7 μm pore size, Sterlitech Kent, Washington) and froze them for subsequent nutrient analysis. We lost nutrient samples from day 11, thus we resampled the mesocosms on day 18. We filtered two water samples (Grade A, 1.6 μm pore size, Sterlitech Kent, Washington) from each mesocosm to quantify water column chlorophyll *a*. Filters were frozen for later chlorophyll estimation. On day -33, we placed six 7.6 cm^2 clay tiles with a 27.5 mm^2 fritted glass disc attached with silicone (LECO cover crucible AL P 1000; GE Silicone 1* All Purpose) on the substrate surface to allow algal colonization for sampling of benthic algal production. We removed two glass fritted discs on each sampling day and froze them for later estimation of benthic algal biomass.

We quantified soluble reactive phosphorus (SRP) with the colorimetric method (EPA Method 365.3; Murphy and Riley, 1962; Stainton et al., 1974) and ammonium (NH_4-N) using the phenol method (5.2.6 EPA Method 350.1; ASTM, 2012) for the filtered water samples. To measure chlorophyll *a* concentration, we cold-extracted water column (filters) and benthic (fritted discs) samples with acetone and measured the extractant spectrophotometrically with a correction for pheophyton (ASTM, 2012).

We followed Tank et al. (2017) to measure ecosystem metabolism as gross oxygen production on days 4, 11, 25 and 39. We quantified ecosystem metabolism by measuring dissolved oxygen production and respiration in light and dark cycles, respectively, on the glass fritted discs in 50 mL centrifuge tubes. We measured dissolved oxygen (HACH HQ40d multiple parameter meter, Loveland, Colorado) to estimate initial oxygen concentrations. We placed fritted disks in centrifuge tubes filled with the respective mesocosm's water and sealed the tubes. After allowing the discs to metabolize for an average of 1.75 hours (SD = 0.23 hours) in a common mesocosm, we re-measured the dissolved oxygen within the tubes. We then removed the water and repeated the filling process with the same tube/glass fritted disc pair. After filling the tubes, we immediately placed them in the dark in a common mesocosm for an average of 2.62 hours (SD = 0.47 hours). We then measured final dissolved oxygen and collected and froze the discs. Gross primary production (mg DO cm^{-1} hr^{-1}) was calculated from the addition of net primary productivity (difference in DO in the light cycle) and the absolute value of the respiration (DO difference in the dark cycle).

To determine the decay rates of mussel tissue, we placed the combined shell and soft tissue of each of 5 *A. ligamentina* in fine mesh bags (pantyhose) in each mortality treatment (original weight mean = 297.8 g, range = 77.5 g - 461.5 g). We chose *Actinonaias ligamentina* because it was the most abundant mussel species within each mesocosm, is thermally sensitive, and most likely to be lost during a drought (Atkinson et al., 2014). We weighed the bags every 12 hours for 4.5 days, and then daily for 10 days until the shells were empty and the weight was stable. We calculated total tissue (including both the soft tissue and the shell) decay rates and soft tissue decay rates following Strayer and Malcom (2007). Soft tissue decay rates were determined by assuming the minimum weight measurement consisted of only shell material and

subtracting that measurement from each weight measurement. To examine organic matter decomposition rates, we incubated three cotton strips (8cm x 25mm) in the bottom of each mesocosm beginning on day 7 (Tiegs et al., 2013). We removed strips on days 18, 28, and 38; these dates mirror the decomposition study by Novaias et al. (2017) and reflect incubation times of 11, 21, and 32 days. Strips were preserved with 85% ethanol and later dried at 40°C. We determined the tensile strength of each cotton strip using a tensiometer (Mark 10 MG100) torn at 2 cm/min following Tiegs et al. (2013). As such, the tensile strength reflects the remaining organic matter of the original cotton strip and is reported in pounds.

All statistical analyses were conducted with R Core software version 3.5.3 (R Core Team, 2019). We used mixed linear models to test for differences among our dependent variables based on the fixed factor treatment, the fixed continuous variable sampling date, the interaction between the fixed variables, and a random intercept accounting for mesocosm. We included the mesocosm as a random intercept to account for the repeated measures over time on each replicate; this allows each mesocosm to have a different starting value and accounts for mesocosm dependency. Each model was checked visually for normality and homogeneity of variance of its residuals (Zuur et al., 2009); we $\log_{10}$ transformed water column ammonium, water column chlorophyll *a*, and benthic chlorophyll *a* to meet these assumptions. We used the function *lmer()* (from the R package *lme4* (Bates et al., 2015)) to perform all mixed models as we had different sample sizes for each treatment: 9 control mesocosms, 5 mortality mesocosms, and 4 live mussel mesocosms. We used the function *anova()* to conduct a type III ANOVA with Satterthwaithe's method and obtain p-values for all models as implemented in the *R* package *lmerTest* (Kuznetsova et al., 2017). We then used Tukey post hoc tests to conduct multiple

comparisons if the null hypothesis was rejected for each dependent variable as implemented in the package *emmeans* (Lenth, 2018).

Mesocosm experiment results

Mussel decay: *Actinonaias ligamentina* soft tissue and shell had an average instantaneous decay rate of -0.016 day^{-1} across all mortality mesocosms. Within 7 days, most soft tissue had decayed within the bags. The average instantaneous decay rate of the soft tissue alone was -0.336 day^{-1}. We did not observe shell dissolution within the time frame of our experiment.

Nutrients: Following the mass mortality event, the mortality treatments had a large increase in ammonium. Ammonium (NH_4-N) was significantly higher in the mortality treatments compared to the control treatments ($F_{2,120} = 10.92$, $p < 0.001$; Figure 3-3A). Sampling day was also significant in predicting ammonium amount in the system ($F_{1,120} = 14.34$, $p < 0.001$). The interaction between treatment and sampling day was not statistically significant ($F_{2,120} = 1.17$, $p = 0.31$). Overall, ammonium in the water column significantly increased by 94.4% directly after the mass mortality event, while ammonium in the control mesocosm increased by 9.6%, although this was highly variable (ranged from 84.1% to -62.5%). SRP generally increased during the experiment ($F_{1,103} = 6.91$, $p < 0.01$; Figure 3-3B). While SRP was not significantly different between treatments ($F_{2,16} = 0.37$, $p = 0.70$), the interaction between treatment and sampling day was statistically significant ($F_{2,103} = 4.67$, $p < 0.02$). Between the die-off and the end of the experiment, SRP increased 38% in tanks that experienced the mussel die-off but decreased by 51% in control tanks.

Primary production and ecosystem metabolism: Mortality treatments had higher gross primary production than the control mesocosms ($F_{2,30} = 4.11$, $p < 0.03$). Mortality treatments had higher gross primary production than live treatments, but there was not a statistical difference

between the two groups ($t_{22} = 2.27$, $p = 0.08$). Sampling day was significant in explaining gross primary production ($F_{1,54} = 77.81$, $p < 0.001$). The interaction between the two terms was also not statistically significant ($F_{2,54} = 1.94$, $p = 0.16$). There was not a difference in water column chlorophyll *a* concentration between treatments ($F_{2,19} = 0.54$, $p = 0.59$), although water column chlorophyll did increase through time ($F_{1,105} = 12.51$, $p < 0.001$; Figure 3-3C). The interaction between the two terms was also not statistically significant ($F_{2,105} = 0.76$, $p = 0.47$). In late July and August, some control and live mesocosms experienced algal blooms, while mortality mesocosms had low water column chlorophyll *a* concentrations. Benthic chlorophyll *a* concentration was higher in mortality and live treatments than control treatments ($F_{2,19} = 9.10$, $p < 0.002$; Figure 3-3D). Sampling day did not predict benthic chlorophyll *a* concentration ($F_{1,106} = 0.59$, $p = 0.45$) and the interaction between treatment and sampling day was not significant ($F_{2,106} = 0.89$, $p = 0.41$). Note that ecosystem metabolism and benthic chlorophyll *a* concentrations are significantly correlated as they were measured from the same glass fritted discs ($R^2 = 0.28$, $p < 0.001$). While these variables are correlated, one measures ecosystem structure (biomass) and the other ecosystem function (respiration).

Organic matter decomposition: Higher tensile strength corresponds to a higher percentage of the original remaining cotton strip; thus, higher tension indicates less decomposition. Tensile strength of the cotton strips decreased with time ($F_{1, 36} = 4.95$, $p < 0.04$) and was significantly different between treatments ($F_{2,18} = 5.60$, $p < 0.02$; Figure 4). The mean tensile strength of an unincubated cotton strip is 65.6 lbs. (SD = 2.0 lbs.).

Below, we apply these results to an actual mussel die-off to extrapolate how mussel die-offs can impact nutrient cycling in river reaches following a mass mortality event.

SCALING UP: SHORT AND LONG-TERM NUTRIENT RELEASES FOLLOWING A MASS MORTALITY EVENT

As described above, an extreme drought in the Kiamichi River in 2011 led to massive mussel mortality. We combined quantitative data on these mussel losses with nutrient release data from our mesocosm experiment to extrapolate how mussel losses impact short and long-term nutrient cycling and storage for several river reaches.

On July 30 and 31, 2011, we (CLA and CCV) sampled mussels at three sites (K2, K3 riffle, and K3 pool) severely impacted by the drought. The K2 and K3 pools were isolated pools that still contained water but were very shallow (< 10 cm) and warm (K3 exceeded 40°C) (Vaughn et al., 2015). K3 contained a riffle that was completely dry. For K2 and K3 pools, we measured mussel abundance and composition by sampling ten, 0.25 m^2 quadrats following Vaughn et al. (1997); we identified and measured the length of both dead and live individuals. We returned live individuals to the mussel bed. For the K3 dry riffle we laid out 10 transects across the dry mussel bed and identified shells from 14 quadrats across each transect. We used species-specific, length-soft tissue dry mass regression equations (Hopper et al., 2018) to calculate the soft tissue mass of each mussel. We calculated areal nutrient pulses ($\mu g\ L^{-1}\ m^{-2}$) released to the river as a consequence of mussels dying as the product of nutrients released by decomposing mussel tissue to the water column in the mesocosm at sampling day 4 ($\mu g\ L^{-1}\ g^{-1}$) by the biomass loss of mussels at a site on an areal basis ($g\ m^{-2}$). Based on our extrapolation, this mussel die-off resulted in a large pulse of both nitrogen and phosphorus (Figure 3-5). This nutrient pulse is equivalent to the areal nitrogen excretion of a mussel assemblage for 20 hours, phosphorus excretion for 195 hours (Atkinson et al., 2018), and to the phosphorus release from

dissolving shells for two years (Wegner et al., 2018). This represents a large pulse of phosphorus that likely stimulates primary production.

Freshwater mussel soft tissue represents short term storage of nutrients since the soft tissue decays quickly, while the shell represents long term nutrient storage. We wanted to determine the role of shell material as a potential long-term nutrient sink and site of nutrient release following mortality. While shell decay can be highly variable in freshwater ecosystems (Strayer and Malcom, 2007), we used the average shell decay rates from a previously published study on the Kiamichi and Little Rivers in Oklahoma (Atkinson et al., 2018) and the Sipsey River, Alabama (Atkinson, *unpublished*) to estimate spent shell biomass and nutrient release (C, N, and P) over time. Specifically, using the average decay rate ($k = -0.053$ year^{-1}) and the average shell size per site, we estimated shell biomass (g m^{-2}) over an 80-year timeframe and the subsequent nutrient release, assuming a constant rate, from spent shells following the punctuated mortality event in the Kiamichi River in 2011. We expect this estimation to be realistic as the shell decay rate was measured over a year with shell from the Kiamichi River, thus accounting for how discharge, water chemistry, and season affects shell decay rates (Strayer and Malcom, 2007; Ilarri et al., 2019).

At K3, the mass of relic shells (2.4 kg m^{-2}) exceeded shell mass of living mussels (1.6 kg m^{-2}), while all mussels in the dry reach perished, resulting in 1.7 kg m^{-2} of shell material exposed. While some shell material may have been exported due to terrestrial scavengers, we assumed that it remained in the stream channel and was submerged once flow resumed. Site K2 did not experience complete drying and the low flows did not result in as much mortality as K3 and resulted in 1.5 kg m^{-2} of relic shell while 5.0 kg m^{-2} was maintained in live mussels. Based on the modeling described above, shell material decay (Figure 3-6A) would result in a slow

nutrient release at each of these sites (Figures 3-6B-D). For example, 413 g C m^{-2}, 4.8 g N m^{-2}, and 0.4 g P m^{-2} remained in the shell of dead mussels at K3 in the reach that did not dry, which would then be slowly released by shell decayed (Figures 3-6B-D). The surviving, living mussels at K3 still maintained nutrients in their shell and continued to store nutrients and potentially grow and store additional material. When mortality is equal to the production of shells, shell mass is maintained at a steady state. But large-scale die-offs lead to a pulse in relic shells and lower production of shell material. This represents a long-term loss of mussel-driven nutrient storage and shell habitat within stream reaches (Wenger et al., 2018).

IMPLICATIONS & CONCLUSIONS

Based on the presented case studies, our mesocosm experiment, and our extrapolated nutrient pulse due to a mussel die-off, we conclude that stream ecosystems are severely altered following mussel mass mortality events. Mussel loss is governed by drought severity, location within the river network, and species-specific drought tolerances. In the short term, decomposing carrion from mussel die-offs releases a large pulse of nutrients into the water which stimulates food web productivity. In the long term, the overall loss of mussel biomass, and the loss of functional traits as more sensitive species decline, leads to decreases in ecosystem function which may take decades to recover (Figure 3-1).

While we have frequently observed algal blooms in the field following mussel die-offs, we did not observe algal blooms within our mesocosm experiment. In our small mesocosms, the decomposition of mussel tissue likely altered the microbial community to favor heterotrophs, which potentially out-competed water column algae for available nutrients. Our extrapolation from the observed mussel die-off in the Kiamichi River predicted a large phosphorus pulse. After inducing a die-off of the invasive bivalve *Corbicula*, McDowell et al. (2017) observed a smaller

increase in ambient phosphorus concentration than expected. They posited that algal uptake of SRP accounted for difference between the predicted increase in water column SRP and what was measured. Further exploration of the interacting factors driving algal bloom formation after mussel die-offs during drought is warranted.

The frequency and severity of hydrologic drought is predicted to increase in the southcentral and southeastern U.S. as a consequence of climate change and increasing human demand for water (Baron et al., 2002; Golladay et al., 2016). This region also contains the highest diversity of freshwater mussels globally (Williams et al., 1993; Haag, 2010). Thus, future mussel mass mortality events are highly likely and we need to both understand their ecological effects and how to mitigate them. Individual mussel species' tolerances to maximum water temperature and minimum dissolved oxygen concentrations vary and are an area of active research (Jeffrey et al., 2018; Archambault et al., 2014). Understanding how mussels acclimate and potentially adapt to increased water temperatures and reduced water availability will be critical to protecting this diverse guild (Galbraith et al., 2012; Gough et al., 2012). However, it is unlikely that the drought sensitive species will rebound to their former abundance without changes in water management and restoration of populations through mussel propagation.

Freshwater mussels are not the only organism threatened by mass mortality events and rivers are not the only ecosystem altered through these events. Our research provides an example of how the loss of an abundant, long-lived organism has cascading and long-term impacts on ecosystems. These impacts are analogous to loss of a forest in terrestrial ecosystems; habitat provision and nutrient sequestration is altered as the community shifts and takes decades to rebound (Ellison et al., 2005; Boyd et al., 2013). The loss of this long-lived organism and the subsequent release of this nutrient pulse has large impacts on stream ecosystems.

ACKNOWLEDGMENTS

TPD, CCV and CLA designed the mesocosm experiment and TPD performed it. CLA, CCV and SWG provided field data on mussel losses and shell dissolution rates. TPD performed analyses and wrote the manuscript with input from all authors.

Funding to conduct the mesocosm experiment was provided by a University of Oklahoma Biological Station fellowship to TPD and NSF DEB-1457542 to CCV. Oklahoma mussel surveys were funded by the Oklahoma Biological Survey and an EPA STAR fellowship to CLA. Georgia mussel surveys were funded by the Jones Center at Ichauway, Georgia Department of Natural Resources, and The Nature Conservancy. We appreciate field and laboratory help from K. Ashford, M. Carman, N. Ferreira Rodríguez, J. Hartwell, E. Higgins, J. Lopez, R. Prather, B. van Ee, and M. Winebarger. We thank the Vaughn lab, Atkinson lab, D. Knapp, C. Curry, M. Patten, J. Wesner, and three anonymous reviewers for their advice on the manuscript. Fish were handled in accordance with the recommendations of American Fisheries Society's Guidelines for the use of Fishes in Research. The protocol was approved by the University of Oklahoma's Institutional Animal Care and Use Committee (Protocol number R17-023). This paper was completed as part of a dissertation at the University of Oklahoma and is a contribution to the program of the Oklahoma Biological Survey.

REFERENCES

Allen, D.C., Vaughn, C.C., Kelly, J.F., Cooper, J.T., and Engel, M.H. (2012). Bottom-up biodiversity effects increase resource subsidy flux between ecosystems. *Ecology* 93(10), 2165-2174.

Archambault, J.M., Cope, W.G. an Kwak, T.J. (2014). Survival and behaviour of juvenile unionid mussels exposed to thermal stress and dewatering in the presence of a sediment temperature gradient. *Freshw Biol* 59(3), 601-613.

ASTM [American Society for Testing and Materials]. (2012). *Standard methods for the examination of water and wastewater*. American Public Health Association, American Water Works Association and Water Environment Federation, Washington, D.C., USA.

Atkinson, C.L., Julian, J.P., and Vaughn, C.C. (2012). Scale-dependent longitudinal patterns in mussel communities. *Freshw Biol* 57(11)**,** 2272-2284. doi: doi:10.1111/fwb.12001.

Atkinson, C.L., Julian, J.P., and Vaughn, C.C. (2014). Species and function lost: Role of drought in structuring stream communities. *Biol Conserv* 176**,** 30-38. doi: 10.1016/j.biocon.2014.04.029.

Atkinson, C.L., Sansom, B.J., Vaughn, C.C., and Forshay, K.J. (2018). Consumer aggregations drive nutrient dynamics and ecosystem metabolism in nutrient-limited systems. *Ecosystems* 21(3)**,** 521-535.

Atkinson, C.L., and Vaughn, C.C. (2015). Biogeochemical hotspots: temporal and spatial scaling of the impact of freshwater mussels on ecosystem function. *Freshw Biol* 60**,** 563-574.

Baron, J.S., Poff, N.L., Angermeier, P.L., Dahm, C.N., Gleick, P.H., Hairston, N.G., et al. (2002). Meeting ecological and societal needs for freshwater. *Ecol Appl* 12(5)**,** 1247-1260.

Barnhart, M.C., Haag, W.R., and Roston, W.N. (2008). Adaptations to host infection and larval parasitism in Unionoida. *J N Am Benthol Soc* 27(2), 370-394. doi: 10.1899/07-093.1.

Baruzzi, C., Mason, D., Barton, B., and Lashley, M. (2018). Effects of increasing carrion biomass on food webs. *Food Webs* 17, e00096. doi: 10.1016/j.fooweb.2018.e00096.

Bates, D., Maechler, M., Bolker, B., Walker, S. (2015). Fitting linear mixed-Effects models using *lme4*. *Journal of Statistical Software*, 67(1), 1-48. doi:10.18637/jss.v067.i01.

Baustian, M., Hansen, G., de Kluijver, A., Robinson, K., Henry, E., Knoll, L., et al. (2014). "Linking the bottom to the top in aquatic ecosystems: mechanisms and stressors of benthic-pelagic coupling", in: *Eco-DAS X symposium proceedings. Association for the Sciences of Limnology and Oceanography, Waco, Texas*, 25-47.

Bódis, E., Tóth, B., Szekeres, J., Borza, P., and Sousa, R. (2014). Empty native and invasive bivalve shells as benthic habitat modifiers in a large river. *Limnologica* 49**,** 1-9. doi: 10.1016/j.limno.2014.07.002.

Boyd, I.L., Freer-Smith, P.H., Gilligan, C.A., and Godfray, H.C. (2013). The consequence of tree pests and diseases for ecosystem services. *Science* 342(6160), 1235773. doi: 10.1126/science.1235773.

Cherry, D.S., Scheller, J.L., Cooper, N.L., and Bidwell, J.R. (2005). Potential effects of Asian clam (*Corbicula fluminea*) die-offs on native freshwater mussels (Unionidae) I: water-column ammonia levels and ammonia toxicity. *J N Am Benthol Soc* 24(2)**,** 369-380.

Cooper, N.L., Bidwell, J.R., and Cherry, D.S. (2005). Potential effects of Asian clam (*Corbicula fluminea*) die-offs on native freshwater mussels (Unionidae) II: porewater ammonia. *J N Am Benthol Soc* 24(2)**,** 381-394.

DeCicoo, L. and Blodgett, D. (2017). hydroMap: Watershed boundaries. R package version 0.1.4.

Ellison, A.M., Bank, M.S., Clinton, B.D., Colburn, E.A., Elliott, K., Ford, C.R., et al. (2005). Loss of foundation species: consequences for the structure and dynamics of forested ecosystems. *Front Ecol Environ* 3(9), 479-486.

Fey, S.B., Siepielski, A.M., Nussle, S., Cervantes-Yoshida, K., Hwan, J.L., Huber, E.R., et al. (2015). Recent shifts in the occurrence, cause, and magnitude of animal mass mortality events. *Proc Natl Acad Sci U S A* 112(4), 1083-1088. doi: 10.1073/pnas.1414894112.

Gagnon, P.M., Golladay, S.W., Michener, W.K., and Freeman, M.C. (2004). Drought responses of freshwater mussels (Unionidae) in coastal plain tributaries of the Flint River Basin, Georgia. *J Freshw Ecol* 19(4)**,** 667-679. doi: 10.1080/02705060.2004.9664749.

Galbraith, H.S., Blakeslee, C.J., and Lellis, W.A. (2012). Recent thermal history influences thermal tolerance in freshwater mussel species (Bivalvia:Unionoida). *Freshw Sci* 31(1)**,** 83-92. doi: 10.1899/11-025.1.

Golladay, S. W., Martin, K.L., Vose, J. M., Wear, D.N., Covich, A.P., Hobbs, R.J., Klepzig, K.D., Likens, G.E., Naiman, R.J., and Shearer, A.W. (2016). Achievable future conditions as a framework for guiding forest conservation and management. *Forest Ecology and Management* 360:80-96.

Golladay, S.W., Gagnon, P.M., Kearns, M., Battle, J.M., and Hicks, D.W. (2004). Response of freshwater mussel assemblages (Bivalvia:Unionidae) to a record drought in the Gulf Coastal Plain of southwestern Georgia. *J N Am Benthol Soc* 23(3)**,** 494-506.

Gough, H.M., Gascho Landis, A.M., and Stoeckel, J.A. (2012). Behaviour and physiology are linked in the responses of freshwater mussels to drought. *Freshw Biol* 57(11)**,** 2356-2366. doi: doi:10.1111/fwb.12015.

Haag, W.R., and Stoeckel, J.A. (2015). The role of host abundance in regulating populations of freshwater mussels with parasitic larvae. *Oecologia* 178(4), 1159-1168. doi: 10.1007/s00442-015-3310-x.

Haag, W.R. (2010). A hierarchical classification of freshwater mussel diversity in North America. *Journal of Biogeography* 37(1), 12-26. doi: 10.1111/j.1365-2699.2009.02191.x.

Haag, W.R. (2012). *North American freshwater mussels: natural history, ecology, and conservation.* Cambridge University Press.

Haag, W.R., and Warren, M.L. (2008). Effects of severe drought on freshwater mussel assemblages. *Trans Am Fish Soc* 137(4)**,** 1165-1178. doi: 10.1577/T07-100.1.

Hopper, G.W., Gido, K.B., Vaughn, C.C., Parr, T.B., Popejoy, T.G., Atkinson, C.L., et al. (2018). Biomass distribution of fishes and mussels mediates spatial and temporal heterogeneity in nutrient cycling in streams. *Oecologia***,** 1-12.

Ilarri, M.I., Amorim, L., Souza, A.T., and Sousa, R. (2018). Physical legacy of freshwater bivalves: Effects of habitat complexity on the taxonomical and functional diversity of invertebrates. *Sci Total Environ* 634**,** 1398-1405. doi: 10.1016/j.scitotenv.2018.04.070.

Ilarri, M.I., Souza, A.T., and Sousa, R. (2015). Contrasting decay rates of freshwater bivalves' shells: Aquatic versus terrestrial habitats. *Limnologica* 51**,** 8-14. doi: 10.1016/j.limno.2014.10.002.

Ilarri, M.I., Souza, A.T., Amorim, L., and Sousa, R. (2019). Decay and persistence of empty bivalve shells in a temperate riverine system. *Sci Total Environ* 683, 185-192. doi: 10.1016/j.scitotenv.2019.05.208.

Jeffrey, J.D., Hannan, K.D., Hasler, C.T. and Suski, C.D. (2018) Hot and bothered: effects of elevated Pco2 and temperature on juvenile freshwater mussels. *Am J Physiol Regul Integr Comp Physiol* 315(1), R115-R127.

Kuznetsova, A., Brockhoff, P.B., and Christensen, R.H.B. (2017). lmerTest Package: Tests in Linear Mixed Effects Models. *2017* 82(13)**,** 26. doi: 10.18637/jss.v082.i13.

Lenth, R. (2018). Emmeans: Estimated marginal means, aka least-squares means. *R Package Version* 1(2).

Lennox, R.J., Crook, D.A., Moyle, P.B., Struthers, D.P., and Cooke, S.J. (2019). Toward a better understanding of freshwater fish responses to an increasingly drought-stricken world. *Reviews in Fish Biology and Fisheries* 29(1), 71-92. doi: 10.1007/s11160-018-09545-9.

Lydeard, C., R. H. Cowie, W. F. Ponder, A. E. Bogan, P. Bouchet, S. A. Clark, K. S. Cummings, T. J. Frest, O. Gargominy, D. G. Herbert, R. Hershler, K. E. Perez, B. Roth, M. Seddon, E. E. Strong, and F. G. Thompson. 2004. The global decline of nonmarine mollusks. Bioscience 54:321-330.

Magoulick, D.D., and Kobza, R.A. (2003). The role of refugia for fishes during drought: a review and synthesis. *Freshw Biol* 48**,** 1186-1198.

Matthews, W.J., and Marsh-Matthews, E. (2003). Effects of drought on fish across axes of space, time and ecological complexity. *Freshw Biol* 48(7), 1232-1253. doi: DOI 10.1046/j.1365-2427.2003.01087.x.

McDowell, W.G., McDowell, W.H., and Byers, J.E. (2017). Mass mortality of a dominant invasive species in response to an extreme climate event: Implications for ecosystem function. *Limnol Oceanogr* 62(1)**,** 177-188. doi: 10.1002/lno.10384.

Mosley, L.M. (2015). Drought impacts on the water quality of freshwater systems; review and integration. *Earth-Science Reviews* 140, 203-214. doi: 10.1016/j.earscirev.2014.11.010.

Murphy, J., and Riley, J.P. (1962). A modified single solution method for the determination of phosphate in natural waters. *Analytica chimica acta* 27**,** 31-36.

Novais, A., Batista, D., Cassio, F., Pascoal, C., and Sousa, R. (2017). Effects of invasive clam (*Corbicula fluminea*) die-offs on the structure and functioning of freshwater ecosystems. *Freshw Biol* 62**,** 1908-1916. doi: 10.1111/fwb.13033.

Palmer, M.A., Liermann, C.A.R., Nilsson, C., Florke, M., Alcamo, J., Lake, P.S., et al. (2008). Climate change and the world's river basins: anticipating management options. *Front Ecol Environ* 6(2)**,** 81-89. doi: 10.1890/060148.

R Core Team. (2019). "R: A language and environment for statistical computing. 3.5.33 ed. (Vienna, Austria: R Foundation for Statistical Computing).

Rugel, K., Jackson, C.R., Romeis, J.J., Golladay, S.W., Hicks, D.W., and Dowd, J.F. (2012). Effects of irrigation withdrawals on streamflows in a karst environment: lower Flint River Basin, Georgia, USA. *Hydrol Process* 26(4)**,** 523-534.

Sansom, B.J., Bennett, S.J., Atkinson, J.F., and Vaughn, C.C. (2018a). Long-term persistence of freshwater mussel beds in labile river channels. *Freshw Biol* 63(11)**,** 1469-1481.

Sansom, B.J., Atkinson, J.F., and Bennett, S.J. (2018b). Modulation of near-bed hydrodynamics by freshwater mussels in an experimental channel. *Hydrobiologia* 810(1)**,** 449-463. doi: 10.1007/s10750-017-3172-9.

Smith, N.D., Golladay, S.W., Clayton, B.A., and Hicks, D.W. (2015). "Stream habitat and mussel populations adjacent to AAWCM sites in the Lower Flint River Basin", in: *Proceedings of the 2015 Georgia Water Resources Conference.* (eds.) R.J. McDowell, C.A. Pruitt & R. Bahn. (Athens, Georgia: Institute of Ecology, University of Georgia).

Spooner, D.E., and Vaughn, C.C. (2008). A trait-based approach to species' roles in stream ecosystems: climate change, community structure, and material cycling. *Oecologia* 158**,** 307-317. doi: 10.1007/s00442-008-1132-9.

Stainton, M., Capel, M., and Armstrong, F. (1974). *The Chemical Analysis of Freshwater*. Miscellaneous Special Publication 25. Department of the Environment, Freshwater Institute. *Research and Development Directorate. Winnipeg, Manitoba, Canada*.

Strayer, D.L. (2014). Understanding how nutrient cycles and freshwater mussels (Unionoida) affect one another. *Hydrobiologia* 735(1)**,** 277-292.

Strayer, D.L., and Malcom, H.M. (2007). Shell decay rates of native and alien freshwater bivalves and implications for habitat engineering. *Freshw Biol* 52(8)**,** 1611-1617. doi: 10.1111/j.1365-2427.2007.01792.x.

Subalusky, A.L., Dutton, C.L., Rosi, E.J., and Post, D.M. (2017). Annual mass drownings of the Serengeti wildebeest migration influence nutrient cycling and storage in the Mara River. *Proc Natl Acad Sci U S A* 114(29), 7647-7652. doi: 10.1073/pnas.1614778114.

Tank, J.L., Reisinger, A.J., and Rosi, E.J. (2017). "Nutrient limitation and uptake," in *Methods in Stream Ecology (Third Edition)*. Elsevier, 147-171.

Tiegs, S.D., Clapcott, J.E., Griffiths, N.A., and Boulton, A.J. (2013). A standardized cotton-strip assay for measuring organic-matter decomposition in streams. *Ecol Indic* 32**,** 131-139. doi: 10.1016/j.ecolind.2013.03.013.

USGCRP [U.S. Global Change Research Program]. (2017). *Climate Science Special Report: Fourth National Climate Assessment*, Volume I [Wuebbles, D.J., D.W. Fahey, K.A. Hibbard, D.J. Dokken, B.C. Stewart, and T.K. Maycock (eds.)]. Washington, DC, USA, 470 pp., doi: 10.7930/J0J964J6.

Vaughn, C.C. (2018). Ecosystem services provided by freshwater mussels. *Hydrobiologia* 810**,** 15-27. doi: DOI 10.1007/s10750-017-3139-x.

Vaughn, C.C., Atkinson, C.L., and Julian, J.P. (2015). Drought-induced changes in flow regimes lead to long-term losses in mussel-provided ecosystem services. *Ecol Evol* 5(6)**,** 1291-1305. doi: 10.1002/ece3.1442.

Vaughn, C.C., Taylor, C.M., and Eberhard, K.J. (1997). "A comparison of the effectiveness of timed searches vs. quadrat sampling in mussel surveys", in: *Conservation and Management of Freshwater Mussels II: Initiatives for the Future. Proceedings of a UMRCC symposium*), 16-18.

Wenger, S.J., Subalusky, A.L., and Freeman, M.C. (2018). The missing dead: The lost role of animal remains in nutrient cycling in North American Rivers. *Food Webs***,** e00106. doi: https://doi.org/10.1016/j.fooweb.2018.e00106.

Williams, J.D., Warren Jr, M.L., Cummings, K.S., Harris, J.L., and Neves, R.J. (1993). Conservation status of freshwater mussels of the United States and Canada. *Fisheries* 18(9)**,** 6-22. doi: 10.1577/1548-8446(1993)018<0006:CSOFMO>2.0.CO;2.

Yang, L. H., J. L. Bastow, K. O. Spence, and A. N. Wright. 2008. What can we learn from resource pulses? Ecology 89:621-634.

Zuur, A.F., Ieno, E.N., Walker, N.J., Saveliev, A.A., and Smith, G.M. (2009). *Mixed effects models and extensions in ecology with R*. Springer

FIGURE CAPTIONS

Figure 3-1. Conceptual model depicting ecosystem function shift due to unionids at short and long time scales. Pre mass mortality information based on 25°C, downstream values for 1991 in Vaughn et al. (2015) for the biofiltration and community structure data and on Atkinson and Vaughn (2015) for downstream nutrient excretion and storage information. *Loss of nutrient capacitance dependent on mussel recruitment. Time increases to the left and the impact on mussels of four main ecosystem functions is described and depicted. Capital letters refer to distinct processes in the model, while lower case letters refer to sources: [a]Vaughn et al. (2015), [b]Atkinson and Vaughn (2015), [c]McDowell et al. (2017), [d]Gagnon et al. (2004), [e]Cherry et al. (2005), [f]Cherry et al. (2005), [g]Atkinson et al. (2014), [h]Atkinson et al. (2018), [i]Ilarri et al. (2018).

Figure 3-2. Map of case study locations within the southern continental USA. In the bottom panel, large streams (stream order ≥ 8) are depicted in light blue to provide context while the focal river basins are depicted in black. The letters next to the river basins indicate which bottom panel corresponds to those river basins. Southeastern Oklahoma (A) contains three rivers: the Kiamichi, Little, and the Mountain Fork. K2 and K3 are sites on the Kiamichi discussed in the 'short and long-term nutrient releases following bivalve mortality' section of this manuscript. The lower Flint River (B) is in southwestern Georgia; rivers discussed in the case study section are named. Code from the R package *hydroMap* (DeCicoo and Blodgett, 2017).

Figure 3-3. Ambient concentrations of NH_4-N (μg L^{-1}; A), SRP (μg L^{-1}; B), water column chlorophyll *a* concentrations (μg L^{-1}) and benthic chlorophyll *a* concentrations (μg cm^{-2}) in control, live mussel, and dead mussel treatments. The dashed line represents when the mass

mortality event was induced in 5 live mussel mesocosms. Points represent the mean, while the lines indicate the standard deviation. Ammonium is statistically different within control and dead treatments based on a Type III ANOVA, Tukey HSD, $p < 0.05$. Benthic chlorophyll *a* was higher in live and mortality treatments than control treatments based on a Type III ANOVA, Tukey HSD, $p < 0.05$.

Figure 3-4. Tensile strength (lbs.) as a proxy for decomposition of organic matter within different treatments. Cotton strips have a starting mean tensile strength of 65.61 lbs. (SD = 1.97 lbs). Points represent the mean, while the lines indicate the standard deviation. Decomposition was higher in the mortality treatments than the live treatments and is statistically significant based on Type III ANOVA, Tukey HSD, $p < 0.02$.

Figure 3-5. Extrapolated nutrient release from Kiamichi mussel beds after a drought-induced mass mortality event. The shell lengths from dead unionids are used to predict mussel soft tissue (A), which was then paired with nutrient data from the mesocosm experiment to predict ammonium release (μg m^{-2}; B) and SRP release (μg m^{-2}; C).

Figure 3-6. Shell decomposition (A) of spent mussel shells following the mass mortality event as a result of low flow and high temperature conditions at 3 sites in the Kiamichi River, OK and the resultant release of carbon (B), nitrogen (C), and phosphorus (D) from the shell material over time. Shell decomposition is modeled based on the shell decomposition rates and shell stoichiometry values from Atkinson et al. (2018) and the empty shells sampled from Southeastern Oklahoma in the drought of 2011.

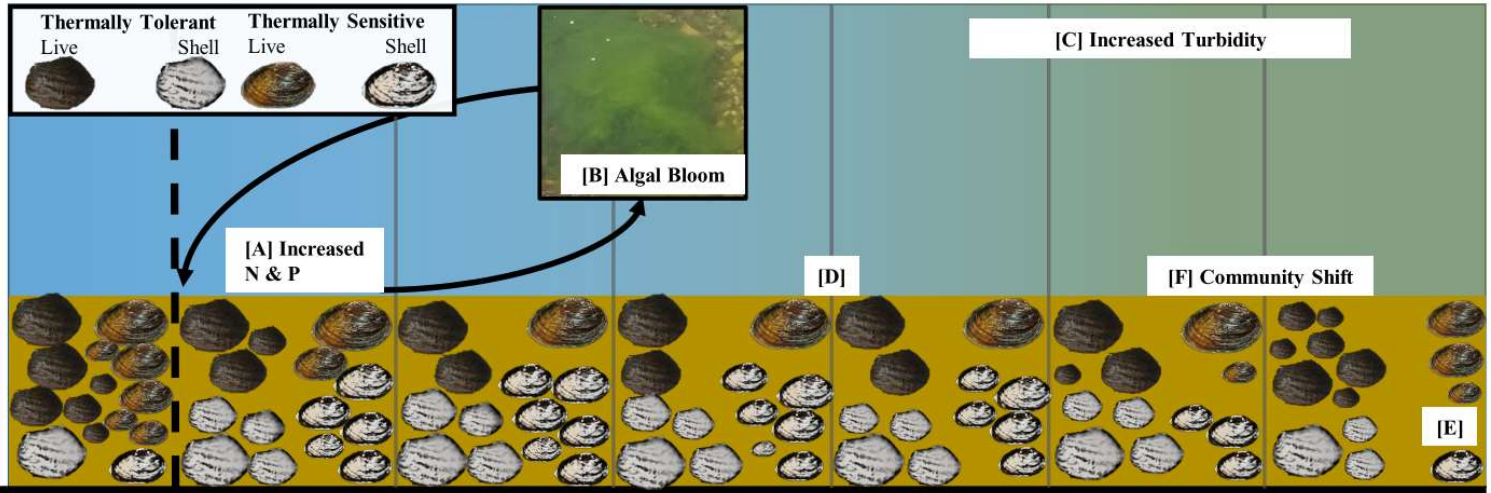

	PRE MASS MORTALITY[a,b]	HOURS	DAYS	WEEKS	MONTHS	YEARS	DECADES
BIOFILTRATION	~5,200 L h^{-1} m^{-2}	Reduced	[B] Reduced biofiltration, paired with increased nutrients, lead to algal blooms[a,c,d]		[C] Potentially altered biofiltration capacity & timing, due to community change		
NUTRIENT REGENERATION	~345 µmol N m^{-2} h^{-1} ~26 µmol P m^{-2} h^{-1}	[A] Increased N & P in the water column[e] & the interstitial space[f]	Increased N & P in the interstitial space[f]			Loss of nutrient capacitance* & shift of excretion stoichiometry because of the homogenized community and reduced biomass	
			[D] Loss of nutrient capacitance, due to individuals lost[g]				
NUTRIENT STORAGE	~47 g N m^{-2} ~4.8 g P m^{-2}	Soft tissue storage reduced while shell is stable[g]			[E] Shells begin dissolving, slowly releasing nutrients into the water column[h]		Storage reduced until biomass completely rebounds
HABITAT	~28 ind. m^{-2} ~5 species m^{-2}	Increased interstitial spaces from shells without tissue			[E] Decreased habitat heterogeneity of mussels & mussel shells[i]		More homogenous benthos

Figure 3-1. Conceptual model of ecosystem function shift due to unionids die-offs.

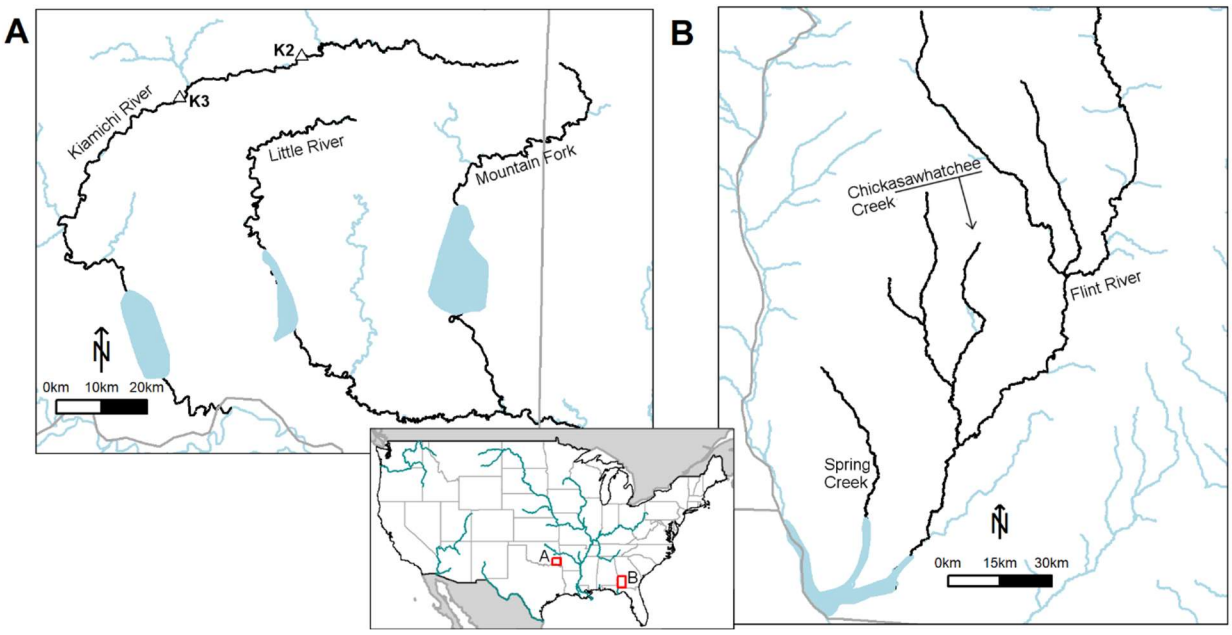

Figure 3-2. Map of case study locations in the Southeastern United States

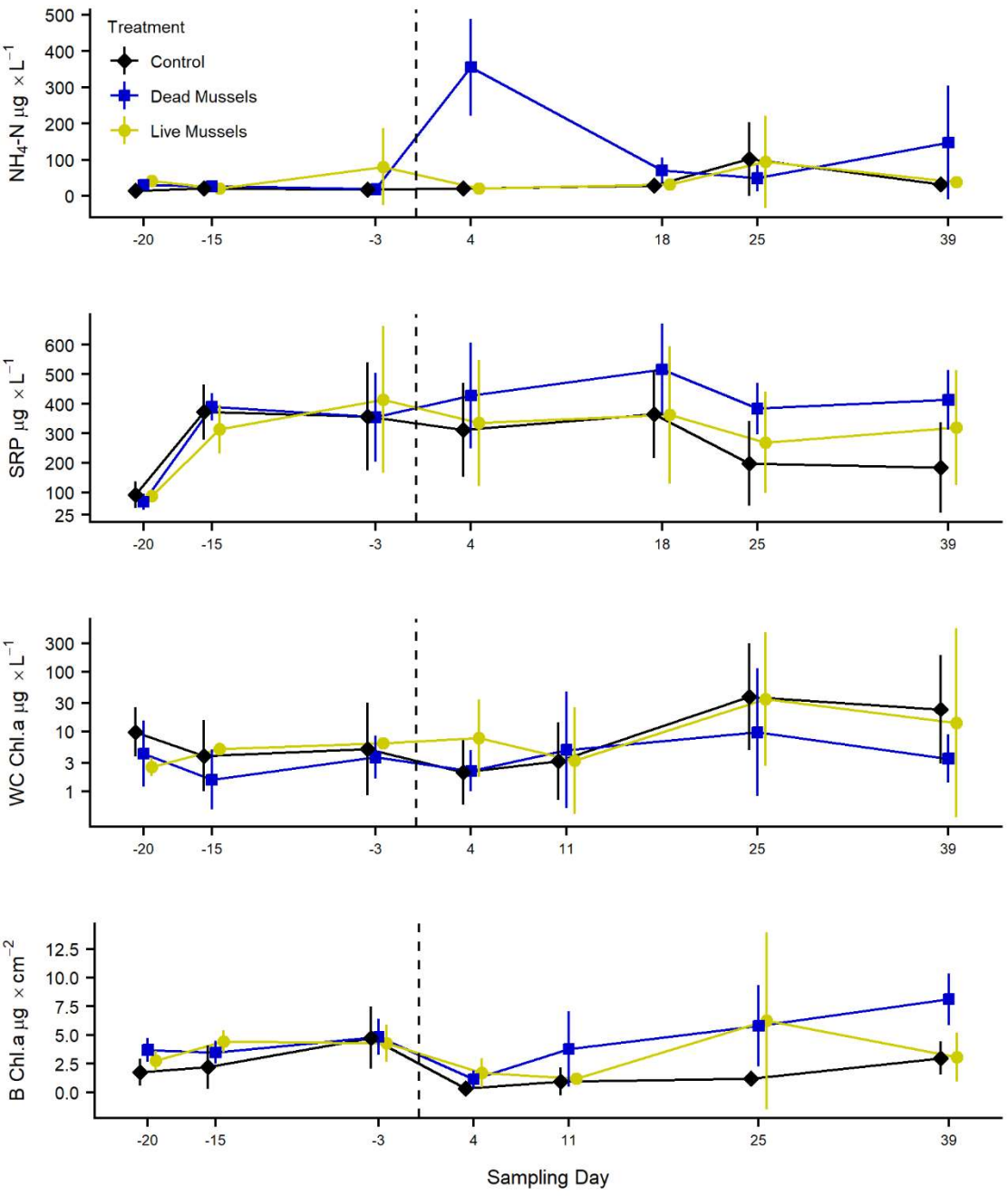

Figure 3-3. Water column nutrients and chlorophyll *a* concentration among treatments

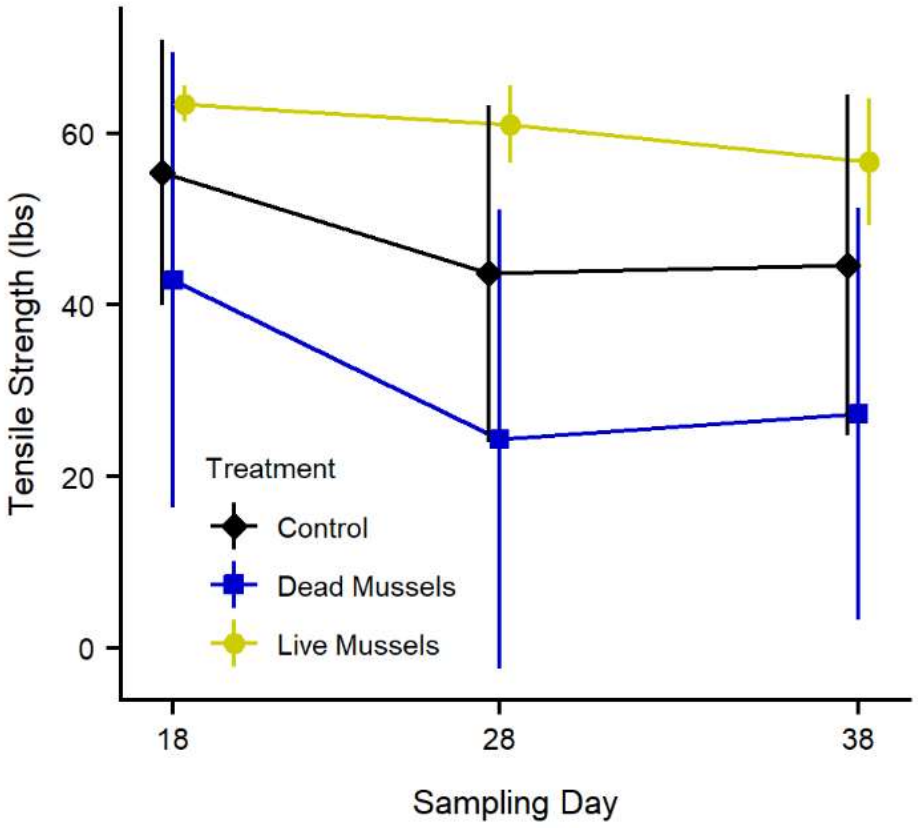

Figure 3-4. Organic matter decomposition among treatments after the die-off

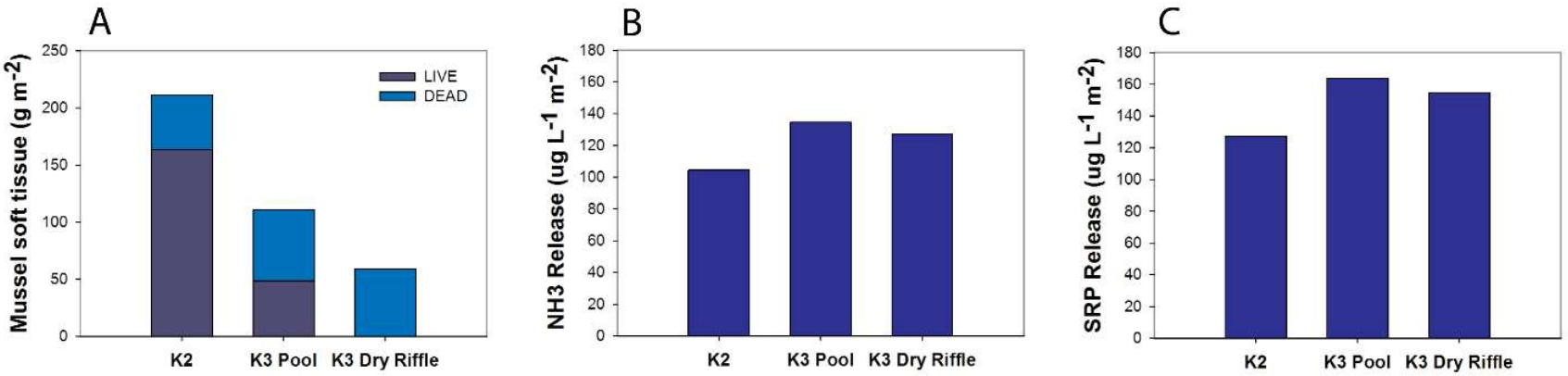

11

12 Figure 3-5. Modelled short-term release of nutrients from soft tissue after a die-off

13

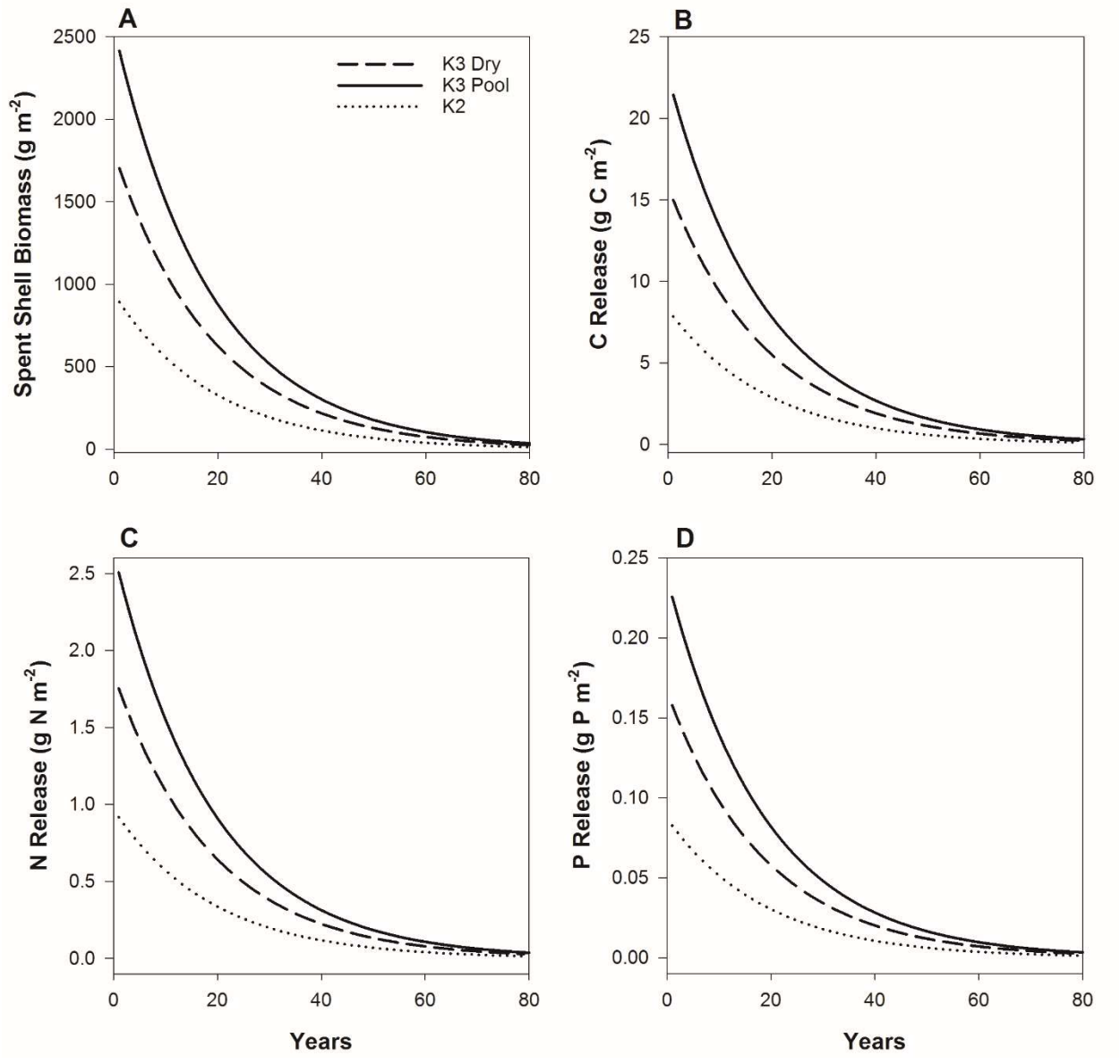

Figure 3-6. Modelled long-term releases of nutrients from shell after a die-off

APPENDIX

Table 3-A1. Sampling record with the corresponding measurements collected and sampling dates and days reported. Filled cells indicate we sampled that ecosystem compartment at that time. Tiles for benthic metabolism and algal chlorophyll *a* quantification were replaced on days -20, 0, and 8 to ensure maximum time for algal colonization.

Day	Date	Physical-chemical parameters	Water column nutrients	Benthic chl. *a*	Water column chl. *a*	Benthic metabolism	Cotton decomp.
-45	5/18/2018	Water added to mesocosm					
-33	5/30/2018	Mussels added to nine mesocosms					
-20	6/12/2018	■	■	■	■		
-15	6/17/2018	■	■	■	■		
-14	6/18/218	Ten Largmouth bass added to each mesocosm					
-3	6/28/2018	■	■	■	■		
-2	6/29/2018	Largmouth bass removed from mesocosms					
0	7/2/2018	Mass mortality induced in five mesocosms					
4	7/6/2018	■	■	■	■	■	
11	7/13/2018	■		■	■	■	
18	7/20/2018	■	■				■
25	7/27/2018	■	■	■	■	■	
28	7/30/2018						■
39	8/10/2018	■	■	■	■	■	■

Table 3-A2. Mean (SD) physical and chemical parameters for control, dead, and live treatments throughout the experiment. Negative days indicate sampling times before the mass mortality event, while positive days are after the event.

		Water Temperature (°C)			Dissolved Oxygen (mg L^{-1})		
Day	**Date**	**Control**	**Dead**	**Live**	**Control**	**Dead**	**Live**
-20	6/12/2018	27.2 (0.4)	27.0 (0.2)	27.0 (0.2)	7.43 (0.71)	7.41 (0.47)	7.45 (0.70)
-15	6/17/2018	27.1 (0.2)	26.9 (0.3)	27.0 (0.3)	7.36 (0.19)	7.40 (0.27)	7.57 (0.11)
-3	6/28/2018	31.2 (0.6)	31.0 (0.8)	30.9 (0.8)	9.81 (1.34)	9.31 (0.91)	10.69 (3.25)
4	7/6/2018	31.7 (0.2)	31.8 (0.2)	31.6 (0.3)	9.51 (1.06)	8.56 (1.25)	10.00 (2.39)
11	7/13/2018	29.9 (0.5)	30.4 (0.7)	30.0 (0.3)	9.09 (1.31)	12.22 (2.94)	10.25 (2.31)
18	7/20/2018	30.2 (0.5)	29.7 (0.3)	29.6 (0.2)	8.55 (1.20)	8.23 (1.13)	9.39 (2.48)
25	7/27/2018	31.8 (0.3)	31.8 (0.2)	31.7 (0.3)	10.83 (1.70)	14.54 (3.86)	12.41 (3.85)
39	8/10/2018	30.9 (0.2)	31.1 (0.2)	30.8 (0.3)	10.89 (1.38)	11.48 (2.44)	12.18 (2.41)

		Conductivity (µS cm^{-1})			Water Addition (mL s^{-1})		
Day	**Date**	**Control**	**Dead**	**Live**	**Control**	**Dead**	**Live**
-20	6/12/2018	399 (23)	418 (19)	401 (19)			
-15	6/17/2018	345 (15)	345 (12)	349 (17)	26 (28)	11 (16)	17 (15)
-3	6/29/2018	385 (59)	381 (64)	376 (64)			
4	7/6/2018	373 (71)	387 (84)	366 (83)			
11	7/13/2018	377 (73)	369 (84)	363 (77)	11 (27)	19 (17)	20 (22)
18	7/20/2018	396 (72)	390 (69)	373 (64)			
25	7/27/2018	402 (67)	386 (53)	384 (70)			
39	8/10/2018	382 (68)	377 (56)	358 (64)			